The Thoracic Respiratory Interneurone: Physiology, Morphology and Pharmacology, With Reference To The Transmission Of Respiratory Drive.

By

Shane Anthony Saywell

Submitted to the University of London for the Degree of Doctor of Philosophy.

January 2000

Sobell Department of Neurophysiology

Institute of Neurology

Queen Square

London

WC1 3BG

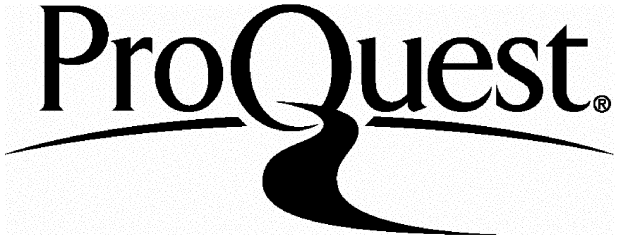

Abstract.

The central respiratory drive generated in the medulla is transmitted to the motoneurones of the cervical and thoracic cord that innervate the muscles that produce respiratory movements. This respiratory drive is thought to be transmitted to the motoneurones monosynaptically from the bulbospinal neurones and polysynaptically via interneurones.

In this study in the anaesthetized paralysed cat, the strength of the bulbospinal input to thoracic interneurones was investigated using intracellular spike-triggered averaging. Similarly, spike-triggered averaging was performed in motoneurones to identify any bulbospinal input for comparative purposes and to re-assess the strength of this input. No input to the interneurones was identified. However, the input to the motoneurones was found to be more abundant than previously thought.

Some of the intracellularly penetrated interneurones were injected with Neurobiotin to allow morphological characterisation. Interneurones with somata located in laminae VII to X of the spinal cord were labelled and had a varied morphology. These neurones had extensive dendritic projections throughout the ventral horn with a predominant rostrocaudal orientation. The majority of the interneurones had axons that projected to the contralateral cord where the axons descend in the medial and ventral funiculi. Interneurones with ipsilateral and rostral projections were also identified. The axons were found to give off up to four collateral branches with the collaterals projecting within the ventral horn.

The collaterals tended to be fine possessing both *en passant* and *terminaux* boutons.

Renshaw cells that exhibited respiratory phasing of their discharge have also been characterised by intracellular labelling in the thoracic cord. These cells were shown to have similar morphology and axonal projections to those seen in the lumbar cord.

The thoracic motoneurones receive a stronger monosynaptic drive than previously thought, but an input to the interneurones has not been identified. The interneurones represent a diverse morphological population that predominantly have a crossed descending axon. These interneurones have fine collateral projections with generally small terminal fields and they may be inhibitory or excitatory. The fine nature of the collaterals is supported by Renshaw cell collaterals being larger and stained at long distances from the injection site. The thoracic Renshaw cells are similar in character to those of the lumbar cord.

Acknowledgements.

I would like to thank Dr. Peter Kirkwood for the opportunity to undertake this study and for his guidance and friendship during the study. I would similarly like to thank Dr. Timothy Ford and Dr. Christopher Seers for their encouragement and friendship. Also I would like to thank Dr. Andrew Todd for the immunohistochemical data contained in this thesis. I would like to thank all members of the Sobell Department of Neurophysiology for their comradeship, and my family as without their support this thesis would not have been possible. The Medical Research Council is also gratefully thanked for its financial support.

Contents.

Chapter 1. Literature survey.

Chapter 2. Methods.

Chapter 3. Thoracic Motoneurones.

Chapter 4. The Respiratory Thoracic Interneurone (Excluding Renshaw Cells).

Chapter 5. The Thoracic Respiratory Renshaw cell.

References.

Appendix.

List of Figures.

Abbreviations.

AP.	Action Potential.
Böt C.	Bötzinger Complex.
CRDP.	Central Respiratory Drive Potential.
CI.	Critical Interval.
CUSUM.	Culmative Sum.
Cys5.	Cyanine 5.18.
cVRG.	Caudal Ventral Respiratory Group.
DAB.	Diaminobenzidine.
DRG.	Dorsal Respiratory Group.
GAD.	Gamma Amino Decarboxylase.
EBSN.	Expiratory Bulbospinal Neurones.
EPSP.	Excitatory Post Synaptic Potential.
FITC.	Fluorescein Isothiocyanate.
FSP.	Focal Synaptic Potential.
HRP.	Horseradish Peroxidase.
IPSP.	Inhibitory Post Synaptic Potential.
ISIH.	Interstimulus Interval Histogram.
LRSC.	Lissamine Rhodamine.
PBS.	Phosphate Buffered Saline.
PBST.	Phosphate Buffered Saline with Triton-X100.
Pre-Böt C.	pre-Bötzinger Complex.
PITH.	Peri-interval Time Histogram.

SD.	Standard Deviation.
rVRG.	Rostral Ventral Respiratory Group.
STA.	Spike-Triggered Averaging.
T.	Threshold.
TP.	Terminal Potential.
VRG.	Ventral Respiratory Group.
$V_{m.}$	Membrane Potential.

Chapter 1. Literature survey.

1.1.1. The Mechanics of Breathing.

In the mammal breathing is the fundamental prerequisite of life: without adequate provision of oxygen and removal of carbon dioxide, metabolic processes essential for the maintenance of existence cannot proceed. In mammals breathing can be divided into two processes: respiration and ventilation. Respiration involves the absorption of oxygen into the circulation, the metabolic processes at a cellular level and the reciprocal process of carbon dioxide excretion. Ventilation, on the other hand, is the process of generating the flow of air in to and out of the alveoli in the lungs thus allowing gaseous exchange to occur. Ventilation in mammalian systems is achieved by changing the volume of the thoracic cavity in which the lungs reside resulting in the displacement of volumes of gas. These volume changes are achieved by movements of the thoracic and abdominal musculature along with the diaphragm. The control of the musculature involved in ventilation is however complex, as any factor that affects the rigidity of the thorax or changes in the resistance to gaseous flow will cause changes in ventilatory function. Consideration of the relationship of all these factors is beyond the scope of this thesis. However, before presenting the results of this study consideration will briefly be given to the muscles involved in achieving respiratory movements, the central pattern generator thought to initiate breathing movements, the motoneurones involved in innervation the of the musculature and finally, spinal

interneurones involved in this process. Wherever possible the discussion will be limited to the feline respiratory system as this animal has historically been the favoured experimental model used in neurophysiology, and is the model used in this study although the rat is increasingly becoming the favoured model animal.

1.1.2. The Respiratory Muscles.

The mechanics of breathing and the consequent gaseous displacement can be considered to be principally dependent on the function of two *systems*; that may be considered as 'pumps', these being the; 'axial' and 'radial' pumps (see Monteau and Hilaire 1991 for review). The axial pump is so called as it involves changes in the volume of the thoracic cavity that occur along the axis of the animal; i.e., in the rostrocaudal direction. Conversely, the radial pump, involves changes in the volume of the thoracic cavity that occur by increasing the radius of the cavity. The axial pump may be considered to be almost entirely dependant on the activity of the diaphragm, the only other muscles contributing to this pump in certain behaviours being the abdominal muscles. The radial pump is dependant on the activity of principally the intercostal and parasternal muscles that act to raise or lower the rib cage and hence alter the radius of the thorax. It must be emphasised that these pumps do not act independently and the activity of the muscles of the pumps are co-ordinated centrally and linked by thoracic and abdominal pressure changes (see Iscoe 1998 for review), as the activity of these muscles affect the rigidity of the thorax and, hence, the mechanical advantages of neighbouring muscles. A third

category of respiratory phased muscles have been termed 'accessory' muscles (See Cohen 1979 for review), and are mainly the muscles of the neck and upper airways. However, other muscles may be considered to have a respiratory function and hence considered as accessory, these include muscles that affect the rigidity of the thorax and consequently affect respiratory function (for review see Monteau and Hilaire 1991).

1.1.3. The Diaphragm.

The diaphragm is the principal muscle responsible for inspiration. The diaphragm is responsible for up to 80% of the volume changes that occur in the lungs and is the principal muscle of the axial pump. The diaphragm consists of striated muscle of many fibre types, (for review see Monteau and Hilaire 1991) and is a dome-shaped sheet of muscle attached to the lower ribs, the sternum and the vertebrae. The diaphragm thus separates the thorax from the abdomen. The diaphragm contracts as a whole and contraction results in the muscle flattening and moving down into the abdominal cavity thus increasing the volume of the thoracic cavity. The diaphragm is innervated by the phrenic nerves that in the cat leave the spinal cord between C4 and C6 with no innervation received from any other segment of the spinal cord.

1.1.4. The Intercostal Muscles.

The intercostal muscles are arranged as two sheets of muscle between, and attached to the ribs (see Sears 1964a and De Troyer & Ninane 1986 for

illustrations and Monteau and Hilaire 1991 for review). The fibres of the external intercostal muscles run diagonally in a ventrocaudal direction, whereas, the fibres of the internal intercostal muscles run diagonally in the in the dorsocaudal direction. This orientation led to the theory that the external intercostals raise the ribs and are thus inspiratory and the internal intercostals lower the ribs and are expiratory (Hamberger 1749). In the cat a mixed respiratory phasing of the intercostals has been demonstrated (Le Bars & Duron 1984), with only the intermediate region of the intercostal muscles showing reciprocal activity with the external intercostals being inspiratory, and the internal intercostals expiratory. Electromyographic recordings in the dog, however, have shown that the external intercostals are active during inspiration and the internal intercostals are active during expiration (De Troyer & Ninane 1986) supporting the theory of Hamberger (1749). The distribution of respiratory activity thorough an intercostal space varies (Legrand & De Troyer 1999b), with the greatest amount of activity in the regions of the greatest mechanical advantage (De Troyer, Legrand & Wilson 1999a), and the external intercostal muscles being inspiratory and the internal intercostal muscles expiratory.

The contribution of these muscles to ventilation is thus twofold; firstly, they cause the thoracic cage to rise and fall, thus expanding and contracting its radius, secondly, contribute to the rigidity of the thorax and prevent the diaphragm pulling in the thoracic cage in when it contracts.

The intercostal muscles are innervated by nerves branching from the ventral ramus arising from the thoracic segments T1-T12 in the cat (Eccles *et*

al. 1962; Sears 1964a; Tani, Kida & Akita 1994). The ventral ramus divides into an internal branch (the internal intercostal nerve), and runs along the inside of the thoracic wall (see Sears 1964 and Tani, Kida & Akita 1994 for illustrations) and an external branch that runs between the internal and external intercostals. The internal intercostal nerves contain axons from both expiratory and inspiratory motoneurones (Eccles *et al.* 1962; Sears 1964a), whereas, the external intercostal nerve contains only axons of inspiratory motoneurones (Sears 1964a).

The intercostal muscles are thus the principal muscles involved in the function of the radial pump with the external intercostals acting to raise the rib cage and the internal intercostals acting to lower the rib cage. The intercostal muscles receive all of their innervation from branches of the ventral ramus and these branches contain inspiratory and expiratory motoneurone axons in the internal nerve and only inspiratory activity in the external nerve.

1.1.5. The Parasternal and Paravertabral Muscles.

In addition to the muscles mentioned above there are two other sets of muscles located between the sternum and the ribs and between the vertebrae and the ribs that exhibit respiratory activity, these being; the intercartilagenous and triangularis sterni muscles located between the sternum and the ribs and the levator costae muscle located between the spine and the ribs.

The intercartilagenous muscles (parasternal muscles) are located in

bundles between the sternum and the ventral most portions of the ribs in the first 7 intercostal spaces (Monteau & Hilaire 1991) and have an inspiratory function; i.e. they raise the ribs thus contributing to the radial pump. The triangularis sterni muscle is located between the sternum and the 7 most 'cephalic' intercostal spaces and is thought to have an expiratory function, in the cat (Duron 1981) and in the rat (Monteau & Hilaire 1991).

The mechanical advantage of the inspiratory parasternal muscles and the level of their activity show a gradient in the rostrocaudal direction (De Troyer, Legrand & Wilson 1996; Legrand *et al.* 1996), with the greatest mechanical advantage and activity in the rostral muscles, decreasing caudally. These observations help confirm the parasternal muscles as making a significant contribution the functioning of the radial pump in the dog as was first demonstrated in humans (Taylor 1960).

The levator costae muscles are located in the proximal intercostal space between the lateral process and the next caudal rib (for illustration see Hilaire Nicholls & Sears 1983). The levator costae muscles are inspiratory phased muscles with the strength of the activity greatest in caudal segments (Hilaire Nicholls & Sears 1983). Similar inspiratory phasing has also been demonstrated in the human (Goldman, Loh & Sears 1985). The levator costae muscles are part of the radial pump musculature acting to raise the ribs during inspiration.

1.1.6. The Accessory Muscles.

Any muscle that affects the rigidity of the thorax can be considered to have an 'accessory' respiratory function (Monteau & Hilaire 1991); although, they may or may not directly affect the movement of the thorax. Many muscles of the neck and face have been considered as accessory respiratory muscles (see Cohen 1979). However, other motor behaviours for example, locomotion can affect respiration (Nolan & Waldrop 1997). Hence, other muscle groups may be considered as accessory. Further to this, muscles of the thorax that affect the rigidity of the thorax must be considered as probable accessory muscles. For many of these muscles the respiratory input has not been identified, however, in all likelihood due to their close association with the thorax, some respiratory modulation should be expected.

The muscles that are considered as probable accessory muscles are: multifidus, interspinales, longissimus dorsi, iliocostalis, spino-trapezius and latissimus dorsi. Some of these muscles are represented schematically in Figure 2.1.1 The multifidus muscles are located between the dorsal spinal process and the transverse process of the second segment more caudally. The interspinales muscles are located between adjacent dorsal processes. The longissimus dorsi muscle runs the length of the spine with attachments to the dorsal and lateral spinal processes and the proximal rib. The illiocostalis muscle runs the length of the spine lateral to longissimus dorsi attached the proximal rib. The rotatores muscles are located between the dorsal spinal process and

the lateral process of the adjacent caudal segment. The spino-trapezius and latisimus dorsi muscles are sheet like muscles that attach to the tip of the dorsal process and run over longissimus dorsi and illiocostalis and attach to the forelimb and 13th rib in the case of lattisimus dorsi and the scapula and the spinal processes in the case of the spino-trapezius. All of these muscles are innervated from branches of the dorsal ramus of the thoracic nerves; however, it is not clear in all cases precisely from which branch of the nerve for some muscles. The respiratory modulation of these muscles is also unknown. However, due to their close association with the rib cage, respiratory modulation is likely.

The functioning of the radial and axial pumps can thus be seen to be affected by not only the muscles that are organised to bring about directly the required changes in the volume of the thoracic cavity, but also muscles affecting the rigidity of the thorax. Breathing movements, however, are brought about by the co-ordinated activity of these pumps. This co-ordination must be achieved by the central nervous system and involve a high degree of integration of inputs from many other systems. Breathing, therefore, must be considered a highly integrated movement that is co-ordinated with the functioning of all other motor systems.

1.2.1. The Generation of the Central Respiratory Rhythm.

Ventilation is a rhythmic motor function that has a period between a few hundred milliseconds to minutes in extreme circumstances. Ventilation is under

both voluntary control, as in behaviours like vocalization, and involuntary control; for example, ventilation persists during sleep and under anaesthesia. Thus it is of interest how the respiratory rhythm is generated and integrated into a patterned output that leads to the ventilatory movements. The central origin of the respiratory rhythm as long been identified to lie in the medulla (see Sears 1977; Cohen 1979; Rekling & Feldman 1998 for reviews), and was considered to be centred upon several medullary centres identified principally from lesion experiments or electrical stimulation. Subsequent electrophysiological investigations have revealed neurones with activity phased to various periods of respiration, thus having a respiratory rhythm. Of the neurones in the medulla that exhibit respiratory rhythms only a proportion are bulbospinal; i.e. possessing an axon that projects to the spinal cord. The remaining respiratory neurones in the medulla are motoneurones innervating the upper airways, afferent cells (i.e. P-cells) or presumed propriobulbar interneurones involved in the generation of the central respiratory pattern. Here we will only consider the medullary respiratory interneurones involved in generating the central respiratory rhythm and the bulbospinal neurones thought to transmit the rhythm to the motoneurones of the spinal cord.

From antidromic mapping experiments the location of the bulbospinal neurones have been described and are centred in two regions; one region is the ventrolateral nucleus tractus solitarius and the second does not conform to any discrete anatomical structure, extending rostrally through the nucleus retroambigualis, nucleus ambiguus and rostrally approaching the retrofacial nucleus. These groups of cells are thus referred to as the dorsal respiratory

group (DRG) and the ventral respiratory group (VRG), and the bulbospinal neurones in each group can be further defined by firing pattern, projections and location as summarised in Figure 1.2.1. Once the firing patterns and connectivity of respiratory neurones have been defined, attempts can be made at modelling the rhythm generation mechanism.

1.2.2. The Dorsal Respiratory Group (DRG).

The dorsal respiratory group (DRG) is a discrete aggregation of inspiratory neurones in the medulla. Some neurones of the DRG have been identified as having bulbospinal axons by antidromic activation from the spinal cord (Bianchi 1971;1974; Von Euler *et al.* 1973a,b; Berger 1977), with the soma identified as lying in the ventrolateral nucleus tractus solitarius (NTS) in the cat. Nearly all DRG neurones have a descending axon (Bianchi 1971) which crosses the midline at the medullary level (Bianchi 1971;1974; Berger 1977), and descends contralaterally, usually in the lateral funiculus of the spinal cord.

The firing patterns of almost all the DRG neurones are inspiratory (Bianchi 1971;1974; Berger 1977), with the exception of a small number of expiratory units (Von Euler *et al.* 1973a; Feldman & Cohen 1978). The inspiratory discharge pattern is predominantly augmenting with discharge beginning either in early or late inspiration (Bianchi 1971; Cohen & Feldman 1984) although more varied firing patterns have been described (Von Euler *et al.* 1973a, Bianchi 1974).

The morphology of DRG neurones has been described by several techniques. Firstly the morphology of the inspiratory DRG neurones was described by injection of procion yellow (Von Euler *et al.* 1973a), which revealed cells with somal diameters in the range of 20-60 μm. Intracellular Labelling with horseradish peroxidase (HRP) (Berger, Averill & Cameron 1984; Otake *et al.* 1989) revealed similar neurones in the ventrolateral NTS with mean somal diameters of 38.2 μm in the horizontal plane and 39.4 μm in the transverse plane. The neurones had between 4-10 dendrites and these tended to be orientated in the mediolateral direction for up to 1 mm. The axons originated from either the soma or proximal dendrite (Berger, Averill & Cameron 1984) and projected ventrally and turned medially to cross the midline (Berger, Averill & Cameron 1984; Otake *et al.* 1989). A proportion of these neurones had a bifurcating axon with one branch projecting ipsilaterally and the other contralaterally (Berger, Averill & Cameron 1984; Otake *et al.* 1989). These neurones usually do not give off axon collaterals in the brain stem (Otake *et al.* 1989).

1.2.3. The Ventral Respiratory Group (VRG).

The ventral respiratory group (VRG) is a population of neurones located laterally in the medulla, with the bulbospinal neurones of the VRG having both inspiratory and expiratory activity (see Hilaire and Monteau 1991, Iscoe 1998, Rekling & Feldman 1998 for reviews). The population of respiratory neurones has been extensively mapped (Merrill 1970: Bianchi 1971; 74; Bianchi & Barillot

1982) and extends as a rostrocaudal column within the medulla. The neurones within this column can be separated by their discharge patterns, locations and projections into three groups, thus; the most caudal neurones are mostly expiratory and this region is known as the caudal ventral respiratory group (cVRG), the neurones rostral to the obex are mainly inspiratory and this region is known as the rostral ventral respiratory group (rVRG) and finally the most rostral area of the VRG that contains expiratory neurones is widely referred to as the Bötzinger complex (Lipski & Merrill 1980; Feldman 1981). An area caudal to the Bötzinger complex (Böt C) has latterly been considered separately from the Böt C and is known as the pre-Bötzinger complex (pre-Böt C). This area thus contains many respiratory neurones of many types and thus will be discussed initially in terms of these stated divisions.

1.2.4. Caudal Ventral Respiratory Group (cVRG).

The caudal ventral respiratory group is a group of expiratory neurones extending from the most rostral part of C1 extending in a column rostrally to around the level of the obex, where there is overlap with the inspiratory units of the rVRG. In dorsoventral aspect the neurones are located ventral to the trigeminal nerve tract (Merrill 1970) and almost exclusively have a contralateral spinal axon (Merrill 1970; Bianchi 1971; 1974; Arita, Kogo & Koshiya 1987), descending in a discrete tract in the ventral column (Merrill 1970; Bianchi 1971; 74). The boundaries of the cVRG are rather arbitrary but may be defined as a group of expiratory neurones between the rostral roots of C1 and the obex.

The morphology of cVRG neurones have been described by several techniques. Firstly the morphology of these neurones was described by Kreuter *et al.* (1977) by intracellular staining with procion yellow. Further description of the anatomy of these neurones was achieved by intracellular injection of HRP (Arita, Kogo & Koshiya 1987). This study described expiratory neurones in the cVRG with polygonal or ellipsoid somata. The somata had a mean major diameter of 54.7 μm with 4-6 primary dendrites that projected transversely for up to 900 μm, little dendritic projection along the rostrocaudal axis was evident. The axon was shown usually to originate from the soma and loop rostrally in a dorsomedial direction, crossing the midline around the level of the soma. After crossing the midline the axons travelled caudally in the ventrolateral funiculus. No axon collaterals have been identified for these neurones.

The firing patterns of the cVRG neurones was shown to be expiratory with an augmenting firing pattern (Merrill 1970; Bianchi 1971; 74; Cohen, Feldman & Sommer 1985; Arita, Kogo & Koshiya 1987; Kirkwood 1995). This augmenting pattern has an incremental spike frequency, with an abrupt cession of firing and hyperpolarisation at the onset of inspiration. Further to these expiratory neurones, neurones with an inspiratory discharge pattern have been described in the cVRG of the cat (Arita, Kogo & Koshiya 1987). These inspiratory neurones depolarised abruptly at the onset of inspiration and fired spikes in early inspiration, ceasing firing with the gradual repolarization of the membrane potential later in inspiration. These neurones are classified as early inspiratory neurones. The early inspiratory neurones could not be antidromically

identified from the spinal cord (Arita, Kogo & Koshiya 1987), and are thus thought not to have a spinal axon. The respiratory neurones of the cVRG are thus of two types; augmenting expiratory bulbospinal neurones and early inspiratory neurones that do not posses a spinal axon.

1.2.5. The Rostral Ventral Respiratory Group (rVRG).

The rostral respiratory group is a group of respiratory neurones located rostrally to the cVRG, and principally have an inspiratory firing pattern. Caudally the rVRG begins at the obex: i.e., the junction with the cVRG, and then extends rostrally in a column to around the level of the retrofacial nucleus (for review see Monteau and Hilaire 1991). At the level of the retrofacial nucleus the rVRG neurones overlap with a group of neurones known as the Pre-Bötzinger neurones. The projections and firing patterns of the rVRG neurones are more diverse than those of the other groups of neurones described. The population of neurones having a spinal axon is unclear, as different studies have shown different percentages of neurones projecting to the spinal cord; similarly, the firing patterns exhibited by these neurones differ widely.

For the inspiratory and expiratory neurones of the rVRG many different patterns of discharge have been observed. The inspiratory neurones of the rVRG have been generally classified in accordance with either the changes in the frequency of their discharge or the phase of the inspiratory cycle they discharge in. A predominant group of inspiratory rVRG neurones have an augmenting pattern of discharge (Bianchi 1971; 1974), frequently having an

abrupt cessation of discharge at the end of inspiration. These augmenting inspiratory neurones, however, show variation in the onset of discharge with regard to the inspiratory period. Hence, neurones were described as early or late augmenting inspiratory neurones (Bianchi 1971), whose discharge occasionally continued into the post-inspiratory period. A further group of inspiratory neurones show a decrementing pattern of discharge during inspiration (Bianchi 1974; Merrill 1974). These decrementing neurones begin firing abruptly at the onset of inspiration, in response to a rapid depolarisation (Bianchi 1988), occurring at the onset of phrenic activity, subsequently, cessation of firing is usually associated with a gradual repolarization. Similarly to the augmenting inspiratory neurones, decrementing inspiratory neurones can be subdivided into; early decrementing, or, late decrementing neurones (Bianchi 1974), according to the part of the inspiratory period they discharge in. Finally, two further types of rVRG neurones with inspiratory phased firing have been described, these being; neurones that discharge at a constant frequency throughout inspiration (Bianchi 1974), and neurones that fire tonically whose discharge frequency increases during inspiration (Bianchi 1971). With regard to the discharge patterns of the inspiratory neurones of the rVRG, it can be seen that these neurones represent a heterogeneous population, suggesting that they represent a group of functionally different neurones. The inspiratory neurones of the rVRG thus represent a far more diverse population of neurones than those of the cVRG.

The morphology of rVRG neurones have been described by several techniques. Firstly the morphology of these neurones described by intracellular

injection of procion yellow (Kreuter *et al.* 1977). Subsequently, using intracellular Labelling with HRP (Sasaki *et al.* 1989), augmenting inspiratory neurones were characterised as having aspherical somata with mean diameters of 36 μm, with the major somal diameter orientated in the transverse plane. The axons of these neurones projected predominantly contralaterally (Sasaki *et al.* 1989). Initially the axons projected dorsomedially, then, turned ventromedially to cross the midline, approximately at the level of, or, slightly rostral to the soma. A small number of the neurones had ipsilateral collaterals (Sasaki *et al.* 1989). However, contralateral collaterals could not be identified, probably due to low intensity staining.

1.2.6. The Bötzinger Complex (Böt C) and the Pre-Bötzinger Complex (pre-Böt C).

The final division of the VRG is the rostral-most portion that has become known as the Bötzinger complex (Lipski & Merrill 1980; Feldman 1981). The Bötzinger complex (Böt C) extends from an area rostral to the rVRG, that latterly has become known as the pre-Bötzinger complex (see later for description) to the retrofacial nucleus; the somata of expiratory neurones in the Bötzinger complex are located around the ventromedial edge of the middle portion of the retrofacial nucleus (Otake *et al.* 1987), whereas inspiratory neurones are located more caudal and ventral. The neurones of the Böt C are predominantly expiratory (Lipski & Merrill 1980), and project contralaterally to the DRG (Kalia, Feldman & Cohen 1979; Lipski & Merrill 1980), and to

contralateral phrenic motoneurones (Merrill & Fedorko 1984), together with a small ipsilateral projection (Bianchi & Barillot 1982).

The morphology of augmenting expiratory neurones of the Bötzinger complex has been described by intracellular labelling with HRP. Intracellular labelling (Otake *et al.* 1987) which identified somata in proximity to, but not within, the retrofacial nucleus. The neurones had a mean soma mean size of 35.9 μm for augmenting and 37.8 μm for plateau expiratory neurones. They possessed dendrites that projected in all directions for up to 600 μm. The axons of these neurones initially project dorsomedially and bifurcate close to the level of the soma into an ipsilateral and a contralateral descending branch. The latter branch crosses the midline at the level of the soma or slightly rostral to the soma (Otake *et al.* 1987). Axon collaterals were observed ipsilaterally and consisted of either a few long collaterals or many collaterals of different lengths (Otake *et al.* 1987), contralateral collaterals were not seen. The axon collaterals possessed both *terminaux* and *en passent* boutons, lying within the Böt C, the nucleus paraambiguus, the retrofacial nucleus and the nucleus ambiguus.

Within the Bötzinger complex, neurones with activities related to all phases of the respiratory cycle have been identified. Inspiratory, expiratory and phase spanning units have been identified (Lipski & Merrill 1980; Bianchi & Barillot 1982; Bianchi *et al.* 1988). The inspiratory neurones were observed to have either an incrementing or decrementing pattern of discharge (Bianchi & Barillot 1982; Bianchi *et al.* 1988), therefore described as either augmenting or early burst decrementing (Bianchi *et al.* 1988); the expiratory neurones

displayed similar patterns of discharge to the inspiratory neurones, having either, a late augmenting discharge, or occasionally a decrementing discharge (Bianchi & Barillot 1982; Bianchi *et al.* 1988). The location of the Bötzinger neurones conforms well to a discrete region of the medulla similar to the anatomically defined region shown by Kalia, Feldman & Cohen (1979). Antidromic stimulation, to identify the axonal trajectories of the Böt C neurones, identifies a predominantly contralateral projection (Lipski & Merrill 1980, Bianchi & Barillot 1982; Bianchi *et al.* 1988), which at the level of the NTS consists mainly of expiratory axons (Bianchi & Barillot 1982); a less abundant ipsilateral projection is however evident (Bianchi & Barillot 1982) for both inspiratory and expiratory neurones.

Recently, an area lying between the rostral most border of the rVRG, and the caudal most portion of the Bötzinger complex, has been identified as an area of interest, representing a potential site for respiratory rhythmogenesis. This area has been named the pre-Bötzinger complex. This site was initially identified as a potential kernel for the genesis of the respiratory rhythm, by transverse microsectioning the medulla successively in a rostrocaudal sequence (Smith *et al.* 1991). Sectioning at the level of the caudal retrofacial nucleus (in the rat) caused disruption of the respiratory rhythm with the rhythm being completely abolished by further caudal sectioning. Rhythmically discharging (bursting) neurones were identified as potential pacemaker cells in this region (Smith *et al.* 1991; see Rekling & Feldman 1998 for review). The pre-Bötzinger complex has been identified by retrograde transsynaptic transfection of pseudorabies virus, to a region containing a high density of third

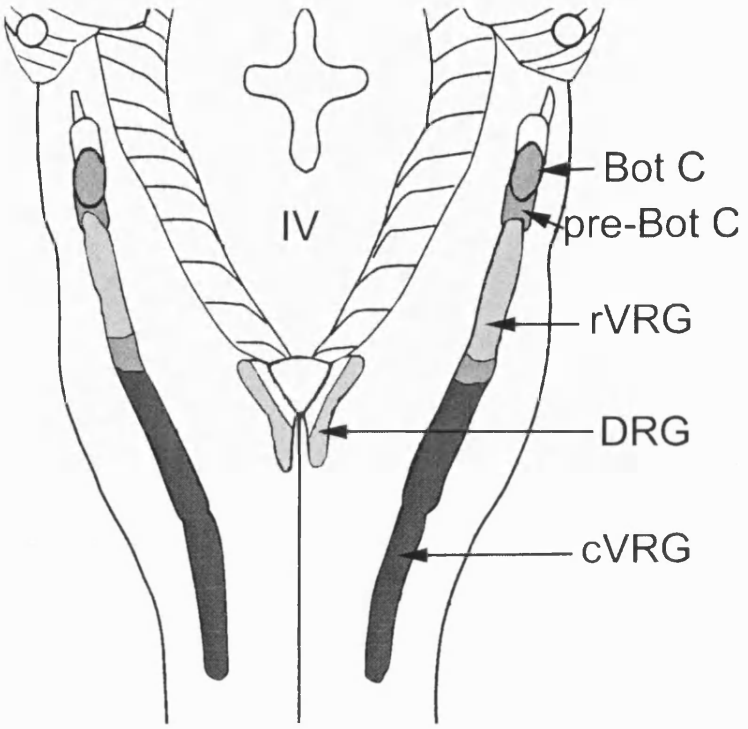

Figure 1.1.1. Schematic of the location of medullary respiratory neurones. ■ Expiratory neurones.
■ Predominantly inspiratory neurones.
■ Inspiratory and expiratory neurones.
VI. Fourth ventricle.

order neurons (Dobbins & Feldman 1994). Hence, as the pre-Böt C contains a high concentration of rhythmically active propriobulbar neurones, for which any perturbation of their function results in a disruption of respiratory function (Rekling & Feldman 1998 for review), the pre-Böt C is regarded as a putative site for respiratory rhythmogenesis.

1.3.1. The Respiratory Motoneurones and the Innervation of the Respiratory Muscles.

It is well established that the respiratory rhythm generator is located within the medulla, and this rhythm generator provides the signal that brings about the contraction of the respiratory muscles. The innervation of these muscles is provided by motoneurones and they can be considered as the first order neurones. The respiratory drive generated by the medullary rhythm generator must thus be transmitted to the motoneurones, this can be achieved in one of two ways; either the respiratory drive can be directly transmitted to the motoneurones by the axons of the medullary neurones, thus providing a monosynaptic input, or, the drive can be transmitted via intervening interneurones, i.e. via a polysynaptic input. Motoneurones with respiratory functions involved in control of the upper airway tract and functioning of some accessory muscles (Cohen 1979) are located in the medulla, receiving their respiratory drive from local circuits. However, motoneurones innervating the principal respiratory muscles, the diaphragm, intercostals and the parasternal muscles are located in the spinal cord and thus must receive a long descending input. The nature and strength of this input to the cervical motoneurone pools

that innervate the diaphragm and the thoracic motoneurone pools that innervate the intercostals and parasternal muscles is of great interest. Demonstrating a direct connection between bulbospinal neurones and motoneurones can be achieved by employing either anatomical or electrophysiological techniques, with only the latter providing direct evidence of the strength of the input (Kirkwood *et al.* 1999 see Appendix). Two principal electrophysiological techniques have been employed to establish the presence of a direct bulbospinal input to motoneurones; cross-correlation (see Kirkwood 1991 for review) and spike-triggered averaging (STA). This will be considered in detail later. Before moving on to a detailed consideration of the transmission of the respiratory drive to motoneurones the location, morphology and firing characteristics of the spinal motoneurones that innervate the respiratory muscles will be considered.

1.3.2 The Phrenic Motoneurones.

Phrenic motoneurones are the neurones that innervate the ipsilateral region of the diaphragm. Intracellular recordings from respiratory phrenic motoneurones that innervate the diaphragm have identified characteristic inspiratory slow potentials and firing patterns (Berger 1979; Jodkowski *et al.* 1987; 1988). The slow potentials have either a ramp of depolarisation or an abrupt onset; similarly, the firing patterns are either augmenting or abrupt onset plateau (Berger 1979; Jodkowski *et al.* 1987; 1988). In an extensive study by Berger (1979) subpopulations of phrenic motoneurones were identified according to the depolarising membrane potential trajectories. Phrenic

motoneurones were thus subdivided into three categories; type A motoneurones; for motoneurones that had a membrane trajectory consisting of two linear components; type B and type A/B motoneurones had non linear membrane trajectories with type B having a slower rate of post-inspiratory hyperpolarisation (Berger 1979). The end of inspiratory depolarisation in phrenic motoneurones is due partly to active inhibition (Berger 1979) as the hyperpolarisation at the end of inspiration can be reversed to a depolarisation by the injection of current as demonstrated by Sears (1964c) in intercostal motoneurones, thus indicating active inhibition.

The phasic activity of phrenic motoneurones is thus due largely to the monosynaptic excitatory input from the inspiratory neurones of the DRG and VRG (see Monteau & Hilaire 1991), with active inhibition occurring during expiration from medullary inhibitory neurones or segmental inhibitory interneurones. Evidence of a monosynaptic crossed input to phrenic motoneurones from the contralateral DRG neurones was obtained by cross-correlation (Cohen *et al.* 1974; Cohen & Feldman 1984; Davies, Kirkwood & Sears 1985a), with a similar input being identified from inspiratory bulbospinal neurones of the VRG (Davies, Kirkwood & Sears 1985a). Subsequently, the strength of the connections was assessed (Davies, Kirkwood & Sears 1985b), and estimated to be inadequate to drive the firing of the motoneurones, representing only 22% of the required input. The inhibitory input is partly derived from the expiratory bulbospinal neurones of the Böt C (Merrill 1982; Merrill & Fedorko 1984) whose axons are evident at the level of the phrenic nucleus, whereas no inputs from the expiratory cVRG have been identified

(Merrill 1982). Alternatively, inhibitory inputs may be derived from the activity of segmental inhibitory interneurones (Kirkwood 1981 *et al*; Iscoe and Duffin 1996).

From retrograde labelling studies the somata of phrenic motoneurones have been found to be located in the ventral most portion of the ventral horn (Rexed's Laminae IX) (Rexed 1954) of the spinal cord, extending from cervical segments C4 to C6 in the cat (Gordon & Richmond 1990), and are distributed within the segment in a unimodal peak (Webber, Wurster & Chung 1979; Berger *et al.* 1984; Gordon & Richmond 1990). These retrograde tracing studies have identified somata of different diameters intermingled throughout the lamina (Webber, Wurster & Chang 1979); although, clusters of neurones have been latterly described (Berger *et al.* 1984; Gordon & Richmond 1990).

The detailed morphology of the phrenic motoneurones has been revealed by intracellular injection of HRP (Cameron, Averill & Berger 1983), and confirmed earlier observations that phrenic motoneurone somata are oval/ellipsoid in nature (Webber, Wurster & Chang 1979) with their major somal diameter orientated in a rostrocaudal direction. Phrenic motoneurones have a mean of 9.7 dendrites (Cameron, Averill & Berger 1985) that project rostrocaudally, often remaining within the phrenic nucleus and projecting dorsally around the edges of the ventral horn, frequently entering the white matter and occasionally crossing the midline (Cameron, Averill & Berger 1983).

1.3.3. The Thoracic Motoneurones.

The second group of motoneurones that innervate the muscles of the thorax are the thoracic motoneurones. The muscles innervated by divisions of the thoracic nerve have been described earlier; however, the principal respiratory muscles innervated by the thoracic motoneurones are the internal intercostals, external intercostals, the parasternal and the levator costae muscles.

The thoracic motoneurones can be further subdivided into categories according to both the branch of the thoracic nerve in which their axons are located and according to the respiratory related activity of the motoneurone. Respiratory thoracic motoneurones whose axons run in the external nerve are exclusively inspiratory (Sears 1964a). The internal nerve contains both inspiratory and expiratory motoneurones. Except for motoneurones innervating the levator costae the respiratory activity of the motoneurones of the dorsal ramus have as yet not been described.

From intracellular recordings in thoracic motoneurones, periodic depolarisations of the membrane potential were described (Eccles, Sears & Shealy 1962; Sears 1964c), that occurred in phase with either inspiration of expiration. An artifactual origin of these fluctuations was excluded and the depolarisations were termed 'slow potentials' (Eccles Sears & Shealy 1962; Sears 1964c). The persistence of these slow potentials in the deafferented

preparation excluded a proprioceptive, origin indicating a central drive acting on the motoneurones. These fluctuations of the membrane were thus termed the central respiratory drive potentials (CRDP) (Eccles Sears & Shealy 1962), as they occurred in phase with either the inspiratory or expiratory respiratory cycle. The origin of the CRDP was concluded to be supraspinal and located in the medulla because CRDPs were never observed in spinalised preparations.

Inspiratory slow potentials were characteristically incremental depolarisations occurring during inspiration as timed by the phrenic nerve discharge, that abruptly repolarise at the end of inspiration. Expiratory slow potentials characteristically had an incremental depolarisation during expiration, abruptly repolarising at the end of expiration. During inspiration there is an incremental hyperpolarisation that was shown to be due to inhibition (Sears 1964c).

Direct evidence of a monosynaptic connection between medullary expiratory neurones was obtained by spike-triggered averaging of the expiratory motoneurone membrane potential (Kirkwood & Sears 1973). By averaging the membrane potential of the motoneurone at a time defined by the discharge of expiratory bulbospinal neurone (Kirkwood & Sears 1973), EPSPs with a fast rise time were revealed, indicating a monosynaptic connection. The strength of this connection was later concluded to be weak, as Lipski & Merrill (1983) who, using STA, identified few EPSPs in expiratory thoracic motoneurones from expiratory bulbospinal neurones. Further evidence for a descending monosynaptic input was provided by cross correlations between

the activity of inspiratory bulbospinal neurones and inspiratory motoneurones (Davies, Kirkwood & Sears 1985a) and expiratory bulbospinal neurones and expiratory motoneurones (Kirkwood 1995). Peaks in the cross correlation histograms were evident that had a narrow half, width suggesting a monosynaptic connection between the bulbospinal units and the motoneurones. The occurrence of these peaks at appropriate latencies calculated from measurements of conduction velocities further supports a monosynaptic connection. The likely strength of expiratory bulbospinal input to thoracic motoneurones will be considered in more detail in the introduction to Chapter 3.

The location of the thoracic motoneurones within the ventral horn has been described electrophysiologically by antidromic mapping and retrograde labelling. The inspiratory motoneurone pools were found to be located medially within the ventral horn (Sears 1964b; Kirkwood *et al.* 1988) with the internal nerve inspiratory motoneurones found more laterally (Lipski & Martin-Body 1987) in the ventral horn; whereas, the motoneurones of the expiratory motoneurone pool were found to be located more diffusely within the ventral horn. The somatopic organisation of thoracic (T8) motoneurones, has been anatomically described for some thoracic motoneurones (Fedorko 1982). The somata of internal intercostal motoneurones, are located laterally in the ventral horn; the somata of the motoneurones of the abdominal oblique branch of the external nerve, located more medially. The somata of the motoneurones contained in the main external intercostal, nerve are located ventrally; the extent of the combined motoneurone subtypes forms a pool extending up to 7.2

mm in the rostrocaudal direction (Fedorko 1982). Similar results have been obtained from retrogradely labelled motoneurones after injection of HRP into the muscle (Larnicol *et al.* 1982); the somata of the motoneurones innervating the intercostals, were found within the segment of the labelled muscle, and the caudal portion of the next rostral segment, with the external nerve motoneurones being located deeper than the internal intercostals.

The detailed anatomy of the thoracic motoneurones has been revealed by intracellular labelling using HRP. Intracellular labelling demonstrated a similar somatopic organisation to that previously described, with the internal nerve inspiratory intercostal motoneurones, located more dorsolaterally to the ventromedially located external nerve inspiratory intercostal motoneurones, with internal expiratory intercostal motoneurones interposed between and overlapping both the other motoneurone fields (Lipski & Martin-Body 1987). Intercostal motoneurones somata of varying morphologies have been described (Lipski & Martin-Body 1987), with the somal dimensions tending to be larger in the rostrocaudal direction than the mediolateral. The somata are predominantly ellipsoid, with no apparent morphological difference between types of motoneurones. Similarly, no difference in dendritic character was noted between motoneuronal types, the dendrites being principally tapered (although microdendrites were seen). The dendrites tended to project into the medial and lateral borders of the ventral horn, failing to penetrate the white matter. Substantial rostral and caudal projections were seen averaging 1.3 and 1.16 mm respectively. For the intercostal motoneurones the axons generally have a somatic origin (Lipski & Martin-Body 1987), with no other major morphological

dissimilarity between types or clear differences in the collateral branching patterns (Lipski & Martin-Body 1987).

1.4.1. The Respiratory Spinal Interneurones.

Many aspects of the control of ventilation have been well defined, even fully characterised; the principal and accessory respiratory muscles have been identified, the location of the site of respiratory rhythm identified, along with the neurones transmitting the respiratory drive to the spinal motoneurones, that innervate the principal respiratory muscles. Consequently, it may appear that further investigation of ventilatory control simply involves more detailed characterisation of these elements. However; disparities exist. One such disparity lies in the strength of the descending bulbospinal input to the cervical and thoracic motoneurones. Several investigators (Sears 1977; Davies, Kirkwood & Sears 1985b; Merrill & Lipski 1987; Kirkwood 1995) have estimated the strength of the connection between respiratory bulbospinal neurones and spinal respiratory motoneurones. In each case these investigators, have concluded that the strength of the bulbospinal connection to the spinal motoneurone is inadequate to drive the firing of the motoneurone in the preparation under investigation. As a result it has been suggested (Davies, Kirkwood & Sears 1985b; Merrill & Lipski 1987; Kirkwood 1995) that the apparent deficit in the input to the motoneurones is compensated for by polysynaptic inputs from segmental interneurones. These interneurones have thus been hypothesised to modulate the function of the respiratory motoneurones and possibly act as a segmental pattern generator, that is

modulated by inputs from the bulbospinal respiratory neurones. These interneurones are probably diverse in nature but there are three distinct populations exist that can be described
separately, these are; cervical interneurones, thoracic interneurones, and finally a well characterised type of interneurone, the Renshaw cell.

1.4.2. Cervical Respiratory Interneurones.

Interneurones with respiratory phased discharge patterns have been identified in the cervical cord and can be divided into two groups; the upper cervical interneurones and the lower cervical interneurones. The upper cervical interneurones lie in segments C1-C3 whereas the lower cervical interneurones lie in C4-C6. Hence, these populations will be dealt with separately.

The upper cervical interneurones were first identified during experiments involving transection of the spinal cord. It was demonstrated that after spinalisation at the rostral boundary of C1 spontaneous respiratory activity could after a recovery period re-establish itself (Aoki *et al.* 1978; 1980). The recovery of the respiratory rhythm in spinalised cats suggested that there was a site for rhythm generation within the spinal cord. Interneurones were likely originators of this rhythm, although alternatively, there may be some respiratory medullary neurones remaining in C1 (Aoki *et al.* 1980). The location of the upper cervical interneurones has been mapped electrophysiologically (Aoki *et al.* 1980; Lipski & Duffin 1987; Duffin & Hoskin 1987) and the upper cervical interneurones were found to form a restricted column extending from the cVRG

to the rostral portion of C3, and are found laterally in lamina VII. The upper cervical interneurones have an inspiratory augmenting discharge pattern (Lipski & Duffin 1987), the onset of discharge commencing just before thoracic inspiratory (external) nerve discharge. The upper cervical interneurones have been shown to have axons that descend ipsilaterally for many segments (Lipski & Duffin 1987; Hoskin, Fedorko & Duffin 1988). In the study of Lipski & Duffin (1987), axons were identified as projecting as far as T10; whereas Hoskin, Fedorko & Duffin (1988) demonstrated that almost all (94%) the upper cervical interneurones project to T9 and that they arborise between T9 and L3. The arborisation of these interneurones was shown in the study of Lipski and Duffin (1987) to be at least partly within the phrenic and intercostal nuclei. Although the presence of collateralisation within a particular nucleus does not indicate connection to the neurones of that nucleus, STA between the interneurones and the motoneurones of that nucleus does. In the study of Lipski and Duffin (1987), STA showed no EPSPs in the cervical cord; however, in the thoracic segments one EPSP was seen in an internal intercostal motoneurone and an external intercostal motoneurone, although, Hoskin, Fedorko & Duffin (1988) identified no PSPs using STA in expiratory intercostal motoneurones. The upper cervical respiratory interneurones are thus a population of inspiratory neurones that are contiguous with the caudal-most boundary of the cVRG (Lipski & Duffin 1987), these neurones project ipsilaterally with a terminal field between T9 and L3; collateralisation is evident within the phrenic and thoracic motor nuclei, although little input is revealed by STA, suggesting that any connections are likely to be on distal dendrites or to segmental interneurones.

A second population of respiratory interneurones within the cervical segments are found in the segments C4-C6. The interneurones of the lower cervical segments have both inspiratory (Bellingham & Lipski 1990) and expiratory patterns of discharge (Bellingham & Lipski 1990; Douse & Duffin 1993). The inspiratory interneurones of the C5 segment were identified as having predominantly an incrementing discharge, that usually stopped abruptly at the end of expiration but occasionally went into post-inspiration; however, some neurones fired tonically during expiration and some post-inspiratory neurones were identified (Bellingham & Lipski 1990). The expiratory interneurones of the C5 segment were identified with either phasic incremental, decremental and constant rates of discharge (Bellingham & Lipski 1990; Douse & Duffin 1993), or with tonic expiratory activity. The C5 respiratory interneurones are located throughout the ventral horn dorsal to the phrenic motor nucleus (Bellingham & Lipski 1990; Douse & Duffin 1993), although there presence within the phrenic motor nucleus cannot be excluded (Bellingham & Lipski 1990). There is no apparent segregation of the interneurones within the ventral horn according to their firing characteristics (Douse & Duffin 1993). Approximately half of the interneurones have been identified as having a descending ipsilateral axon with collaterals extending into the phrenic nucleus (Douse & Duffin 1993); evidence for an connection between the interneurones and the phrenic motoneurones has been achieved using STA, and revealed small IPSPs in 3 phrenic motoneurones (Douse & Duffin 1993).

The cervical segments can be seen to possess two distinct types of interneurones, the upper cervical inspiratory interneurones identified so far

have an ipsilateral descending projection, and the lower cervical respiratory interneurones that have intersegmental ipsilateral projections and diverse firing characteristics. The upper cervical interneurones being contiguous with the cVRG may represent an extension of the neurones of the central respiratory pattern generator into the spinal cord; whereas, the lower cervical interneurones are likely to be propriospinal interneurones involved in segmental pattern generation.

1.4.3. The Thoracic Respiratory Interneurones.

Within the thoracic spinal cord, interneurones with respiratory phasing of their discharge pattern have been identified. These thoracic interneurones exhibit a wide variety of discharge patterns (Kirkwood *et al.* 1988) that are related to respiration and have been divided several categories (Schmid *et al.* 1993). These interneurones can be considered as either inspiratory, expiratory (Kirkwood *et al.* 1988; Schmid *et al.* 1993) or multiphasic (Kirkwood *et al.* 1988) i.e. having a maximal firing rate in both phases of respiration. A more detailed description of the characteristics of the thoracic interneurones will be given in the introduction to Chapter 4.

Electrophysiological characterisation has identified the somata of these neurones to be located in the medial ventral horn (Schmid *et al.* 1993) dorsal to and within the thoracic motor nucleus (Kirkwood *et al.* 1988). A similar somal location has been demonstrated with retrograde HRP Labelling (Schmid *et al.* 1993), where somata of variable morphology were identified with a range of

diameters between 10-30 μm.

From antidromic activation it has been demonstrated that these interneurones have axons that descend both ipsilaterally, contralaterally and on occasion bilaterally (Kirkwood *et al.* 1988). However, the predominant projection is to the contralateral spinal cord, with additional evidence for the predominance of this projection being given by retrograde Labelling with HRP (Schmid *et al.* 1993). Little data regarding the extent of a rostral projection is available, although such a projection has been demonstrated for one neurone (Kirkwood *et al.* 1988). Many of the axons of these interneurones have been identified to run in the ventral funiculus (Kirkwood *et al.* 1988) and give off collaterals that project dorsally through the ventral horn. Further evidence of collateralisation within the ventral horn has been obtained from STA of extracellularly recorded signals (Schmid *et al.* 1993; Kirkwood *et al.* 1993). Spike-triggered averaging revealed terminal potentials (TPs) associated with action potentials within the collateral. Focal synaptic potentials (FSPs) were also frequently seen to follow the terminal potential at a latency appropriate for one synaptic delay. These FSPs were of positive- or negative-going and thought to be due to inhibitory and excitatory post synaptic currents respectively. Further interpretation of the physiological characteristics of this group of interneurones will be dealt with in greater detail in the introduction to Chapter 4.

1.4.4. The Renshaw Cell.

The first identified interneurone in the spinal cord was the Renshaw cell; consequently this class of interneurone has been very well characterised, principally in the lumbar segments. Latterly Renshaw cell have been identified within the cervical, thoracic and sacral segments of the spinal cord, although they have been best characterised in the lumbar cord; hence, in the following the Renshaw cell will be described principally in terms of data gathered in the lumbar cord with a more thorough consideration given the Renshaw cell in the introduction to Chapter 5.

It was observed that antidromic stimulation of the efferent nerves of one segment decreased the frequency of discharge of motoneurones in the adjacent segment (Renshaw 1941). This decrease in discharge frequency was postulated to be due to inhibition of motoneurones by interneurones within the spinal cord. Supporting evidence for this hypothesis was first obtained when action potentials of interneurones were recorded in response to antidromic stimulation of motoneurone axons (Renshaw 1946). Intracellular recording in motoneurones identified IPSPs in the motoneurones in response to antidromic stimulation (Eccles, Fatt & Koketsu 1954) with appropriate characteristics to be mediated by the interneurones previously described in the studies of Renshaw (1941; 1946). The inhibition has become known as recurrent inhibition (Eccles, Fatt & Koketsu 1954). Pharmacological investigation of Renshaw cells has indicated that they receive a cholinergic input from the motoneurone collaterals

and that the inhibitory transmitters they release is glycine (Eccles Fatt & Koketsu 1954) and GABA (Cullheim & Kellerth 1981).

The first intracellular Labelling of Renshaw cells was achieved with Procion yellow (Jankowska & Lindström 1971), revealing small neurones lying at the ventromedial edge of the ventral horn. Subsequent intracellular labelling with HRP (Largerbäck & Kellerth 1985; Van Keulen 1979; Fyffe 1990) confirmed the location of Renshaw cell somata within the ventral horn, with the somata having a range of somal morphologies. The dendrites of the Renshaw cell project throughout the ventral horn. The axons of the Renshaw cells were shown to run in the ventral funiculus rostrally, caudally or bidirectionally, periodically giving off collaterals possessing *en passant* and *terminaux* boutons and arbourising within the ventral horn (Largerbäck & Kellerth 1985; Fyffe 1990).

1.5.1. Further Research.

The objective of the study described below was to further characterise the respiratory system of the thoracic spinal cord, using both physiological and anatomical techniques in the anaesthetised cat.

Firstly, for both thoracic motoneurones and interneurones their respiratory modulation is described from intracellular recordings, which were also used in conjunction with the technique of spike-triggered averaging so as to identify any direct connections between expiratory bulbospinal neurones and

either motoneurones or interneurones.

Secondly, penetrated interneurones including Renshaw cells were iontophoretically filled with Neurobiotin to enable staining of the individual interneurone, allowing detailed morphological characterisation. For selected interneurones the terminal field was stained for inhibitory neurotransmitters and examined under the confocal microscope.

These data provide detailed information regarding the strength of descending expiratory drive to neurones of the thoracic cord, along with detailed morphological characterisation of thoracic interneurones and identification of their neurotransmitters.

Chapter 2. Methods.

2.1.1. Preparation.

The experiments were performed on adult cats of either sex, weighing between 2.2 and 3.7 kg, under sodium pentobarbitone anaesthesia (Sagatal), initially 38 mg kg^{-1} intraperitoneal, supplemented intravenously as required. Anaesthesia was assessed by response to a noxious pinch of the forepaw and considered satisfactory if only a minimal limb withdrawal was evident; alternatively, in the paralysed animal, if only minimal changes in either blood pressure or respiratory discharge patterns were observed.

The femoral artery was cannulated to permit blood pressure monitoring and the femoral vein was cannulated bilaterally, for administration of drugs and fluids as required. A tracheotomy was performed and a Y-piece inserted into the trachea to permit artificial ventilation; a bilateral vagotomy was performed. A midline incision was made over the thoracic spine, latissimus dorsi was bilaterally dissected free and attached to the skin to form flaps used later for the construction of a paraffin oil pool. The longissimus dorsi muscle was removed over the segments of interest and a bundle of dorsal ramus nerves dissected free from one or two adjacent segments (T5-T8). The branches of the dorsal ramus nerve prepared for recording were; the posterior branch of the dorsal ramus (Sears 1964a) and an anterior branch of the dorsal ramus innervating iliocostalis. These nerves and some of the muscles they innervate are classified

according to their respiratory activity are illustrated in Figure 2.1.1; from here on the bundle of dorsal ramus nerves will be referred to as the dorsal ramus nerve. The internal and external intercostal nerves (Sears 1964a) of the same two adjacent segments were dissected free and prepared for recording or stimulation. The animals were mounted prone via clamps attached to the vertebrae at T4, T10 and the iliac crest with side clamps at the level of the laminectomy. The head was fixed by a plate screwed to the cranium and the head slightly ventroflexed. A laminectomy was performed usually between T5-T10 and the dura mater reflected. Small areas of the pia mater were then dissected away over the dorsal columns of T5-T8 and a pressure plate applied over this area to stabilise the cord. In some experiments the dorsal roots were sectioned in one segment. A pool was constructed from the dorsal skin flaps and filled with paraffin oil to prevent evaporation and hence damage to the tissue. Bilateral pneumothoraces were performed to minimise movements related to the ventilatory pump.

An occipital craniotomy was performed, the dura reflected and small patches of the pia removed from a site approximately 2.5 mm lateral and 2.5 mm caudal to the obex on the right side overlying the nucleus retroambiguus. A pressure plate was then applied to the medulla around the pial holes to aid stability.

The animal was paralysed with gallamine triethiodide (Flaxedil) and ventilated with O_2 enriched air as to produce an end-tidal CO_2 of around 4 %. In order to stimulate a powerful respiratory drive CO_2 was added to the air and an

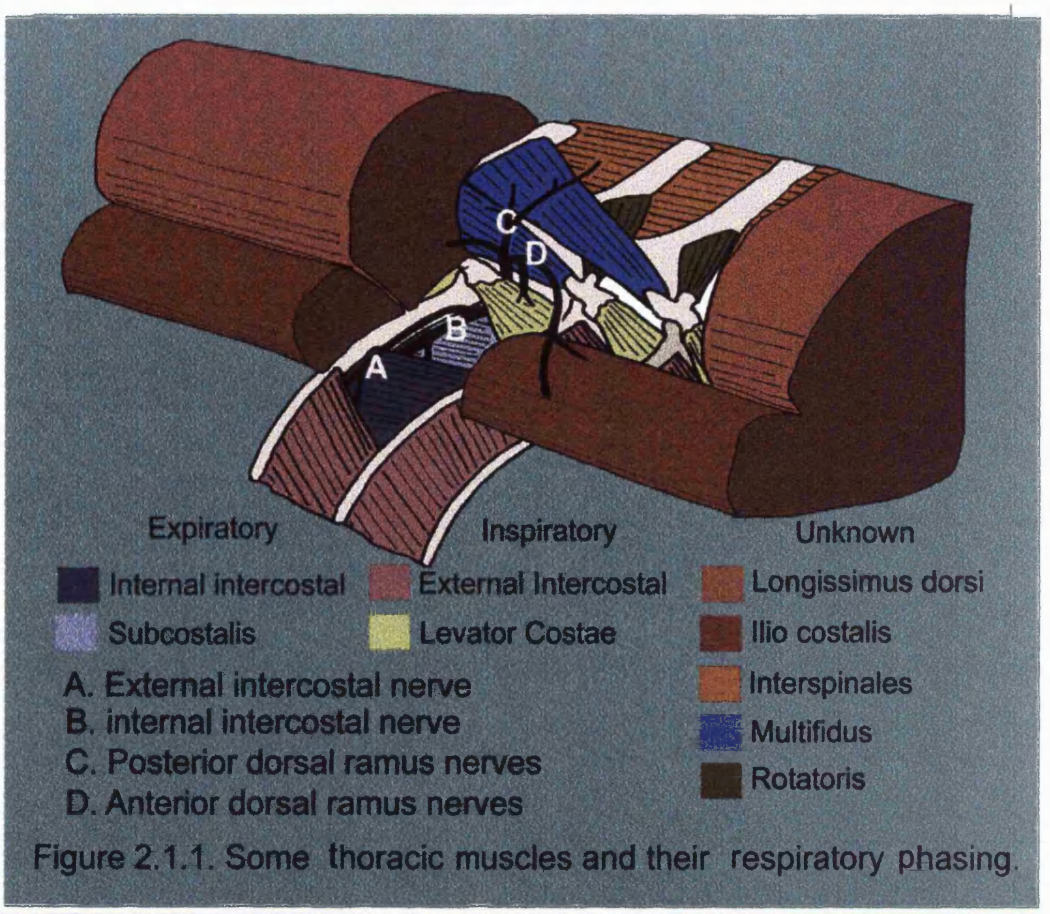

Figure 2.1.1. Some thoracic muscles and their respiratory phasing.

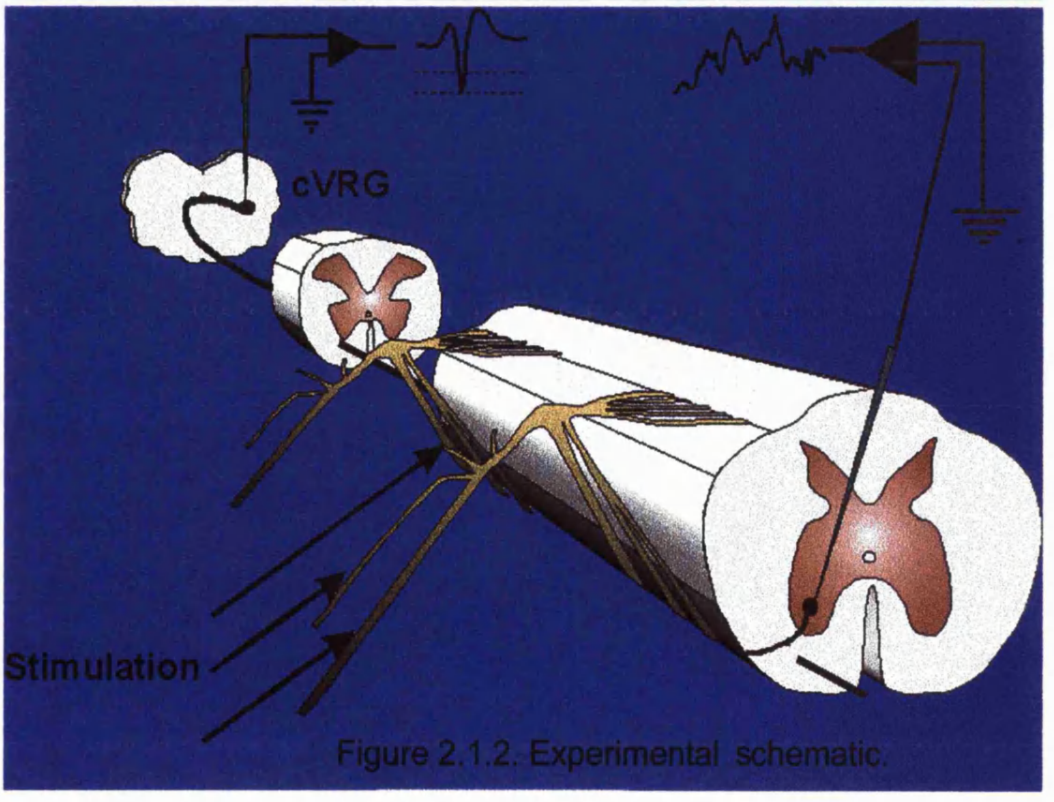

Figure 2.1.2. Experimental schematic.

end tidal CO_2 around 6-7 % was maintained. The core temperature was assessed via a rectal probe and maintained at 37 °C by a heating blanket. In the event of hypotension (mean B.P. <80 mmHg) either dextran was infused or noradrenaline administered to restore the blood pressure. The bladder was emptied manually as required.

2.2.1. Physiological Methods.

2.2.2. Stimulation and Recording.

The dorsal ramus, internal and external nerves were mounted on bipolar platinum wire electrodes for stimulation (7-10 Hz, pulse duration 0.1 ms, at five times threshold (T)) to antidromically activate motoneurones within the segment under investigation, threshold (T) being defined from the afferent volley recorded from an electrode placed on the cord dorsum. The external nerve of the adjacent segment was also mounted on bipolar platinum electrodes to record the inspiratory discharge of the nerve and hence define the inspiratory cycle. The signal from the medullary and the external nerve electrodes were band-pass filtered, with a bandwidth usually of 3 KHz and 300 KHz.

An array of four insulated stainless steel stimulating electrodes was advanced into the cord in the most caudal exposed segment to a depth of approximately 3.5 mm. This arrangement permitted stimulation of the caudal spinal cord to allow identification of units with descending axons on either side.

An electrode (either a glass microelecrode containing 3 M sodium chloride, with a tip broken back to 3-3.2 μm, or an insulated platinum coated microelectrode (Ford, McWilliam, & Shepheard 1986) was inserted into the medulla to a depth of approximately 1.5-2.5 mm where it was used to record expiratory units located in the nucleus retroambiguus. A glass microelectrode containing 2-4 % Neurobiotin in either 0.01 M Tris buffer with 0.5 M KCl or 0.5 M potassium acetate was used as an intracellular electrode in the spinal cord. Potassium acetate was used to eliminate chloride leakage. The tip of the electrode was ground at an angle of 20° and to a impedance between 20-45 MΩ. The electrode was advanced into the cord through a hole in the thoracic pressure plate at an angle of 15° to the vertical (Kirkwood *et al.* 1988). In each segment, before intracellular recordings were attempted with the Neurobiotin filled microelectrode, a series of penetrations were made across the width of the ventral horn at 100 μm intervals using a microelectrode containing 3 M potassium acetate; this allowed mapping of the antidromic motoneurone field potentials to act as reference points (Kirkwood *et al.* 1988) and to define the width and position of the ventral horn.

2.2.3. Unit Identification and Selection Criteria.

Medullary units were selected for investigation if they displayed a clear expiratory phasing with a maximal discharge frequency >30 Hz. A bulbospinal projection of these neurones was identified by invasion of an antidromically stimulated action potential (AP) into the soma. The neurones that had a sharp threshold and relatively constant latency were then tested for collision of the

orthodromic and antidromic APs, collision resulting in annihilation of the antidromic AP; this test was performed at twice the axonal threshold, with the critical interval (CI) defined as the interval shorter than which the antidromic spike was blocked. The interval at which this collision occurs (measured to within 0.05 ms) was used to estimate the conduction velocity and to provide a latency criterion in the acceptance for EPSPs seen in the segment of interest as being monosynaptic, similar to that in Davies *et al.* (1985a), with the procedure used here being justified in Kirkwood (1995).

If a critical interval could not be observed the neurones were not used for STA. For neurones that demonstrated a critical interval, antidromic activation was tested by the addition of a second stimulus (double shock), to confirm collision; i.e. that the CI was not due to soma being refractory (modification of Swadlow 1982). No values for the CI were found to be the result of a refractory soma.

All medullary units used in STA were identified as expiratory neurones, with an axon projecting through the segment at which the STA was to be performed, and for these neurones accurate estimates of their conduction velocity could be made.

The Neurobiotin containing electrode was advanced into the cord to a depth of approximately 2 mm where upon it was advanced in 2 μm steps in order to obtain intracellular penetrations of neurones. The criteria for identification of a motoneurone was invasion of an antidromic action potential from stimulation of the peripheral nerves. Interneurones were identified

according to a hierarchy of criteria; the inability to antidromically activate the neurones from the peripheral nerves, the ability to antidromically activate the neurones from the caudal stimulating electrode, their firing rate and their depth. In experiments where the dorsal roots were sectioned, Renshaw cells were identified by the presence of a recurrent EPSP, and their characteristic firing. In one experiment where the dorsal roots remained intact one Renshaw cells was identified by its firing characteristics alone.

2.2.4. Data Acquisition.

A total of eight data channels were recorded on magnetic tape. These input channels were; a voice channel, a timing marker channel for the stimulators, an external intercostal nerve recording, the cord dorsum volley, the microelectrode DC channel (20 mV/V), microelectrode AC channel (1mV/V, high-pass filtered, 50 ms time constant), the discharges of the medullary unit and the microelectrode current. The signals of interest were fed into a CED 1401 analogue to digital converter on- or off-line. All analysis was performed using CED Sigavg or CED Spike 2 software.

2.2.5. Spike-Triggered Averaging.

When stable intracellular penetrations were achieved in motoneurones with a membrane potential of $\leq$ -40 mV the synaptic noise was averaged from the high-pass filtered membrane potential recording using the spike of the expiratory bulbospinal unit as the trigger. The criteria of at least a -40 mV

membrane potential is an arbitrary one, but it is felt that in neurones with lower membrane potentials the neurone may be too depolarised to identify any EPSPs and would thus introduce false negatives in the determination of the degree of connectivity. Averages were constructed with a 15 ms duration and with an offset of 5 ms from the trigger spike. The minimum number of sweeps used to construct an average was 1024.

Figure 2.2.1 shows a schematic diagram of the experimental set up.

2.2.6. Neuronal Labelling.

Interneurones were selected for intracellular labelling on the basis of their firing characteristics, slow potentials, size of their membrane potential and the stability of the penetration. If the membrane potential was less than -30 mV or the penetration was not unequivocally intracellular the neurone was not injected.

The interneurones were filled with Neurobiotin by application of positive current pulses of 600 ms cycle duration at a frequency of 1 Hz. A filling period of 50 nA.mins was attempted, and in very stable penetrations longer filling periods were used. After a survival period of 1-8 hrs the animal was given heparin and sacrificed by overdose of anaesthetic prior to transcardially perfusion with 1.5 l of 0.01 M phosphate buffered saline (PBS) followed by 3 l of 4 % paraformaldehyde. The relevant segments of the spinal cord were then dissected free and stored overnight in fixative or PBS.

2.3.1. Anatomical Methods.

2.3.2. Tissue Preparation.

For the segment containing the injected interneurone and the adjacent segments, the dura, arachnoid and pia mater were removed from the cord along with the spinal roots. Sections were then cut in either the transverse or parasagittal plane, at a thickness of between 30-70 μm; sections were cut on either a Vibratome of a freezing microtome. For sections cut on a freezing microtome the tissue was stored overnight in a 20 % sucrose solution in PBS or fixative prior to sectioning. The sections, kept serially in two series of alternate sections, were left to soak overnight in 0.1 M PBS containing 3 % Triton-X100 (PBST) at 4°C.

The first series was then incubated in either avidin-HRP (Sigma) or ABC Elite (Vector) in PBST for between 5 and 48 hours. After six rinses in Tris buffer (pH 7.6), the sections were reacted with diaminobenzidine (DAB), nickel ammonium sulphate and hydrogen peroxide in Tris buffer to reveal the labelled neurone and its processes. The progression of the reaction was followed by viewing the sections under a dissecting microscope. Once a well-stained neurone was identified the reaction was terminated by serial washes in cold Tris buffer; alternately, if excessive background staining became evident the reaction was terminated. The reacted sections were mounted in glycerol and examined under the microscope to identify sections containing the soma or any evidence of a terminal field. For sections in which collaterals and boutons were

evident the orientation of the projection in the section was determined as to decide in which adjacent unreacted section further portions of the terminal field were likely to be found. These selected unreacted sections were then set aside for immunohistochemical processing. The remaining sections were processed in an identical fashion to the first batch of sections.

The sections were mounted on gelatinised slides and air dried for at least 24 hours. They were counterstained with neutral red (1 % solution), serially dehydrated through acetone and cleared in xylene. The slides were then coated with DePeX mounting medium and coverslipped.

2.3.3. Immunohistochemistry.

The unreacted sections containing the presumed terminal field were reacted with antibodies to GAD and gephyrin in Dr A.Todds laboratory (Glasgow), and processed for examination under the confocal microscope according to the following protocol.

The sections were incubated overnight in a cocktail of primary antibodies, the antibodies were; sheep anti-GAD (gift of Dr W.R.Oertel) diluted 1:600, plus mouse monoclonal antibody 7a (Boehringer) directed against gephyrin, diluted 1:100 in PBS containing 0.3% Triton X-100. The sections were then rinsed and incubated in a cocktail of secondary antibodies plus avidin-FITC (fluorescein isothiocyanate) overnight. This consisted of anti-mouse IgG conjugated to LRSC (lissamine rhodamine) and anti-goat IgG

conjugated to Cy5 (cyanine 5.18). Both antibodies were from Jackson Immunoresearch, and diluted 1:100 in PBS with 0.3% Triton. The cocktail also included avidin conjugated to FITC from Jackson diluted 1:1000. The sections were then rinsed and mounted on glass slides with glycerol-based mounting medium (Vectashield, Vector Laboratories), containing an anti-fade reagent to minimise bleaching of the fluorescent dyes. This process results in the axon being labelled with FITC, gephyrin with LRSC and GAD with Cy5. The sections were then viewed under a confocal microscope.

2.3.3. Reconstruction and Measurement.

The labelled neurones were examined under a microscope. The morphologies of the neurones and their terminal fields, were reconstructed via drawing tube using a 40x objective. The dimensions of the soma, dendrites, axon and boutons were estimated as follows; for the soma an ellipse was drawn within the soma and the minimum and maximum diameters measured, the mean diameter was calculated according to the equation; major soma diameter + minor soma diameter/2 (Ulfhake & Kellerth 1983), the diameter of the dendrites was measured at a distance of 30 µm from the soma where the dendritic diameter is constant, proximal to the first branch point. However, the dendrite was measured closer to the soma if the dendrite branched close to the soma. The axon diameter was also measured 30 µm from the soma. Structures were considered to be boutons if they were swellings in the collateral branch of greater than 3 times the diameter of the collateral branch, the dimensions of

these presumed boutons were the maximum diameter of the swelling.

Chapter 3. The Thoracic Motoneurones.

3.1.1. Introduction.

The thoracic motoneurone is a site of convergence of many inputs (Aminoff & Sears 1971). Not only have inputs been demonstrated from peripheral afferent fibres (Sears 1964a), but also, bulbospinal (Kirkwood & Sears 1973) and propriospinal inputs (Kirkwood, Sears & Westgaard 1981). Inputs to the motoneurones can be inhibitory, as in recurrent inhibition (Kirkwood, Sears & Westgaard 1981) or excitatory as is the case for bulbospinal inputs (Kirkwood & Sears 1973). Once the inputs to the motoneurones have been identified, the remaining challenge is to assess the strengths of the inputs in order to either estimate the contribution of the input to driving motoneurone discharge, as is the case with excitatory inputs, or to assess the contribution to the modulation of the firing pattern of the motoneurone, as may be the case for inhibitory inputs, for instance those of the Renshaw cells.

The respiratory system is an ideal system in which to study the strengths of descending connections. Under conditions of light pentobarbitone anaesthesia and in preparations that have had the cerebrum removed, the respiratory bulbospinal neurones of the DRG and VRG continue to discharge in a stereotypical pattern, thus co-ordinating and contributing to the generation and output of a respiratory pattern that is transmitted via the phrenic and thoracic motoneurones to the muscles of the thorax and abdomen. The

strength of this connection to the motoneurones and interneurones of the spinal cord can then be assessed indirectly by cross-correlation (Kirkwood & Sears 1991) or directly by STA (Kirkwood & Sears 1973). Due to the persistence of this respiratory pattern under these experimental conditions the respiratory system has become a widely studied system for investigation of neuronal connectivity and motor control.

Descending inputs to the phrenic (Merrill, Lipski, Kubin & Fedorko 1983; Lipski, Kubin & Jodkowski 1983) and thoracic motoneurones from respiratory bulbospinal neurones have been identified (Kirkwood & Sears 1973). However, little data is available regarding descending inputs to interneurones and identification of such inputs are of significance in determining the likely origin of their respiratory phasing (Kirkwood *et al.* 1988). Estimation of the size of this input is also of significance due to the apparent inadequacy of the bulbospinal connection to motoneurones to drive their discharge (Davies *et al.* 1985; Merrill & Lipski 1987). Direct assessment of the strength of any bulbospinal input to interneurones will require STA and any input to the interneurones needs to be compared to similar inputs to motoneurones.

A factor that may have resulted in an under-estimation of bulbospinal input to intercostal motoneurones may be a spatial restriction of the bulbospinal axon collaterals to the rostral portion of the segment as suggested by Kirkwood (1995) (see also Kirkwood *et al.* 1999). Consequently reappraisal of the bulbospinal input to thoracic motoneurones is necessary. The data gathered from STA in motoneurones will also act as comparative data in interneurones.

3.1.2. Descending Bulbospinal Inputs to the Respiratory Neurones of the Spinal Cord: Identification and Assessment of Input Strength.

The respiratory neurones in the medulla are known from anatomical studies to project not only to the cervical cord (Feldman, Loewy & Speck 1985; Ellenberger & Feldman 1988) but also to the thoracic (Rickard-Bell, Bystrzycka & Nail 1985; Yates *et al.*1999), the lumbar and sacral cord (Vander Horst & Holstege 1995). However, these studies do not provide data on the strength of the connection (Kirkwood *et al.* 1999), the strength of the connection can only be estimated using physiological methods of cross-correlation and STA.

A monosynaptic connection between expiratory bulbospinal neurones and thoracic motoneurones was demonstrated by Kirkwood and Sears (1973). This connection was identified by spike-triggered averaging of the motoneurone synaptic noise to reveal an EPSP with a latency and rise time appropriate for a monosynaptic connection (Kirkwood and Sears 1973). The observation of a direct connection between bulbospinal neurone and motoneurones proved the existence of a descending input to thoracic motoneurones but did not quantify the size of the connection. Further studies examining the connectivity of expiratory bulbospinal neurones and thoracic motoneurones (Merrill & Lipski 1987) using STA failed to identify abundant connections. For expiratory bulbospinal motoneurone pairs, monosynaptic EPSPs were identified in only 2/57 pairs, indicating little direct connectivity (~4%), and it was concluded that the respiratory drive was transmitted to the motoneurones via segmental

interneurones.

Evidence of connections between expiratory bulbospinal neurones and internal nerve motoneurones have been examined (Cohen, Feldman & Sommer 1985; Davies *et al.* 1985a,b; Kirkwood 1995) using cross-correlation. The resultant cross-correlations suggested that the mean size of the EPSP would be 22 μV. If account is taken of crossing ipsilateral collaterals of the expiratory bulbospinal neurones, it was suggested (Kirkwood 1995) that up to ~66% of the input to expiratory motoneurones to drive their discharge is derived from the bulbospinal input. Connectivity between expiratory bulbospinal neurones and thoracic motoneurones has thus been identified in several studies. However, there are discrepancies as to the significance of the connection as studies using cross-correlation indicate a much stronger connection than those using STA. It is thus of interest how these discrepancies could be accounted for. Using STA to average extracellular terminal and focal synaptic potentials (Kirkwood 1995) identified a non-uniform projection of bulbospinal collaterals within the segment, with a stronger projection in the rostral portion of the segment. Discrepancies in the measurement of the strength of bulbospinal motoneurone connections thus may arise from a spatial restriction in the projection of bulbospinal collaterals (Kirkwood 1995).

Reinvestigation of expiratory bulbospinal inputs to thoracic motoneurones is of importance for several reasons; firstly it will allow resolution of the discrepancies between cross-correlation and STA data, secondly it will allow comparison of the strength of input to motoneurones compared with that

to interneurones, and finally the data will act as control data for reorganisational changes of descending axons in lesion studies (Ford *et al.* 1997). In the current study the rostral portion of the thoracic segments will be surveyed as this is the region of the segment that is thought to have the greatest density of bulbospinal projections.

3.2.1. Results.

3.2.2. Expiratory Bulbospinal Neurone Identification.

A total of 30 bulbospinal units of the cVRG with clear expiratory phased discharge patterns, were used for STA in motoneurones and interneurones (see Chapter 4). Typical example of the firing characteristics are shown in Figure 3.2.1 and 3.2.5 where each expiratory unit can be seen to fire spikes with an incremental frequency, terminating abruptly before the onset of inspiration, as timed by the onset of discharges in the external nerve. An averaged expiratory bulbospinal action potential, recorded at the level of the soma is shown in Figure 3.2.6. In order to confirm that the discriminator levels were set at appropriate points to exclude contamination of the trigger spikes by other nearby units, an inter-stimulus interval histogram (ISIH) was always constructed. The absence of short interval spikes in the ISIH was considered to indicate a well discriminated single unit signal. An example of such a ISIH is shown in Figure 3.2.1 and Figure 3.2.2.B ii. From measurements of the distance between the medullary electrode, the spinal stimulating electrodes, and the critical interval the axonal conduction velocities were calculated,

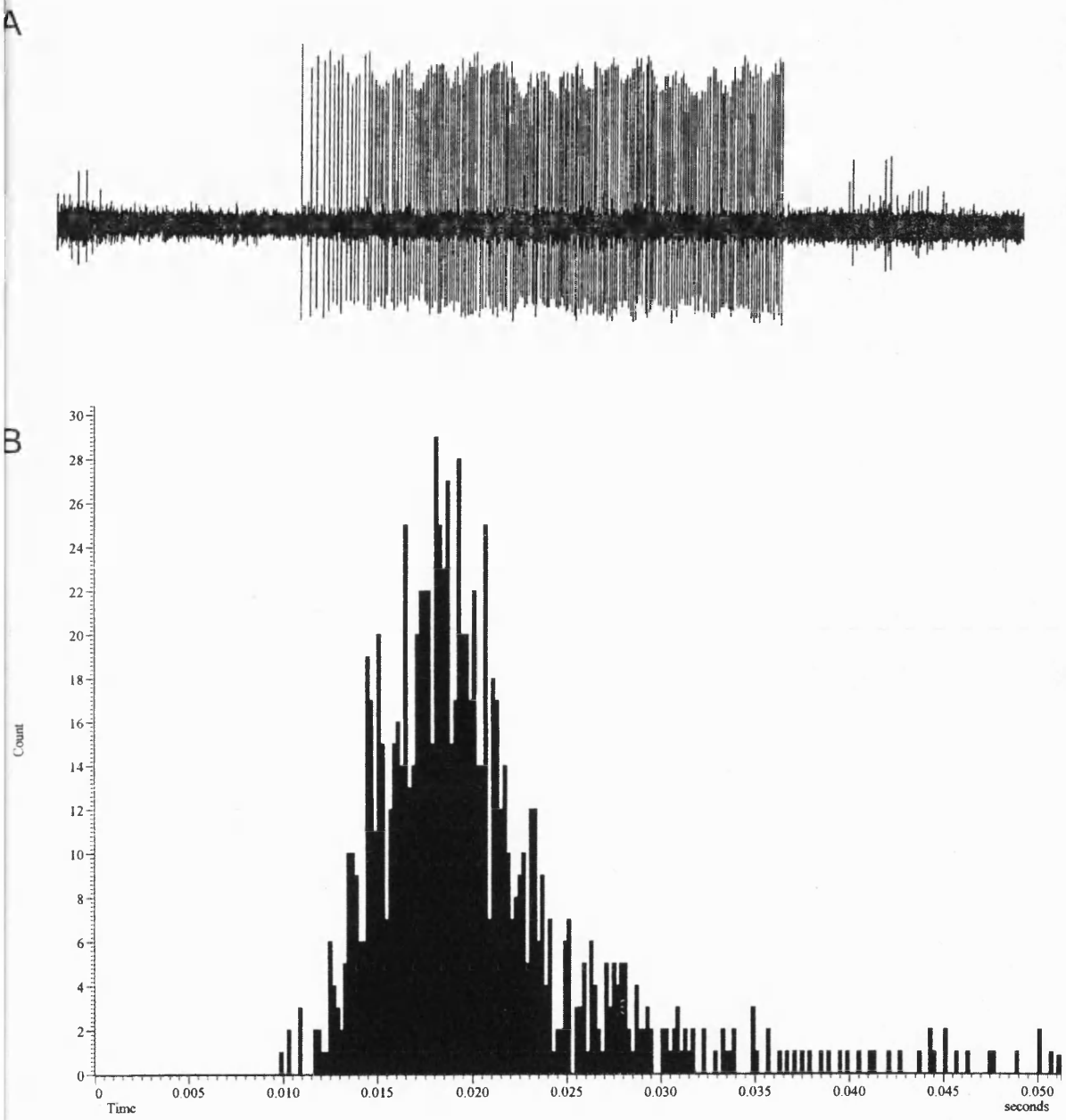

Figure 3.2.1. Example of medullary neurone firing pattern.
A. Extracellular action potentials during expiration.
B. Interspike interval histogram for the action potentials.

with 0.35 ms representing axonal refractory period and the delay in triggering the average from the onset of the bulbospinal AP being subtracted from the critical interval (see Kirkwood 1995). The mean conduction velocity was calculated to be 63.4 ± 16.2 m/s (± SD), the range of values are shown in Figure 3.2.2.A.

3.2.3. Segmental Latencies and EPSP Identification Criteria.

In order to confirm the identity of any averaged potential as an EPSP certain criteria must be satisfied to exclude the potential as being artifactual. The criteria that will help positively identify an EPSP include the latency of the potential, the rise time, the repeatability of the measurement with reference to the number of sweeps used to construct the average.

When identifying a potential the most important consideration is the repeatability of the measurement as if a potential cannot be identified in successive averages it cannot be considered to be genuinely related to the trigger.

The expected time of arrival of an EPSP from a EBSN in a motoneurone is an important consideration in identifying EPSPs, as any potential that occurs earlier than the expected latency can be excluded as being an EPSP arising from the EBSN as it could not arise at a time earlier than the calculated latency.

However EPSPs must arrive at a longer latency than that calculated from antidromic activation, this being due to a number of factors including slowing of

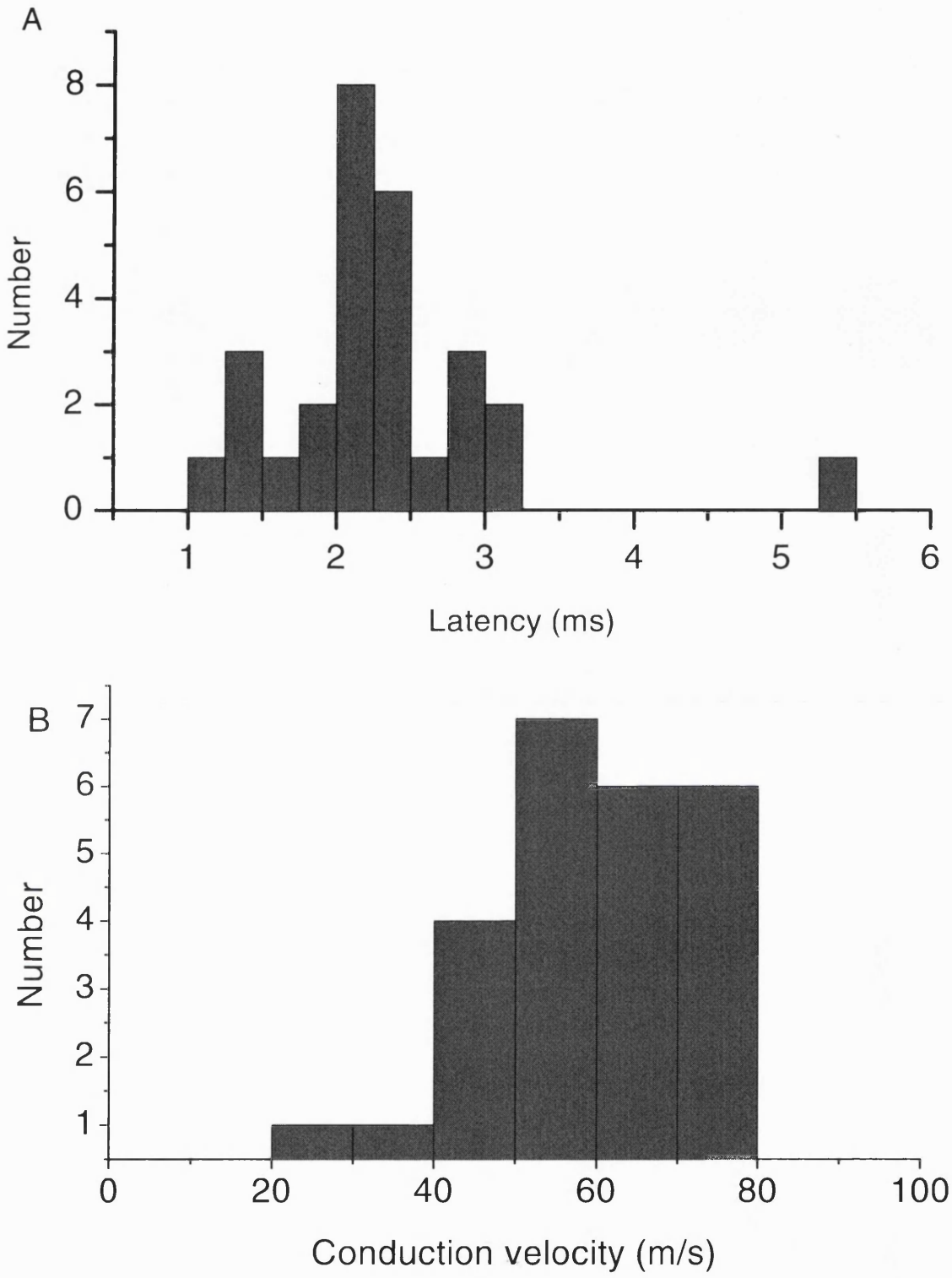

Figure 3.2.2. Bulbospinal neurone latancies and conduction velocities. A. Distribution of the calculated latencies. B. Distribution of the calculated axonal conduction velocities.

the conduction velocity in the collateral branch, and synaptic delay. For each EBSN the minimum latency at which any EPSP would be expected to be seen was estimated from the conduction velocity and the distance between the medulla and the segment under investigation and found to be between 1.1 and 5.4 ms. The distribution of the latencies are shown in Figure 3.2.2.A. For individual potentials thought to be EPSPs the calculated latency was subtracted from the time of onset of the potential to calculate the segmental latency (indicating the conduction delay within the segment). If the segmental latency was negative the potential could not have arised from the EBSN. Allowing for possible errors (0.2 ms) a minimum segmental latency of 0.1 ms was considered necessary to allow for a synaptic delay of 0.3 ms and terminal slowing. The calculated segmental latencies for all the identified EPSPs were in the range of 0.3 to 4.2 ms.

The rise time of the potential is defined as the time taken for the EPSP to rise from 10 to 90% of its value. The rise time is important in identifying that the potential is not due to any form of synchrony.

The number of sweeps used to construct an average is also of importance in identifying potentials as EPSPs above background synaptic noise, because as the number of sweeps increases the background noise will be averaged out allowing identification of smaller potentials.

3.2.4. Motoneurone Firing Patterns and Slow Potentials.

Intracellular recordings were made from motoneurones located in the rostral portion of the spinal cord where the predominant bulbospinal projection is thought to be, in segments T5-T9. The penetrated motoneurones were identified as having axons in the external, internal or dorsal ramus nerves. Motoneurones that had a membrane potential of less than -40 mV no further analysis is carried out here. The membrane potential of the motoneurones studied ranged from -40 to -84 mV (53.9 ± 11.9 mV, mean & SD, n=112) no significant differences were seen between the membrane potential of the groups of motoneurones. A total of 101 motoneurones with axons projecting into one of the three thoracic nerves were thus identified and classified according to respiratory modulation of membrane potential. Motoneurones were consequently classified into three groups inspiratory, expiratory and non-respiratory.

A total of 42 motoneurones were identified as inspiratory, examples of which are shown in Figure 3.2.3. and Figure 3.2.4. An internal nerve motoneurone is shown in Figure 3.2.3. and has an incremental inspiratory slow potential with spikes in late inspiration that abruptly stop at the end of inspiration. The example shown in Figure 3.2.4. is an external nerve motoneurone and has a 5 mV inspiratory slow potential. For the inspiratory motoneurones a total of 9 had axons projecting into the external, 19 into the internal and 14 into the dorsal ramus nerve. A total of 50 expiratory

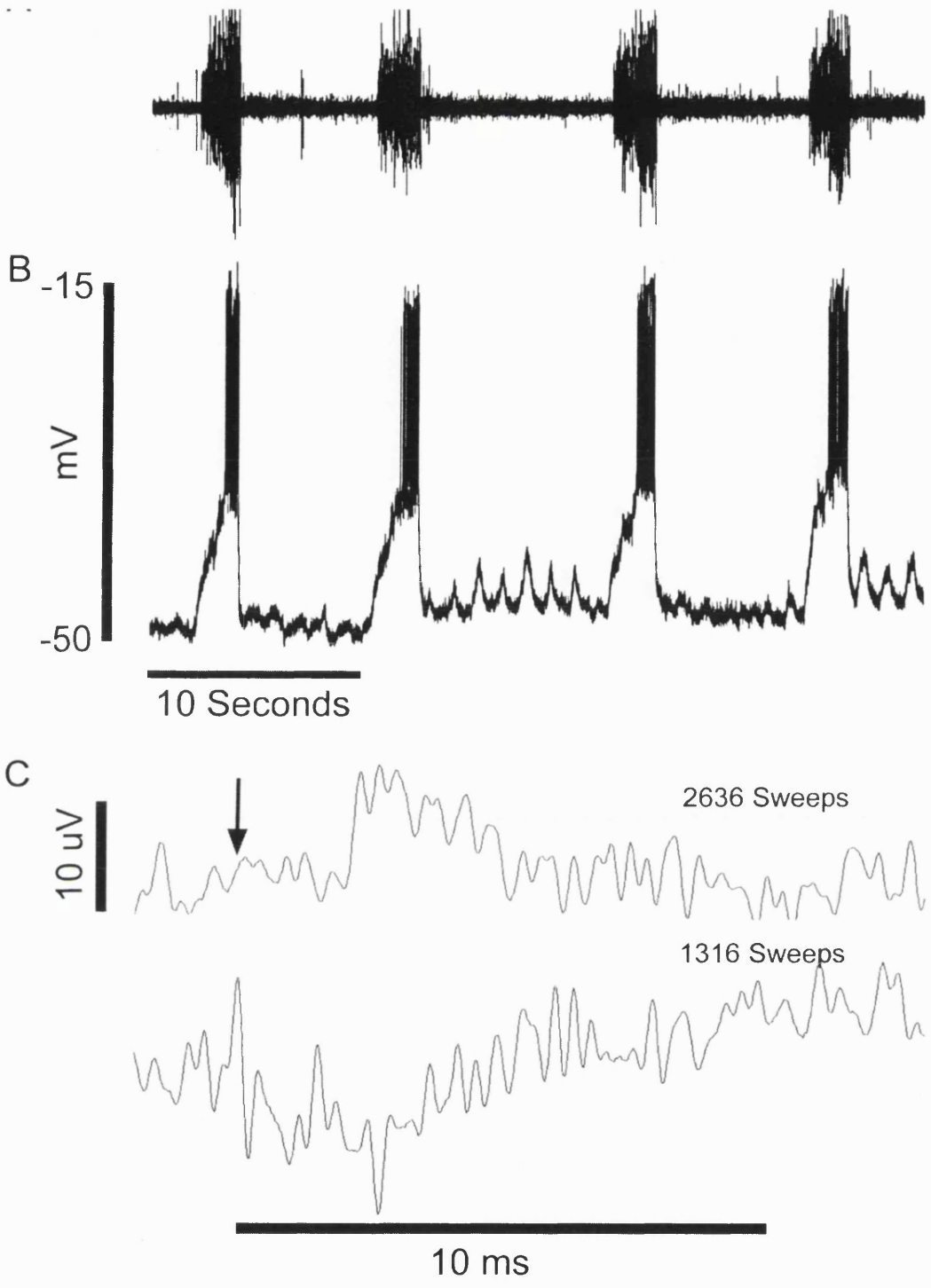

Figure 3.2.3. Intracellular recording from an external nerve motoneurone with an inspiratory CDRP.
A. External nerve discharge used to define inspiration.
B. Intracellular motoneurone recording.
C. Spike-triggered average of the intracellular recording (upper trace) showing the presence of an EPSP, and of the extracellular recording(lower trace). Arrow indicates time of bulbospinal unit discharge.

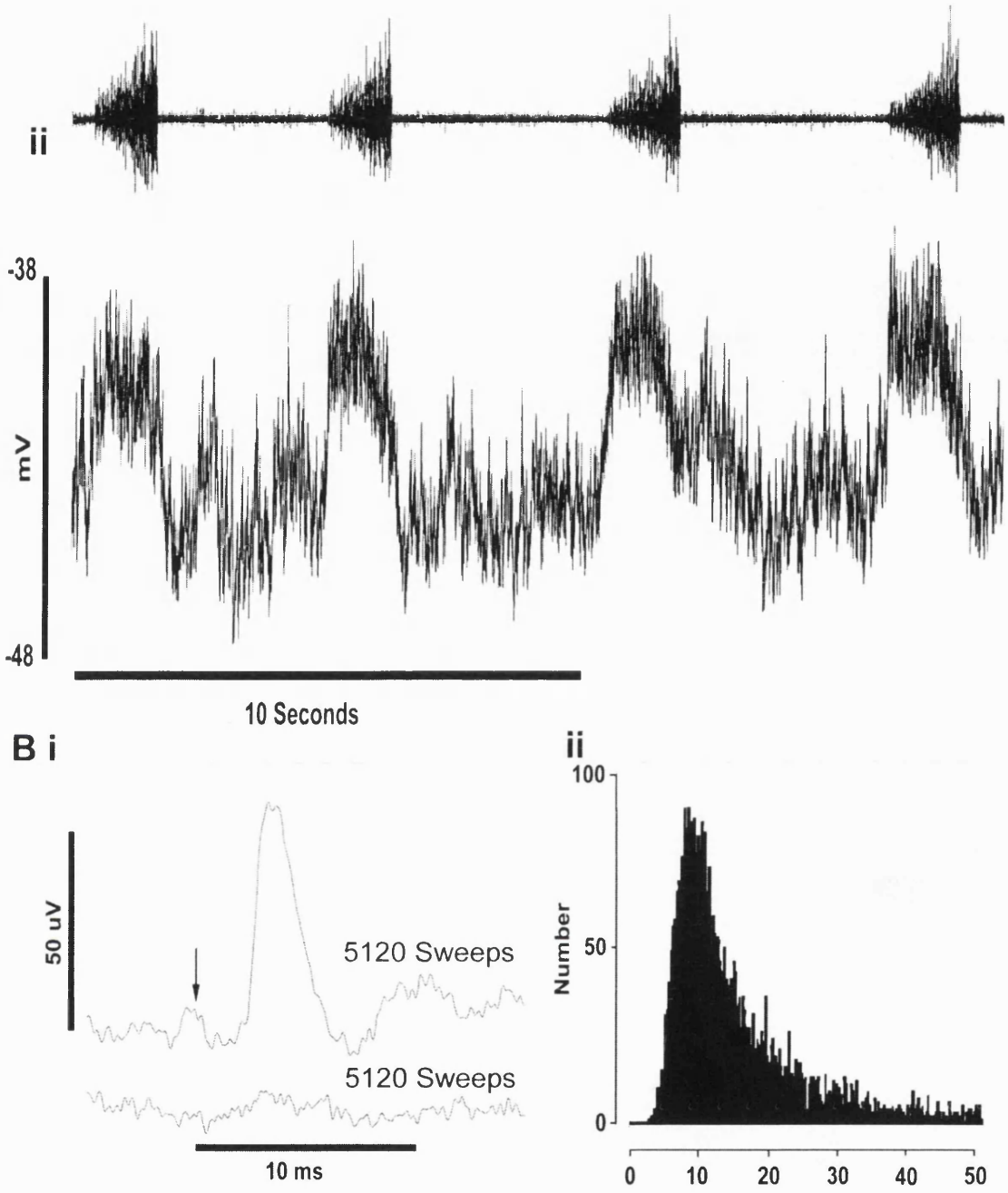

Figure 3.2.4. Intracellular recording from an internal nerve motoneurone with an inspiratory CDRP. A1. External nerve discharge. Aii. Intracellular motoneurone recording. Bi. Spike-triggered average of the intracellular recording (upper trace) showing the presence of an EPSP, and of the extracellular recording(lower trace). Arrow indicates time of bulbospinal unit discharge. Bii. Interspike interval histogram (ISIH) used to trigger the average. The ISIH shows no short intervals

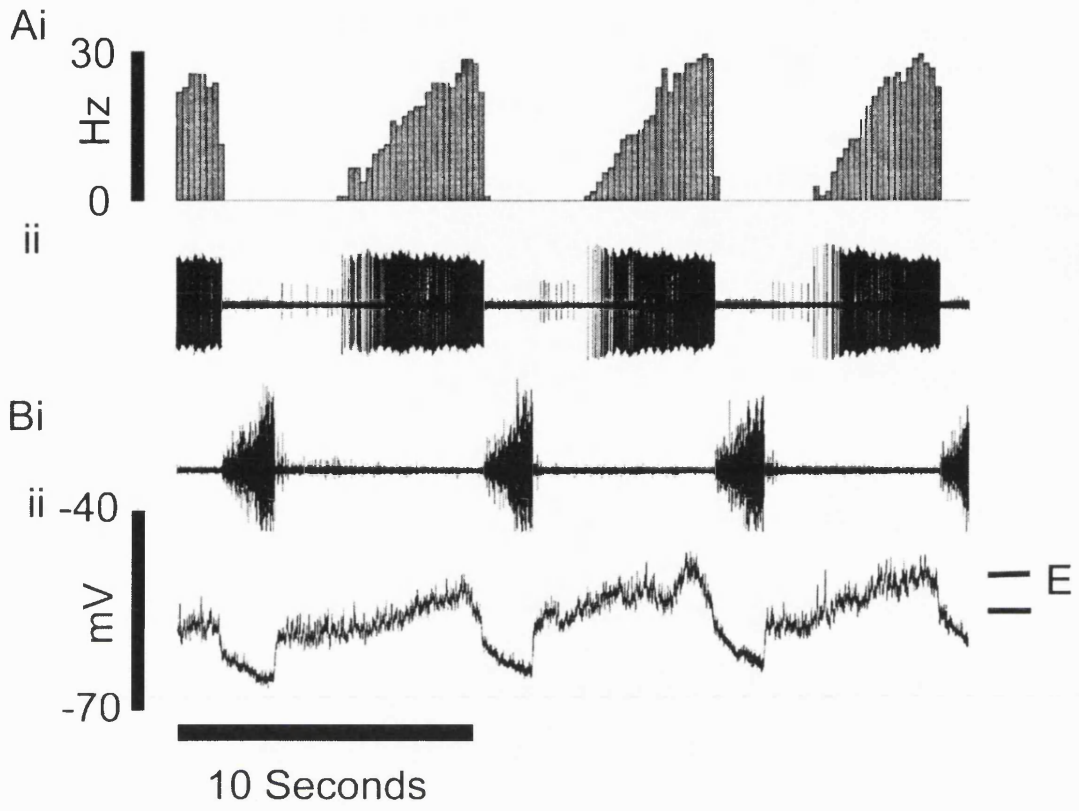

Figure 3.2.5. Intracellular recording from a motoneurone with an expiratory ramp depolarisation Ai. Expiratory bulbospinal neurone firing rate. Aii. Expiratory bulbospinal neurone action potentials. Bi. External nerve recording. Bii. Intracellular recording. E, expiratory ramp.

motoneurones were identified, examples of which are shown in Figure 3.2.5. and Figure 3.2.6. The motoneurones were identified as expiratory upon the basis of their slow potentials i.e. if the motoneurones displayed a depolarisation during expiration as shown in Figure 3.2.5. where a ramp-like depolarisation can be seen in expiration. Alternatively, if a hyperpolarisation was seen in inspiration (presumably due to inhibition, (Sears 1964c) the motoneurone was considered expiratory. An example of a motoneurone with hyperpolarisation in inspiration as shown in Figure 3.2.6.

A further 3 motoneurones were classified as expiratory decrementing, as these motoneurones showed a depolarisation beginning at the end of inspiration and reaching a maximum in early expiration where it began to repolarise as shown in Figure 3.2.7.

For the expiratory motoneurones a total of 44 had axons projecting in the internal and 3 in the dorsal ramus nerve, and none in the external nerve, consistent with previous reports that it only contains axons of inspiratory motoneurones (Sears 1964a).

Intracellular recordings were made from 21 dorsal ramus motoneurones, 4 were classified as expiratory, 1 as expiratory decrementing as shown in Figure 3.2.7. and the remainder were inspiratory. An example is shown in Figure 3.2.4. Inspiratory motoneurones projected into all three nerves with the expiratory motoneurones projecting into just the internal and dorsal ramus nerves.

3.2.5. Spike-Triggered Averaging in Motoneurones.

Spike-triggered averaging was performed on a total of 112 expiratory bulbospinal neurones (EBSN)-motoneurone pairs that received respiratory modulation as defined in Section 3.2.4. In motoneurones that were firing spikes during expiration, STA was not possible, except in a few instances where hyperpolarising current was passed in order to suppress the firing. Averaged potentials were considered to be EPSPs if the potentials satisfied the criteria defined in Section 3.3.3. i.e. if they occurred at an appropriate latency as estimated from the CI, they were greater than 5 μV which was considered the minimum size of an EPSP that could be resolved from synaptic noise. The potentials were also checked for repeatability. For potentials thought to be EPSPs the rise-time from 10-90% of maximum amplitude was calculated and the width of the EPSP at half this amplitude calculated. The rise times were between 0.1-0.8 ms and the half-widths between 0.9 and 7 ms.

In internal nerve expiratory motoneurones EPSPs were identified in 17/41 neurones. The EPSPs ranged in amplitude between 8 and 220 μV, having a mean size of 58 μV ± 55 μV (± SD). An example is shown in Figure 3.3.6.B. for a expiratory motoneurone. For the EPSP shown in Figure 3.3.6.B. it can be seen that the EPSP has a sharp take of from the baseline and has a maximal amplitude of 220 μV. The EPSP from the extracellular record can also be seen to be associated with a terminal potential (TP) and a negative going focal synaptic potential (FSP).

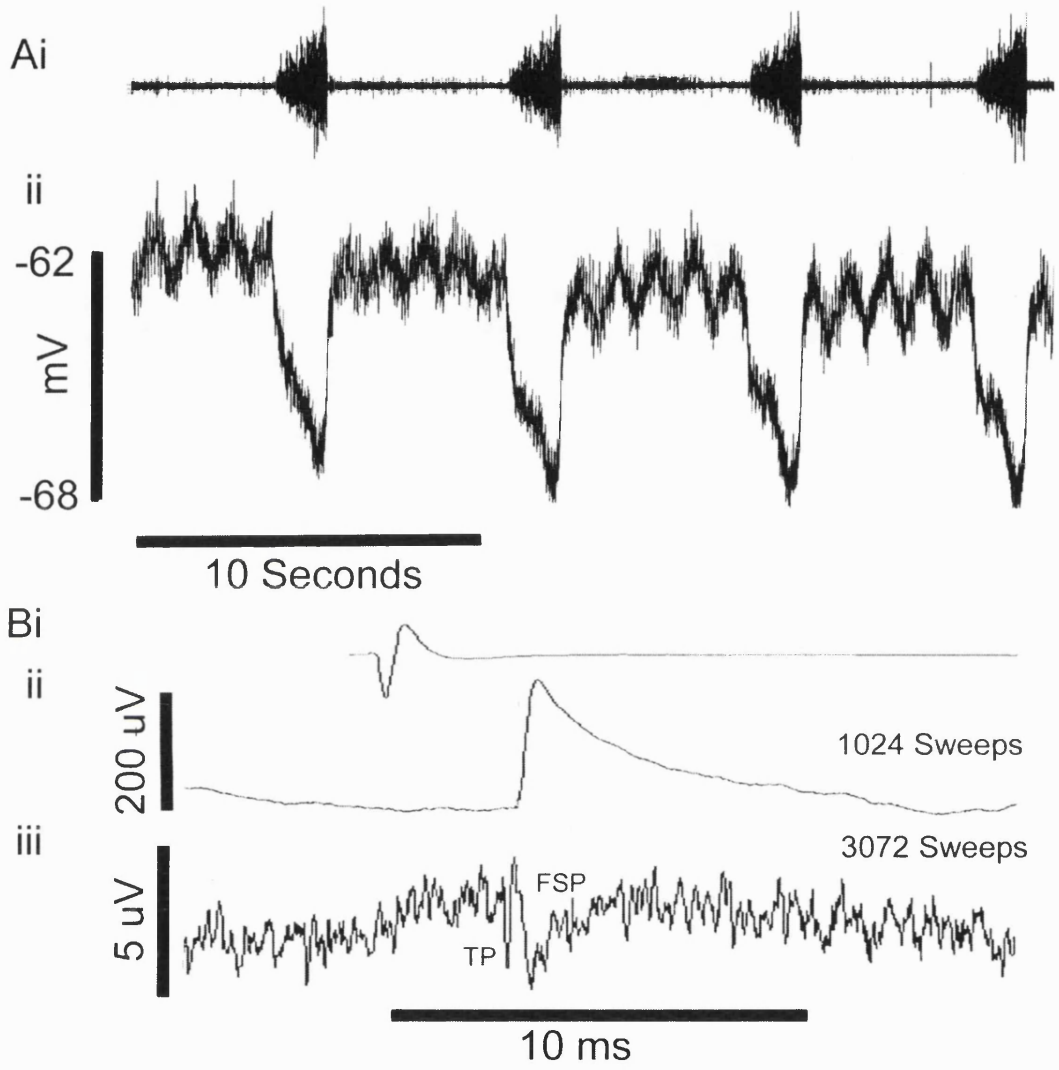

Figure 3.2.6. Intracellular recording from an expiratory motoneurone. Ai. External nerve recording. Aii. Intracellular recording. Bi. Averaged trigger spike. Bii. Spike-triggered averaged EPSP. Biii. Extracellular spike-triggered average showing a terminal potential (TP) and a focal synaptic potential (FSP).

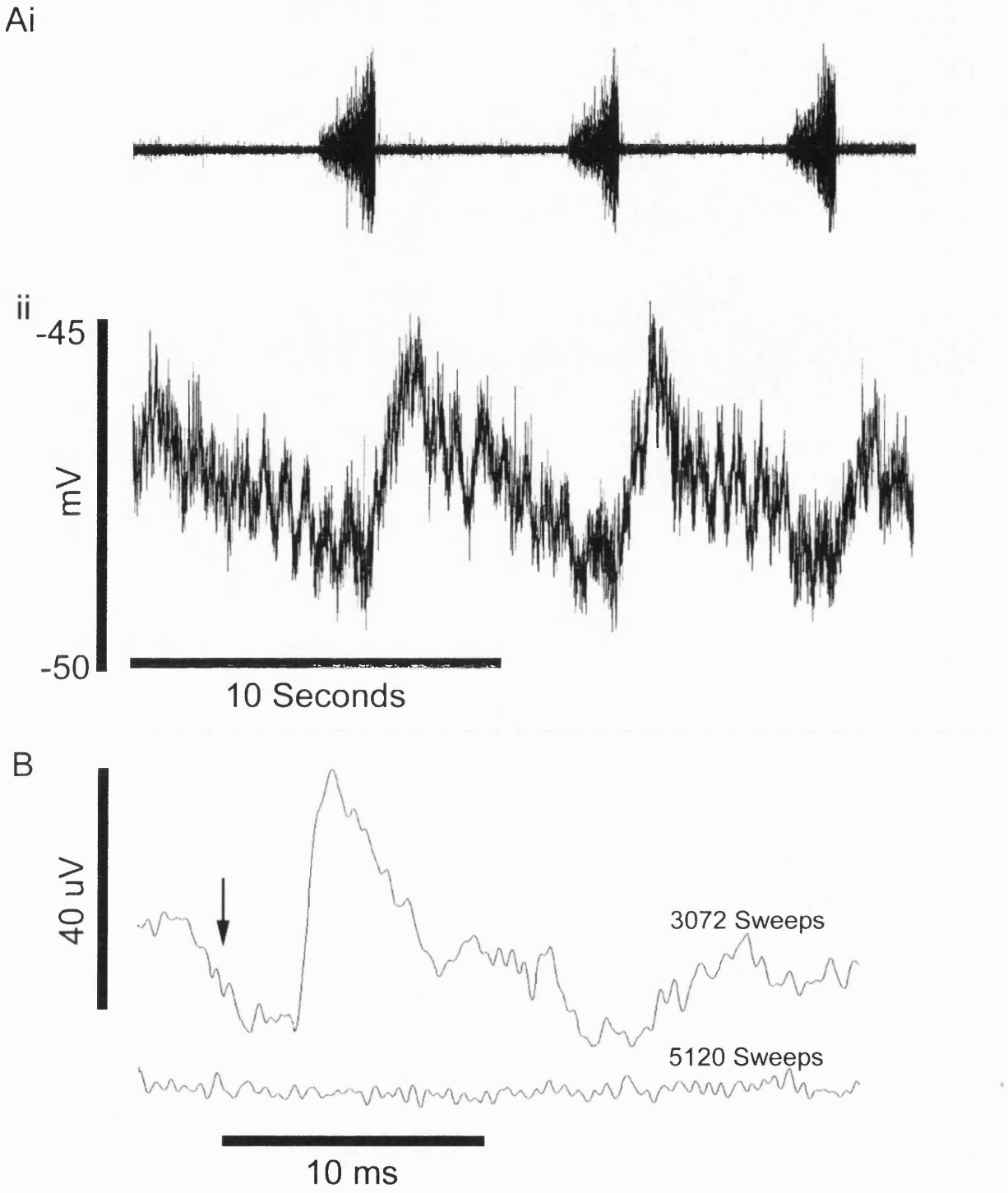

Figure 3.2.7. Intracellular recording from an expiratory dorsal ramus motoneurone. Ai. External nerve recording. Aii. Inracellular recording. B. Spike-triggered average of the intracellular recording (upper trace) showing an EPSP and Extracellular average (lower trace). Arrow indicates time of bulbospinal unit discharge.

Inspiratory phased motoneurones are found in the internal intercostal nerve and STA was performed for these motoneurones in the same way as for expiratory motoneurones. An example of an inspiratory slow potential is shown in Figure 3.2.3.. EPSPs were identified in 2/19 EBSN motoneurone pairs and had amplitudes of 11 and 15 μV.

The motoneurones with axons in the external intercostal nerve only display inspiratory related respiratory discharge patterns. Spike triggered averaging in 12 EBSN-external nerve inspiratory motoneurone pairs was performed. For one of these EBSN-motoneurone pairs an EPSP of an amplitude of 70 μV was identified (Figure 3.2.4) in a motoneurone with a clear inspiratory slow potential.

Spike triggered averaging was also performed for 22 dorsal ramus motoneurones. STA revealed EPSPs in a total of 4/22 EBSN-dorsal ramus motoneurone pairs, 17 with inspiratory modulation, 4 with expiratory modulation and 1 decrementing expiratory modulation. The sizes of the EPSPs ranged from 8-40 μV (20 ±14 μV, mean and SD). An example of an EPSPs identified in an expiratory decrementing dorsal ramus motoneurones are shown in Figure 3.2.7.

3.3.1. Discussion.

Intracellular recordings were made from a large sample of thoracic motoneurones with respiratory related discharges and or slow potentials. These

motoneurones have been extensively characterised (Sears 1964a,b,c) and the motoneurones in this study represent the same population described by Sears (1964c) with the exception of the dorsal ramus motoneurones that have not been previously described. One novel slow potential was however seen in this study that has not been reported before in thoracic motoneurones, that is the expiratory decrementing slow potential.

For motoneurones with a membrane potential ≤-40 mV STA was performed. It was felt necessary to set a minimum value for the membrane potential as in depolarised motoneurones an EPSP may be attenuated and thus introduce false negatives. The value chosen however is quite subjective, other authors have chosen lower values for exclusion of motoneurones from STA; for example, Douse & Duffin (1993) choose -30 mV for STA from interneurones. It is likely that the value chosen here is adequate to avoid the introduction of false negatives.

Spike-triggered averaging, in expiratory motoneurones in the internal intercostal nerve, revealed frequent EPSPs of a wide range of sizes; the variation in size of the EPSP did not appear to be related to the value of the membrane potential. This study has demonstrated a much higher level of connectivity in the rostral portion of the segment between expiratory bulbospinal units and expiratory internal nerve motoneurones than previously described (Merrill & Lipski 1987). The connectivity found in this study is in the order of 42%, thus far greater than that previously reported (Merrill & Lipski 1987) who concluded that the connectivity was around 4%. The greater level of

connectivity seen in this study is possibly due to a different sampling procedure, as only the rostral third of the segment was surveyed. The projections of the expiratory bulbospinal collaterals have been deduced from electrophysiological measurements to be more abundant in the rostral portion of the segment (Kirkwood 1995). It is thus possible that the paucity of the input seen in the study of Merrill and Lipski (1987) arose due to sampling in the caudal portion of the segment that has fewer projections from the EBSNs. This explanation of the difference seems more likely than other variations in the experimental procedure or states of the preparation. However, until a systematic survey of the caudal portion of the segment is completed the uneven distribution of collateral branches cannot be confirmed to account for the differences in connectivity seen.

The higher degree of connectivity identified here supports the conclusion from the cross-correlograms of Kirkwood *et al.* (1995) that the input is far greater than that estimated by Merrill & Lipski (1987).

STA between expiratory bulbospinal neurones and inspiratory motoneurones would not at first sight be expected to reveal connections. However, EPSPs were identified in both external nerve and dorsal ramus inspiratory motoneurones. These connections may be aberrant and of no functional significance, and represent non-specific connection, or transient connections in a reorganising collateral. Alternatively, the bulbospinal neurones giving rise to these EPSPs could be involved in behaviours like vomiting where the inspiratory and some expiratory muscles contract together (Miller, Tan &

Suzuki 1989).

Dorsal ramus motoneurones have been shown here to have both inspiratory and expiratory modulation and have been shown to receive direct input from the expiratory bulbospinal neurones. This indicates that the back muscles innervated by the motoneurones of the dorsal ramus are modulated with respiration and may be involved in respiratory movements. The nature of the involvement is however unclear, as the individual muscles innervated by dorsal ramus motoneurones were not known, although it is likely that these muscles are involved in the co-ordination of postural and respiratory movements.

3.3.2. Summary.

Intracellular recordings have been made from respiratory phased thoracic motoneurones and spike-triggered averaging of their membrane potential performed to identify inputs from expiratory bulbospinal neurones. These recordings have demonstrated that motoneurones whose axons project in the dorsal ramus of the thoracic nerves are respiratory modulated as are the motoneurones contained in the other thoracic nerves. Furthermore, the dorsal ramus motoneurones display a previously unreported expiratory decrementing slow potential.

Spike-triggered averaging has demonstrated monosynaptic connections between EBSNs and all types of thoracic motoneurones. The strength of the

connection between EBSNs and expiratory internal nerve motoneurones was shown to be greater than previously identified by STA, consistent will the stronger connection deduced from cross-correlation measurements. Additionally, unexpected connections between EBSNs and inspiratory phased motoneurones have been identified.

Chapter 4. The Respiratory Thoracic Interneurone (Excluding Renshaw Cells).

4.1.1. Introduction.

Within the ventral horn of the spinal cord it is well established that there are two populations of neurones, motoneurones and interneurones (including ascending relay neurones). The motoneurone is responsible for the innervation of the musculature and their proprieties have been reviewed in a previous chapter. Many interneurones are known to exist within the spinal cord and with one notable exception (the Renshaw cell) have been characterised mostly according to their peripheral afferent inputs. These classifications may not be helpful as spinal interneurones may serve many functions and undoubtedly receive a multitude of different inputs and thus could serve different functions depending on the strongest input at the time (see McCrea 1992 for discussion). However, for the interneurones in the thoracic cord the principal classifying feature has not been the peripheral inputs but the respiratory related phasing of their discharge. In the thoracic cord the activity of interneurones has been hypothesised to provide a substantial proportion of the input required to drive or modulate the firing of thoracic motoneurones (Davies, Kirkwood & Sears, 1985; Kirkwood, 1995). Consequently, for these interneurones classification according to their phasing with reference to the respiratory rhythm may be more helpful, as description in terms of their activity is more likely to help elucidate any role in the generation of a patterned motor output to the thoracic muscles. Central inputs to these interneurones also appear to determine the activity of

these interneurones as they remain active and motor output persists in deafferented preparations, indicating that in this preparation the peripheral afferent input is less significance than the central inputs.

Within the thoracic segments of the spinal cord, interneurones exhibiting a wide variety of respiratory related discharge patterns have been identified. Although some earlier reports exist, a comprehensive survey of the respiratory activity of thoracic interneurones was first achieved by Kirkwood *et al.* (1988). Within the thoracic segments interneurones were identified according to several criteria; the ability to antidromically activate the interneurone from caudally or rostrally located spinal electrodes, the location of the somata within the cord and the firing rate of the neurone (Kirkwood *et al.* 1988); however, only the former criteria unequivocally identifies the unit as an interneurone. The latter two criteria for interneurone identification are based the location of the neurones being more dorsal than the known positions of the motoneurones. Secondly the identity of a unit as an interneurone was based upon the neurones firing at a higher discharge rate than that seen for motoneurones; hence, units were accepted as inspiratory or expiratory interneurones if there discharge frequencies were >100 and 40 Hz (Kirkwood *et al.* 1988), latterly 70 Hz (Schmid et al. 1993) respectively. The positively identified interneurones were classified according to their firing patterns into four categories; inspiratory interneurones, expiratory interneurones, post-inspiratory interneurones and multiphasic interneurones. Inspiratory interneurones had incrementing discharge patterns with the possibility of occasional plateau discharges. The onset of discharge was either in early or late inspiration and at times continued

into post-inspiration (Kirkwood *et al.* 1988; Schmid *et al.* 1993), this being evident more frequently for interneurones that had an early onset discharge and the fastest firing neurones being early onset (Kirkwood *et al.* 1988). Inspiratory phased incrementing interneurones that had a tonic component to their discharge have also been described (Kirkwood *et al.* 1988; Schmid *et al.* 1993). Expiratory interneurones had incrementing, decrementing or tonic discharge patterns (Kirkwood *et al.* 1988; Schmid *et al.* 1993), with early or late onset and tonic patterns (Kirkwood *et al.* 1988). Post-inspiratory interneurones appear to represent a heterogeneous population of neurones with only a small proportion having a decrementing discharge pattern in post-inspiration the remaining interneurones also discharging in other phases of the respiratory cycle. Further groups of expiratory interneurones were defined by Schmid *et al.* (1993) as plateau expiratory, having stable discharge rates during expiration with a decrease in rate during inspiration; variable decrementing units were also seen. Finally multiphasic interneurones include interneurones that discharge in separate bursts in more than one phase of the respiratory cycle (Kirkwood *et al.* 1988). A further feature of the discharge patterns of the interneurones was the regularity of the discharge pattern, hence, the interneurones were divided into regular intermediate or irregular groups, although this grouping was rather subjective (Kirkwood *et al.* 1988).

An estimation of the somatal size of some unidentified thoracic interneurones and an indication of somatal morphology was achieved by retrograde labelling with HRP. Injection of HRP into the thoracic ventral horn (Schmid *et al.* 1993) identified interneurones somata located both ipsilaterally

and contralaterally. The largest density of labelled interneuronal somata were in the region of the injection site in the contralateral ventral horn within laminae VII and VIII. Ipsilaterally located somata were evident although less abundant than contralaterally located somata; the somata being identified as far rostral and caudal as 9 and 3 segments distant from the injection site respectively, the rostral-most located interneurones within the cervical segments indicating a descending projection from cervical interneurones. Somal morphologies of the interneurones were described as multipolar, with round or spindle shaped somata, with the somal diameters in the range of 10-30 μm (Schmid *et al.* 1993), although this may have underestimated the size of the interneurone as no counterstain was used.

For the respiratory thoracic interneurones the trajectories of their axons have been identified by antidromic activation, including microstimulation. The majority of these interneurones projected at least two segments caudal (Kirkwood *et al.* 1988; Schmid *et al.* 1993), with some interneurones activated from electrodes placed up to 5 segments caudal to the location of the soma (Kirkwood *et al.* 1988). It was concluded that the majority of the interneurones with identified descending connections projected at least 3-4 segments caudally. In one instance when a rostral and a caudally located stimulating electrode was employed an interneurone was identified as possessing both a rostral and a caudally projecting axon. The projection of the interneuronal axons were contralateral for 50% of the expiratory interneurones and over 60% for other interneurones types (Kirkwood *et al.* 1988), a similar predominance of contralateral projection was also demonstrated by Schmid *et al.* (1993). A

similar estimation of the extent of the contralateral projection of the interneurones was produced by retrograde labelling, suggesting a relatively extensive contralateral axonal projection close to the somata. Two other axonal trajectories were identified from antidromic mapping; in one instance an expiratory interneurone possessed both a ipsilateral and a contralateral axon; another post-inspiratory interneurone possessed an axon that appeared to cross to the contralateral cord and then re-cross to the ipsilateral cord.

Caudally projecting axons have been locateded by microstimulation. Microstimulation located interneurone axons in the ventral funiculus and because of their parabolic threshold-depth curves were deduced to be unbranched (Kirkwood *et al.* 1988). On the occasions when non-parabolic threshold-depth curves were obtained, collateralisation was deduced to be evident. For one such collateral its course was deduced, indicating an origin in the ventral funiculus and a dorsal projection in the ventral horn (Kirkwood *et al.* 1988). Further evidence of collateralisation in the contralateral ventral horn was provided by STA of extracellular potentials (Schmid *et al.* 1993). Extracellular STA, if performed at a site in close proximity to a stem axon or an axon collateral can reveal waveforms of characteristic shapes (Taylor *et al.* 1978; Munson & Sypert 1979). Waveforms recorded in proximity of a stem axon are typically asymmetrical triangular negative di- or triphasic potentials; whereas, collaterals exhibit a more complex multiphasic waveform, known as a terminal potential (TP) (for discussion see Schmid *et al.* 1993). For regions in the collateral branch that contain synapses focal synaptic potentials (FSPs) can be recorded, and represent current sources or sinks (see Kirkwood, Schmid &

Sears 1993 for discussion) in neighbouring neurones. Frequently TPs are followed by FSPs at an appropriate latency for one synaptic delay indicating the terminal field of the collateral. The sign of the FSP has been taken to indicate whether the input is excitatory or inhibitory in nature; however, for TPs it is not possible to identify unambiguously the component of the waveform associated with the collateral (Munson and Sypert 1979). Extracellular STA in the contralateral cord at approximately the level of the somata revealed both TPs and FSPs (Schmid *et al.* 1993a). In both inspiratory and expiratory interneurones of all varieties of discharge pattern TPs and a subsequent FSP were identified indicating the presence of a terminal field for that neurone, occasionally, TPs alone were evident indicating the presence of only a collateral branch. In the thoracic spinal cord FSPs of three principal types have been identified (Kirkwood, Schmid & Sears, 1993), these being; positive going FSPs and negative going FSPs being either focal or more dispersed in nature. The positive going FSPs represent inhibitory post-synaptic potentials whereas the negative going FSPs represent excitatory post-synaptic potentials; the less focal more dispersed negative FSPs possibly arising from synchronisation of inputs (Kirkwood, Schmid & Sears, 1993).

The existence of two distinct types of FSP associated with two types of input lead to the investigation of whether there was any correlation between the type of activity of the interneurones and the type of FSP, and whether the types of FSPs are segregated within the spinal cord. Two clear correlations between firing characteristics have been demonstrated (Kirkwood, Schmid & Sears, 1993). Phasic inspiratory and expiratory interneurones almost exclusively give

rise to positive going FSPs, implying that these neurones have an inhibitory function; whereas, inspiratory and expiratory interneurones that had a tonic component to their discharge pattern almost exclusively gave rise to a negative going FSP, implying that these neurones are excitatory (Kirkwood, Schmid & Sears, 1993). In one instance it has been demonstrated from intracellular STA in an internal nerve intercostal motoneurone that a positive extracellular FSP represents an IPSP (Kirkwood, Schmid & Sears, 1993). Further to the identification of two populations of interneurones based on correlation between firing characteristics and FSP, it was noted that the phasic inspiratory interneurones have predominantly large diphasic TPs whereas all other categories of interneurones had predominantly complex TPs (Kirkwood, Schmid & Sears, 1993). When comparing the size of the maximum of the terminal potential to the maximum size of the FSP a clear correlation is evident for both positive and negative going FSPs, implying that the size of the pre-synaptic terminal determines the size of the post-synaptic potential.

Despite identification of FSPs in the contralateral cord the target neurones remain obscure. It is well established that spinal motoneurones are located in a reasonably well circumscribed area of the ventral horn, although, interneurones are known to be intermingled (Kirkwood *et al.* 1988; 1999) with the motoneurone population; it is thus of interest to see if there is any focal restriction of the FSPs within the spinal cord. A clear segregation of FSPs was demonstrated for the inspiratory interneurones (Kirkwood, Schmid & Sears 1993), with the positive-going, inhibitory potentials found laterally in the ventral horn in the region of the motoneurones of the internal intercostal nerve;

whereas, interneurones with negative-going excitatory potentials were found more dorsally, implying likely inputs to interneurones or distal motoneurone dendrites. This segregation of input types for inspiratory interneurones was evident for the expiratory interneurones also; however, the segregation was less clear cut. The potentials from the phasic incrementing expiratory interneurones tended to be located within the motor nucleus, with those from the phasic decrementing expiratory interneurones located more dorsally; for expiratory interneurones a less focal pattern was than for the inspiratory ones, evident with most interneurones projecting to the dorsal region of the ventral horn with few interneurones projecting to the motor nucleus (Kirkwood, Schmid & Sears, 1993). A subsidiary observation was made regarding the location of the somata of phasic and tonic interneurones. It was noted that there was a statistically significant segregation of phasic and tonic somata within the ventral horn on the basis of their location deduced electrophysiologically (Kirkwood, Schmid & Sears, 1993), with the phasic units tending to be located deep within the ventral horn and the tonic interneurones located more dorsally. These observations thus indicate that the interneurones project principally to the same location in the contralateral cord to which their somata are located.

In summary, the respiratory interneurones of the thoracic cord have so far been physiologically characterised. The studies of Kirkwood *et al.* (1988) and Schmid *et al.* (1993) have identified distinct populations of both inspiratory and expiratory interneurones. The projections of these interneurones have been identified to be principally contralateral by physiological (Kirkwood *et al.* 1988) and anatomical (Schmid *et al.* 1993) techniques, with evidence for

collateral projection within the ventral horn obtained from microstimulation (Kirkwood *et al.* 1988) and extracellular STA (Schmid *et al.* 1993; Kirkwood, Schmid & Sears, 1993). Similarly, STA has provided evidence for inhibitory and excitatory sub-populations within the overall population of interneurones (Kirkwood, Schmid & Sears, 1993). However, this population of neurones remains far from fully characterised and the functional roles of this population of neurones remain speculative.

One reason for the incomplete characterisation is that the techniques thus far employed are subject to certain limitations. From antidromic stimulation it cannot be concluded that all the interneuronal axons are stimulated (Kirkwood *et al.* 1988), as there may be a sub-population of interneurones, whose axons project within parts of the spinal cord that would not be stimulated by the electrode array. Similarly, interneurones with a rostrally projecting axon have not been extensively tested for. Evidence supporting the possibility that a proportion of the interneurone axons are either ascending or fail to be stimulated by the caudal stimulating electrodes was provided in the study of Kirkwood, Schmid & Sears (1993). In this study contralateral TPs and FSPs were identified from interneurones that could not be identified antidromically from two segments caudal, raising the possibility that there was a technical failure to activate the axons, the interneurones possessed ascending axons, the axons do not run in the ventral horn or the axons do not project for two segments. Limitations similarly exist for the electrophysiological characterisation of the axon and collateral trajectories. Microstimulation has only identified axons that run in the tip of the ventral horn, and by the same

reasoning as before can not be concluded to identify the entire population; likewise, microstimulation cannot be considered to unequivocally identify axon collaterals. Identification of TPs and FSPs by STA has given a less equivocal description of the projection of axon collaterals, however, the collaterals tend to be rare and widely spaced (Schmid *et al.* 1993), hence, mapping electrophysiologically would be extremely painstaking and still reveal little information about the identity of the target neurones.

Retrograde labelling experiments also have limitations with regard to the population of interneurones they identify, further to the limitations implicit to the technique. Injection of label into a tissue will only label neurones whose axons or collaterals project into the region occupied by the deposited label. In the retrograde labelling experiments of Schmid *et al.* (1993), where a total of three injections were made in the lateral and medial ventral horn, the neurones retrogradely labelled cannot be assumed to be part of the same population identified electrophysiologically, with axons running in the tip of the ventral horn. If this were to be the case all the neurones labelled must of had collaterals that project to the sites of label deposition. Retrograde labelling also has two fundamental limitations as a technique used to characterise neurones, these being; no physiological data is gathered hence no real functional conclusions can be drawn, and secondly the morphology is poorly described. Retrograde labelling produces only approximate estimates of somal size and morphology, with little data on the number of dendrites, and no data on the projection of dendrites or axon collaterals. The latter two characteristics are of fundamental importance in assigning a likely function to the interneurones and evaluating

their role in driving and modulating motoneurone firing. As the majority of inputs to the interneurones are likely to be on the dendrites, it is important to identify to which areas the dendrites project and if any of the dendrites project contralaterally (c/w cervical motoneurones) allowing a bilateral input to the neurones. Similarly the terminal fields of the axon collaterals needs to be identified so that likely targets for the interneurones can be identified.

The objective of this study was to characterise the respiratory interneurones of the thoracic cord using intracellular recording and labelling techniques. Intracellular recording from the interneurones has allowed measurement of the magnitude of the respiratory related fluctuations in membrane potential and tests of bulbospinal-interneuronal connectivity by STA, while intracellular labelling has permitted morphological characterisation of the interneurones and identification of the axonal projection and collateral arbors. Following the identification of collateral arbors containing boutons, immunohistochemical techniques and confocal microscopy has been used to identify likely transmitters acting at their synapses. This study has thus further characterised this interneuronal population in terms of physiology, anatomy and pharmacology.

Such characterisation of the interneuronal population, alongside the new data gathered for thoracic motoneurones will act as control data for further experiments, in which the thoracic spinal cord will be used to investigate plasticity and regeneration of long descending bulbospinal projections and intersegmental projection of interneurones following lesioning. This study will

thus provide control data for planned investigations into the plasticity in functional connectivity, gross morphology, terminal fields and transmitter systems.

4.2.1. Results.

4.2.2. Firing Characteristics and Patterns of Respiratory Modulation of Thoracic Interneurones (Excluding Renshaw Cells).

Surveys of the rostral portion of the segment (T5-8) were made and interneurones were identified upon a hierarchy of criteria. Neurones that could be antidromically activated from the caudal spinal stimulating electrodes were considered to be unequivocally identified as interneurones. The remaining neurones were identified as interneurones according to their characteristic high frequency and irregular firing rates due to injury of the neurone when first penetrated and their position. The identity of these neurones as interneurones being confirmed by intracellular filling and identification of the axonal trajectory as being funicular rather than projecting toward the ventral roots.

In total intracellular penetrations were made in 45 interneurones for a long enough duration to allow thorough physiological characterisation. Frequently, penetrations were made in interneurones that were of an inadequate duration to allow assessment of their respiratory modulation and identification of any caudal axonal projections; these incompletely characterised neurones are not considered further. A number of stable penetrations were

made intra-axonally, and, if the penetration was assessed to be in the proximal portion of the axon, close to the soma, they were considered to be candidates for STA (see Chapter 4.3.3.) and intracellular labelling (see Chapter 4.4.1). A penetration was considered to be axonal if the action potential did not arise from any identifiable post-synaptic potential and had an abrupt take off from the baseline; in some cases the site of penetration could be confirmed histologically (see Chapter 4.4.1.). The penetration was considered to be close to, or in the soma if synaptic noise or respiratory modulation of the membrane potential could be seen; alternatively, if post-synaptic potentials could be evoked from either the peripheral nerves or the spinal electrodes the penetration was considered somatic (see Chapter 4.4.1. for further discussion).

The physiologically characterised interneurones fell into three principal categories; inspiratory modulated interneurones, expiratory modulated interneurones and interneurones with no or little respiratory modulation. These classifications are considered separately below.

In total thirteen of the interneurones displayed inspiratory phasing of their activity. Six of these inspiratory interneurones continued to fire action potentials tonically during expiration, an example of which can be seen in Figure 4.2.1. The tonic inspiratory interneurones displayed a constant firing pattern with an increasing frequency of discharge during inspiration as defined by the external nerve discharge. This increase in discharge rate reached a maximum at the end of inspiration or post-inspiration (Richter & Ballantyne 1983) and decreased back to the tonic firing rate during the post-inspiratory

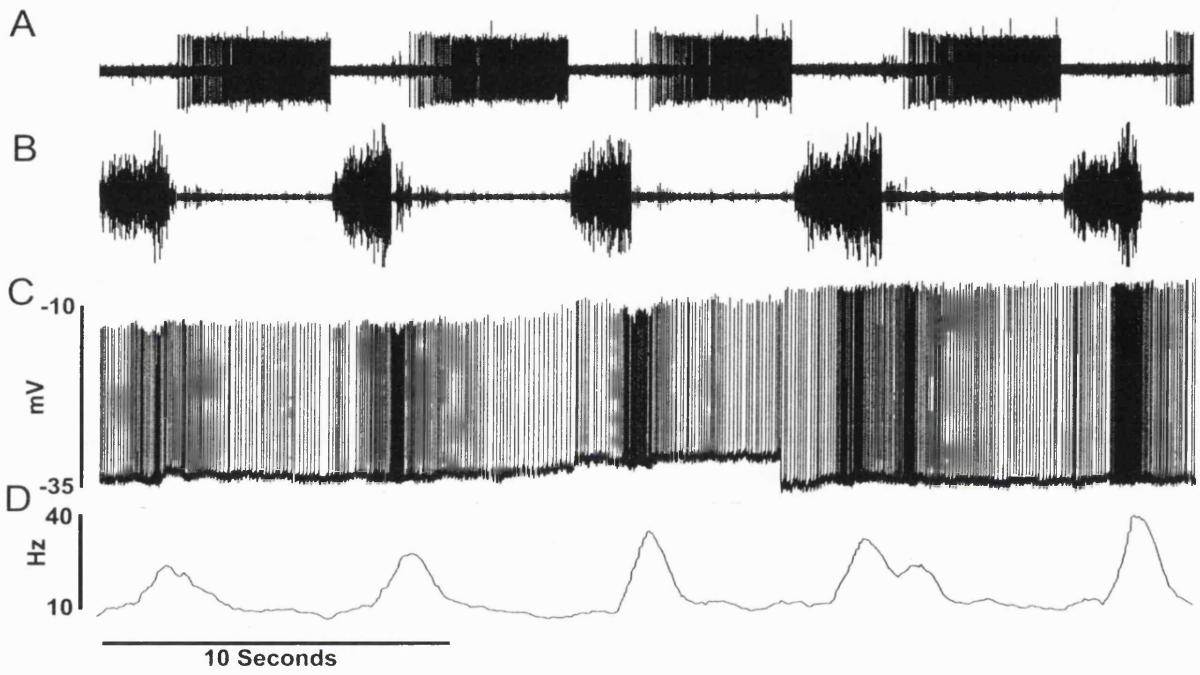

Figure 4.2.1. Intracellular recording from a tonic inspiratory interneurone. A. Expiratory bulbospinal neurone discharge. B. External nerve recording. C. Intracellular (presumed axonal recording. D. Firing frequency of the interneurone.

period. Individual interneurones showed variability in the inspiratory phasing of their discharge, an example is given in Figure 4.2.1, where it can be seen from traces C and D that the maximum firing frequency occurs in differing parts of the inspiratory cycle. This interneurone fires maximally in late inspiration in the first and last cycle, in the remaining cycles maximal firing occurs in post-inspiration with the exception of the penultimate cycle; in this cycle there are two clear components to the discharge, one in inspiration and the other in post-inspiration. None of the tonic inspiratory interneurones showed appreciable variation in the firing frequency during the tonic component of their discharge, an example of an interneurone penetrated intra-axonally is shown in Figure 4.2.1, where it can be seen that the interneurone continues to fire at around 10 Hz throughout expiration. The interneurone with the tonic activity shown in Figure 4.2.1 was intracellularly labelled and the location of the soma is shown in Figure 4.3.2.D and the fully reconstructed cell is shown in Figure 4.3.7.

All of the tonic inspiratory interneurones tested could be antidromically activated from the caudal electrodes, three contralaterally and two ipsilaterally, with one interneurone remaining untested.

The remaining seven inspiratory interneurones showed respiratory excitation only during inspiration. The excitation was evident from one of two features, either discharges of the interneurones only occurred during inspiration or an inspiratory depolarisation could be identified. The firing pattern of the phasic inspiratory interneurones was incrementing, with the maximal discharge frequency reached at the end of inspiration, whereupon the discharge

terminated abruptly. An example of a phasic inspiratory firing pattern is shown in Figure 4.2.2.

For three interneurones identified as having an inspiratory CRDP, the membrane potential became more depolarised during inspiration. However, the depolarisation was not sufficiently large to cause the interneurone to fire. The magnitude of this CRDP was in the order of 1 mV for all three interneurones. Antidromic activation from the caudal segments identified descending axonal projections for 6/7 inspiratory interneurones. Five were activated from ipsilateral electrodes, two of these were also activated from the contralateral electrodes, and one activated from only the contralateral electrodes.

A further thirteen interneurones were classified as expiratory on the basis of their firing pattern or CRDP. For seven of the expiratory interneurones clear phasic firing patterns were evident, an example of which is shown in Figure 4.2.3 Figure 4.2.4 and Figure 4.2.5. The expiratory discharge patterns of these neurones were incrementing, decrementing or plateau. Incrementing expiratory interneurones, an example of which is shown in Figure 4.2.3, began to discharge during the post-inspiratory period, reaching a maximum firing frequency at the onset of inspiration, where there would be an abrupt cessation of their firing. The discharges as seen in Figure 4.2.3 coincide with a depolarisation of the membrane potential during expiration. Frequently during the inspiration the membrane potential could be seen to become more hyperpolarised, this hyperpolarisation was frequently incremental as in Figure 4.2.3, with the membrane potential becoming rapidly depolarised at the onset

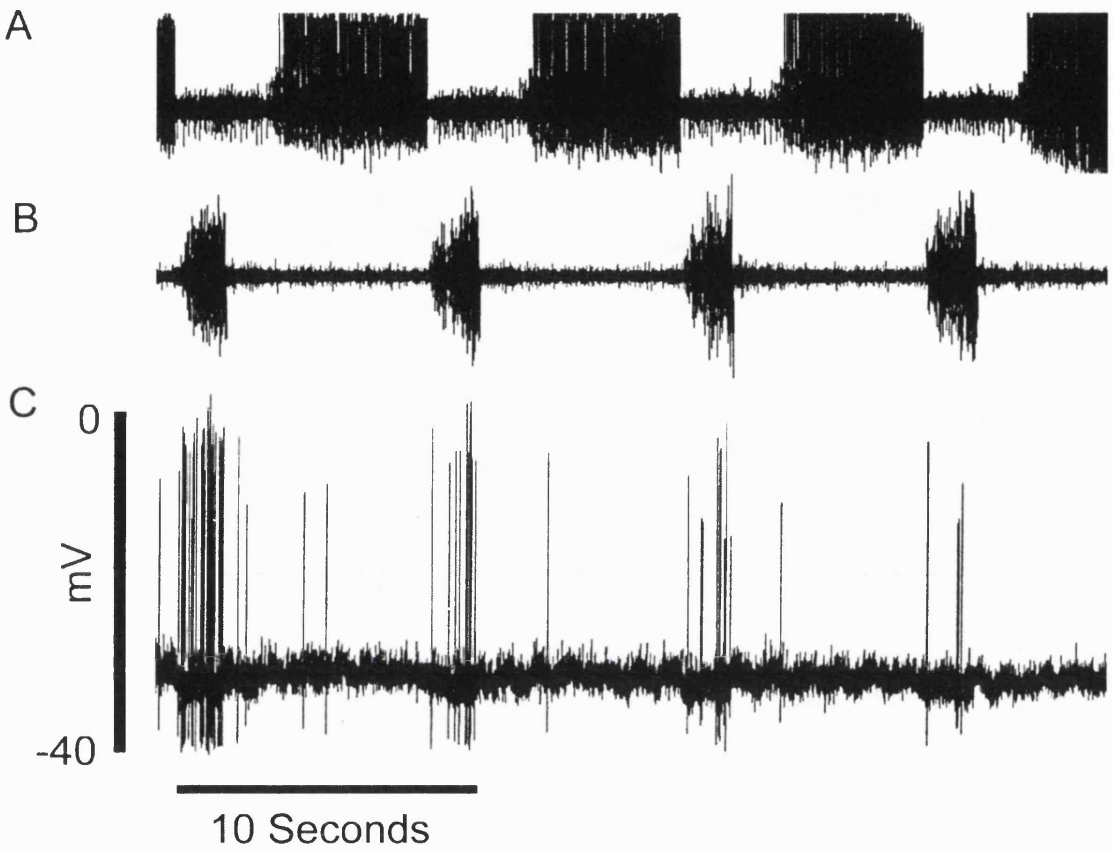

Figure 4.2.2. Intracellular recording from a phasic inspiratory interneurone. A. Expiratory bulbospinal neurone discharge. B. External nerve recording. C. Intracellular (presumed axonal) recording.

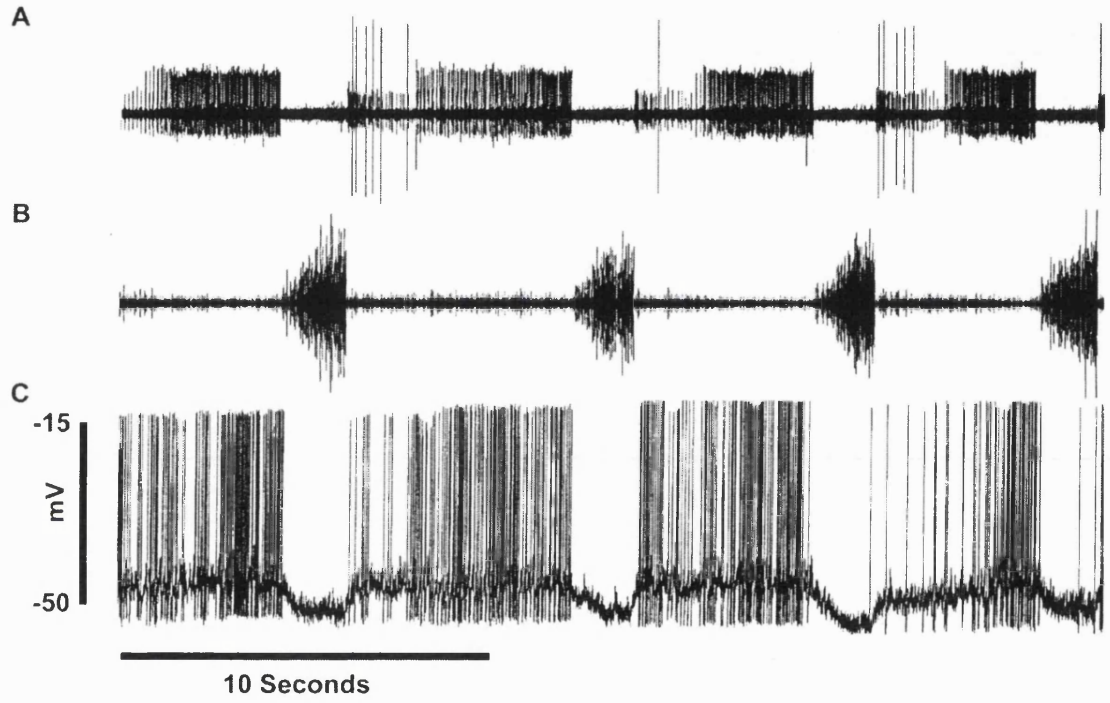

Figure 4.2.3. Intracellular recording from an incrementing expiratory interneurone. A. Expiratory bulbospinal neurone discharge.B. External nerve recording. C. Intracellular recording.

of the post-inspiratory period.

Interneurones with a decrementing expiratory activity were the most abundant, representing 4/7 firing expiratory interneurones, an example of which is shown in Figure 4.2.4. Decrementing expiratory interneurones began to fire rapidly in the post-inspiratory period, and continue to discharge at a decreasing frequency during either the initial or whole expiratory period. For early decrementing interneurones that spanned the respiratory period the firing terminated abruptly at the onset of inspiration; no decrementing units were seen to begin to fire at any other time than at the beginning the post-inspiratory period. The discharge of the decrementing expiratory interneurones was often associated with a depolarisation of the membrane potential as can be seen in Figure 4.2.4.

A final type of expiratory discharge pattern identified was a plateau expiratory pattern as shown in Figure 4.2.5. Plateau expiratory interneurones began firing at the end of inspiration and continued to fire at a constant rate throughout expiration.

This can be seen in the Figure 4.2.5.D where the interneurone fired at a relatively constant frequency of 70 Hz during expiration, with an abrupt termination of firing at the beginning of inspiration.

Interneurones (6/13) were also identified as expiratory from modulation of their membrane potentials. These showed either a clear depolarisation during expiration but without firing action potentials, accompanied by a

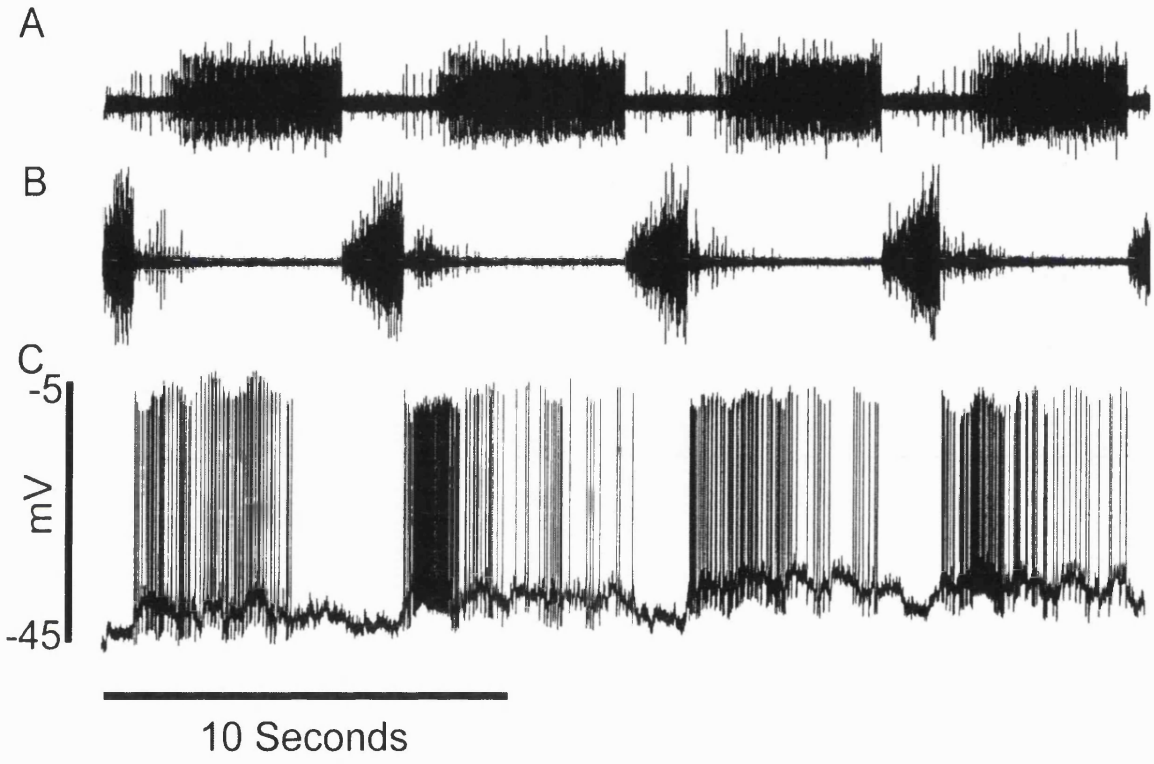

Figure 4.2.4. Intracellular Recording from a Decremental Expiratory Interneurone. A. Expiratory bulbospinal neuron discharge.B. External nerve recording. C. Intracellular recording.

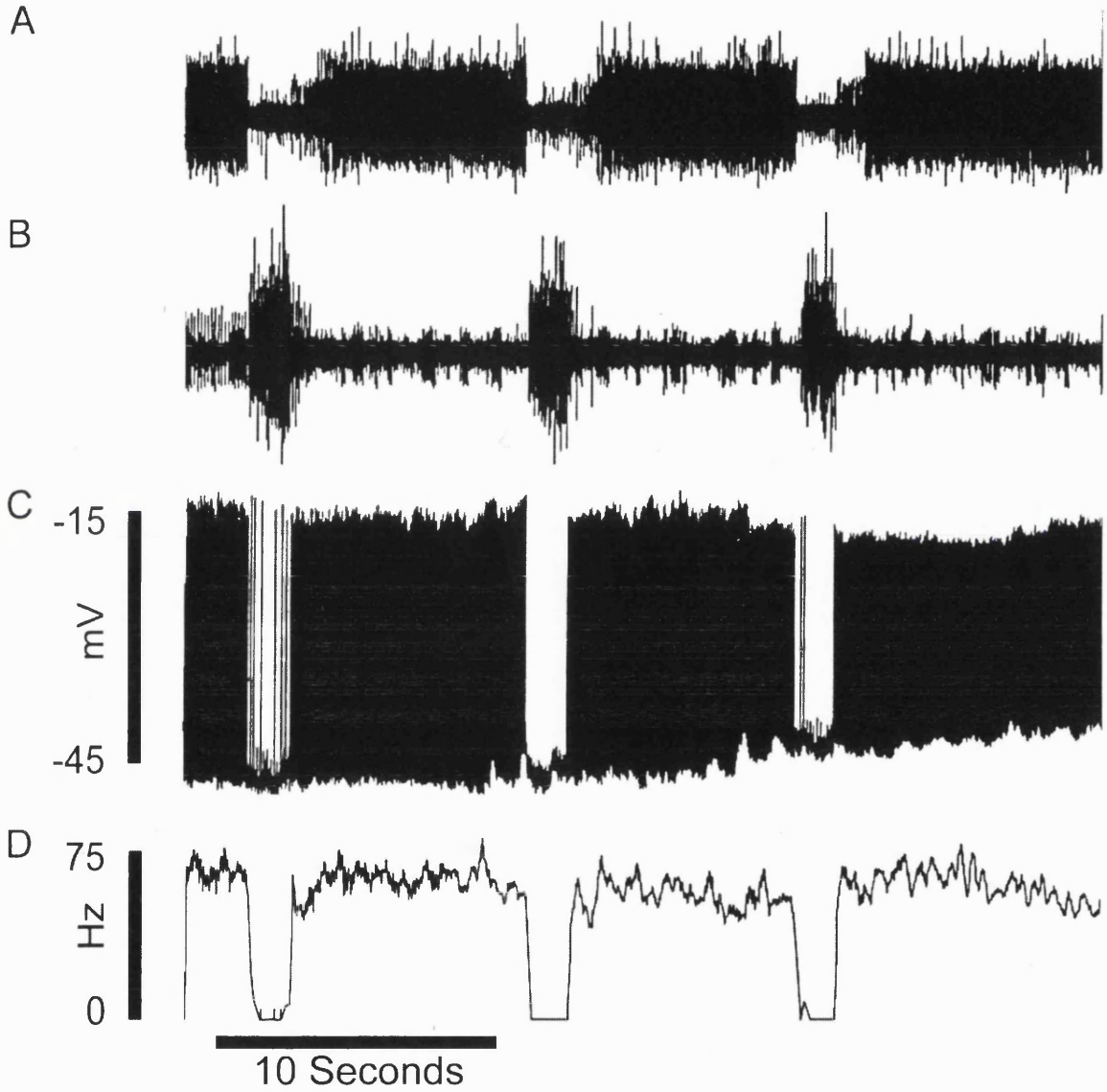

Figure 4.2.5. Intracellular recording from a phasic expiratory plateau interneurone. A. Expiratory bulbospinal neurone discharge.B. External nerve recording. C. Intracellular recording (presumed axonal). D. Firing frequency.

hyperpolarisation during inspiration, or only a hyperpolarisation during inspiration. These hyperpolarisations appeared to be incremental of the type previously described by Sears (1964c) for motoneurones. Examples of these slow potentials are shown in Figure 4.2.6. One interneurone was identified as having some form of respiratory modulation by an alternative criteria; this being the inability of the antidromic spike stimulated by the caudal electrodes to invade the soma during inspiration.

In total 9/13 expiratory interneurones could be antidromically activated from the caudally located stimulating electrodes. Of these six were activated from contralateral electrodes, with one interneurone also activated by the ipsilateral electrodes, two were activated from the ipsilaterally electrodes only with the remainder not being antidromically activated. No obvious relationship between axonal projection and activity was evident.

A number of interneurones were identified for which there appeared to be little or no respiratory modulation. In these interneurones no relationship between firing patterns and a respiratory cycle could be identified. Alternatively, no modulation of the membrane potential grater than 1 mV could be identified. A total of eighteen interneurones fitted this category, eight fired tonically with the remaining interneurones not firing at all. Eight of these interneurones were

identified as having a descending axon from antidromic stimulation, these axons were activated ipsilaterally for four interneurones two also being.

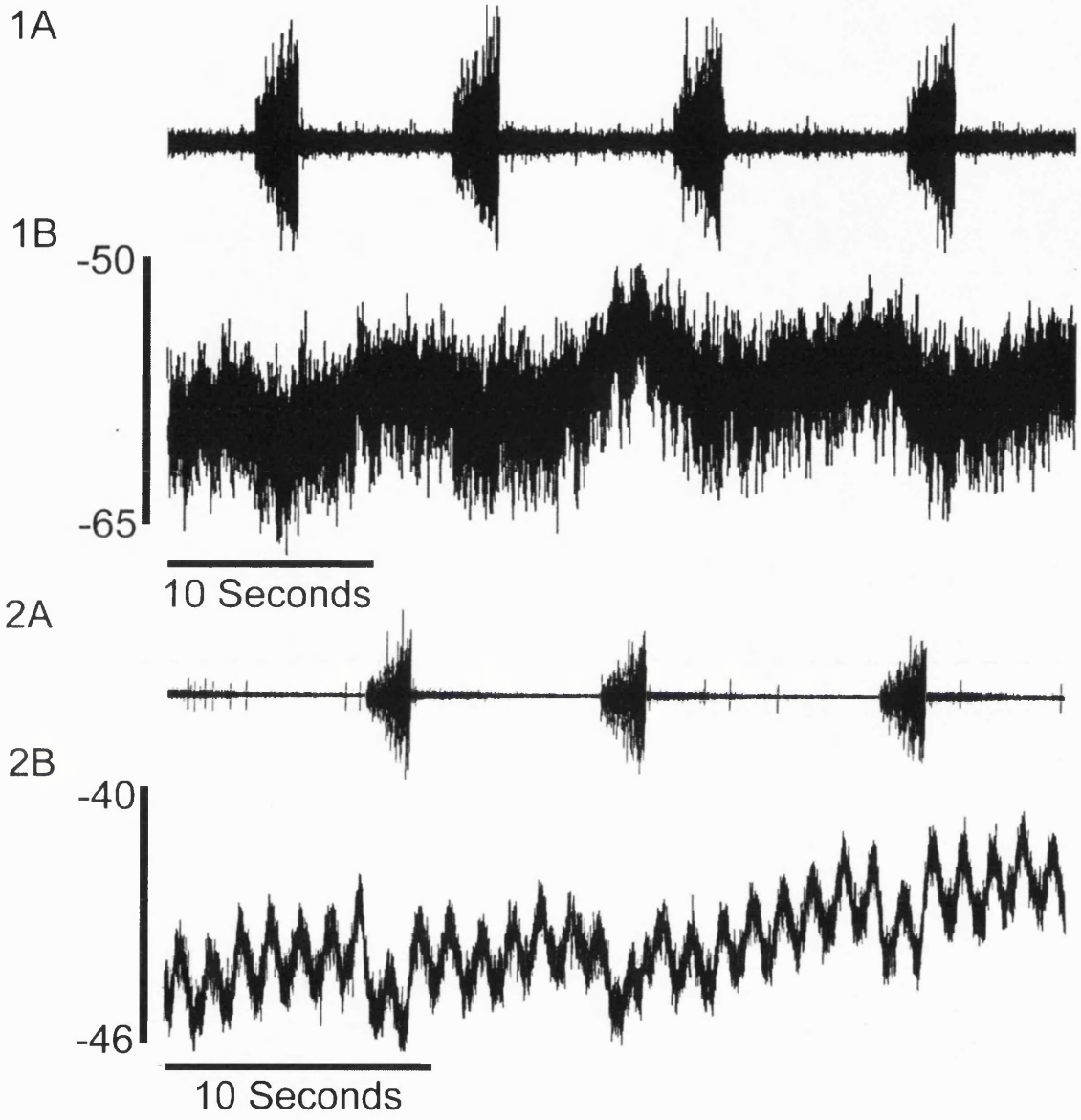

Figure 4.2.6. Intracellular recordings from expiratory interneurones. 1A. External nerve recording. 1B. Intracellular recording. 2A. External nerve recording. 2B. Intracellular recording, note movement artifact at approximately 1Hz from artificial ventilation.

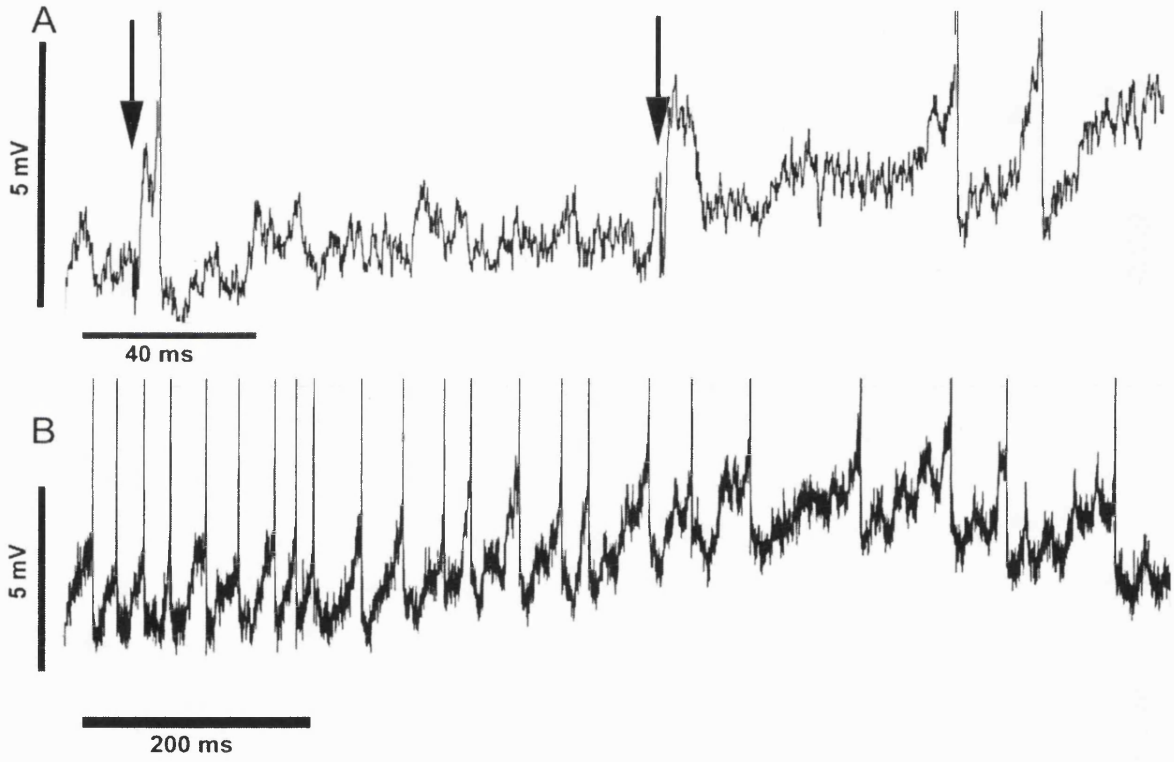

Figure 4.2.7. Intracellular recordings from axons penetrated close to the soma. A. EPSPs in response to peripheral nerve stimulation (arrows indicate time of stimulation). B. Synaptic noise seen within an axon.

activated contralaterally and exclusively contralateral activation for the remainder activated contralaterally and exclusively contralateral activation for the remainder.

One further interneurone could not be classified as its CRDP altered during the penetration. This interneurones could not be antidromically activated from the caudal spinal electrodes. The activity of these interneurones and their projections are summarised in Table 4.2.1.

Table 4.2.1.

	Number	V_m. Mean + SD	Antidromic activation			
			C	I	Bi	N
Expiratory	13	-43 ± 10.2	5	2	1	1
Inspiratory						
Phasic	7	-41.7 ± 9.1	1	3	2	1
Tonic*	6	-39 ± 8.9	3	3	-	-
Non-Respiratory	17	41.4 ± 10.8	4	1	3	9
Multiphasic	1	-22	-	-	-	-

* One interneurone was not tested for antidromic activation.

Membrane potentials and antidromic activation from the spinal electrodes. C, contralateral, I, Ipsilateral, Bi Bilateral, N, not antidromically activated respectively

4.2.3. Spike-Triggered Averaging in Interneurones.

From the intracellular recordings described in section 4.2.2 a total of 33 penetrations were identified as somatic or close to the soma and were stable enough to allow STA to be performed for greater than 1024K sweeps. STA was performed for some penetrations that were thought to be in the proximal portion

of the axon, as described earlier. Figure 4.2.7 shows high gain DC recordings from interneurones in which an axonal penetration was confirmed histologically (see section 4.4.1). The penetrations were identified as being approximately 350 and 75 μm from the soma and are from the interneurones whose activity is shown in Figure 4.2.5 and 4.4.13 respectively. The morphology of these interneurones is also shown in Figures 4.3.6 and 4.3.13 the approximate site of the penetration is indicated in Figure 4.3.6. For the recording in Figure 4.2.7.A EPSPs can be clearly identified in Figure 4.2.7.A response to peripheral nerve stimulation and in Figure 4.2.7.B synaptic noise seen. It was thus considered that STA in these proximal axons may identify EPSPs arising from any bulbospinal input.

The interneurones tested with STA had membrane potentials ranging from -30 to -60 mV (-40.5 ± 10.6 mean and SD); the membrane potential typically being lower than that for motoneurones and accompanied by higher levels of synaptic noise. The criteon used for selecting motoneurones for STA according to the size of the membrane potential was relaxed to -30 mV for interneurones because of the lower membrane potentials frequently encountered. The same criteria were used for identifying EPSPs in interneurones as for that of motoneurones; that is, a positive potential with a fast rise time beginning at an appropriate latency, as calculated from the conduction velocity of the bulbospinal unit and that could be repeatably identified.

It was only possible to perform STA in interneurones that had a

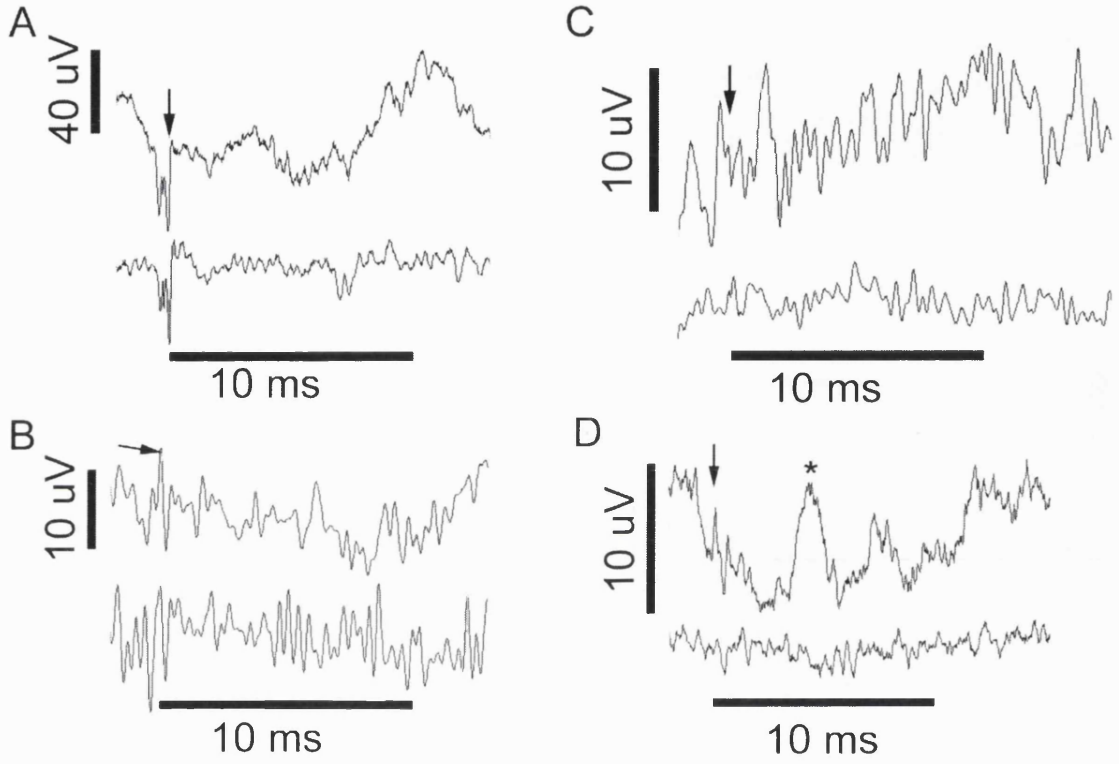

Figure 4.2.8. Examples of STA in different types of interneurones.Upper traces are intracellular averages and lower traces are extracellular averages. Arrow indicates the time of the trigger. A & B. Expiratory interneurones. C Inspiratory interneurone.
D. Non-respiratory interneurone. Note the deflection in D indicated by the asterisk is not an EPSP as it did not occur at an appropriate latency and was not repeatable.

substantial period of the expiratory cycle free from discharges that would contaminate the average, consequently, STA was not possible in some interneurones. However, many of the interneurones that fall into categories that fire during expiration had substantial periods when the spike discharges inactivated, or hyperpolarising current was passed to prevent firing, thus permitting STA. STA was performed for a total of 2 tonic inspiratory interneurones, 5 phasic inspiratory interneurones, 11 expiratory interneurones, 14 non-respiratory interneurones and 1 unclassifiable interneurone. No EPSPs were unequivocally identified. Figure 4.3.1 shows examples of the negative results obtained for interneurones in all the main categories. It was possible to identify TPs from some of these averages indicating bulbospinal collaterals in the region of the interneurones. In one instance (Figure 4.3.1.A) a possible EPSP was identified in an expiratory interneurones the activity of which is shown in Figure 4.2.6. However, this potential has a long rise time, although the potential does occur at an appropriate latency which is rather long but does correspond to the unusually slow conduction velocity of the bulbospinal neurone. This potential also follows a terminal potential indicating the presence of a bulbospinal collateral in the vacinity of the interneurone.

4.3.1. Discussion Relating to Physiological Investigations.

The firing patterns of the respiratory interneurones of the thoracic spinal cord have been previously described from extracellular recordings (Kirkwood *et al.* 1988; Schmid *et al.* 1993) and hence can be compared to the interneurones

in this study. It is however difficult to make direct comparisons between the activity of neurones recorded intracellularly and extracellularly, as the effect of the intracellular microelectrode upon the firing pattern is never known, this being especially so for somal recordings. It is however felt that comparison is worthwhile to assess if the interneurones in this study are likely to be part of the same population as those previously described. Similarly, the slow potentials observed can be compared to those seen in respiratory motoneurones, as can the data from STA.

4.3.2. Physiologically Identified Interneurones Firing Patterns, CRDPs and Axonal Projections.

The interneurones identified in this intracellular study appear to conform to the populations of interneurones previously described in the extracellular studies of Kirkwood *et al.* (1988) & Schmid *et al.* (1993). However, in the present study the inspiratory interneurones have been classified slightly differently, and also according to their CRDPs. A group of inspiratory interneurones with a tonic component to their discharge has been identified with similarities to previously described interneurones. In the study of Kirkwood *et al.* (1988) & Schmid *et al.* (1993) a population of tonically firing interneurones was described with incrementing firing rates during inspiration; here we have identified a similar population. As in these previous studies the present population has common properties with the interneurones described as phasic inspiratory or post-inspiratory. The tonic inspiratory interneurones described here show respiratory phasing commencing in either late inspiration or post-

inspiration and ending in the post-inspiratory period. An example of this is shown in Figure 4.2.1. This interneurone shows a high degree of variability in its inspiratory phasing as in alternate cycles the onset of the increase in rate occurs either in late inspiration or in post-inspiration, with a clear bursts in both phases in one cycle. This interneurone was typical of the population of tonic inspiratory interneurones in this study. These interneurones thus have characteristics common to all the previously described classifications of inspiratory interneurones i.e. phasic, tonic, and post-inspiratory interneurones (Kirkwood *et al.* 1988; Schmid *et al.* 1993) and they may fire phasically in certain circumstances as was observed by Schmid *et al.* (1993) when a supplementary dose of anaesthetic caused a tonic interneurones to fire phasically.

To classify interneurones as genuinely tonic for intracellular somal penetrations the tonic component of the discharge must be identified as not to arise from injury due to the penetration of the soma with the microelectrode. Injury discharges typically have a very fast firing frequency initially, and as the firing slows the discharges usually become irregular and are often related to movement of the spinal cord due to the action of the respiratory pump; as the microelectrode seals into the neurone the injury discharges generally subside. For these tonically firing inspiratory interneurones the frequency of tonic discharge remained constant. An example of this is shown in the firing rate plot in Figure 4.2.1.D, where the tonic firing frequency remains constant at around 10 Hz. This constant tonic firing frequency is typical of the interneurones classified as tonic inspiratory. Thus it is concluded, that these interneurones are

not the phasic or post-inspiratory interneurones previously described with the tonic component being due to injury discharges. Additional evidence to support this conclusion is provided by the fact that this type of inspiratory/post-inspiratory discharge pattern with a tonic component was seen in interneurones for which the penetration was identified to be axonal, for which injury discharges would not be expected.

This variation in firing pattern of these tonic inspiratory interneurones indicates that there is a high degree of modulation of their firing pattern possibly arising from many sources. There is however no clear indication of the probable functions these neurones are subserving.

The remaining interneurones with inspiratory phasing of their firing or membrane potential are a similar population to those described in the studies of Kirkwood *et al.* (1988) & Schmid *et al.* (1993). For the interneurones that fired during inspiration, incrementing discharge patterns were seen, with the discharges sometimes extending into the post-inspiratory period. In some of the firing interneurones a small depolarisation could be identified in phase with inspiration. The remaining phasic inspiratory interneurones were classified as such according to inspiratory phased depolarisation. This depolarisation is similar to the inspiratory CRDP seen in motoneurones (Sears 1964).

For interneurones with expiratory phasing of their discharge or membrane potential similar types were identified to those in previous studies. For the expiratory interneurones that discharged the predominant pattern was a

decrementing discharge similar to those seen previously (Kirkwood *et al.* 1988; Schmid *et al.* 1993) although less abundant. All of the decrementing interneurones began to discharge in post-inspiration, no interneurones had a late onset to their discharge as seen previously. In the example shown in Figure 4.2.4. a clear abrupt depolarisation of the membrane potential can be seen at the start of expiration, with a similar abrupt repolarisation at the end of expiration. The cause of this depolarisation may be to due to an excitatory input rather than relief of inhibition, although, the origin of this input is unknown.

A further group of interneurones showed an incremental discharge pattern during expiration similar to that previously reported. These expiratory incrementing interneurones frequently had a increase in their membrane potential during the inspiratory phase, an example of which is shown in Figure 4.2.3., this hyperpolarisation during inspiration was frequently incremental. The cause of this hyperpolarisation is unknown, however, there are two possible explanations for the hyperpolarisation. Either, it could be due to the repolarisation of the membrane potential due to the cessation of a phasic excitatory input to the interneurones that drives its discharge; or alternately, the hyperpolarisation could be due to an incremental inhibitory input as seen in motoneurones (Sears 1964) that causes the interneurones to cease its discharge. Neither of these explanation could be confirmed here. The origin of these inputs could be bulbospinal, segmental or most likely from both sources.

One further expiratory phased interneurone had a clear plateau to its discharge similar to those identified previously (Kirkwood *et al.* 1988 & Schmid

et al. 1993). This interneurone had no detectable CRDP. However, the penetration was axonal although relatively close to the soma as determined histologically.

Interneurones were also classified as expiratory on the basis of any respiratory related fluctuations in their membrane potential. These interneurones fell into two categories; those with an apparent depolarisation in expiration and those with an apparent hyperpolarisation in inspiration. The expiratory depolarisation is most likely due to an excitatory input, for the example shown in Figure 4.2.6.A an incremental depolarisation can be seen, suggesting that the interneurones receives an incremental excitatory input. The interneurone that hyperpolarised in inspiration, as shown in Figure 4.2.6.B, has a slow potential typical to that seen during inhibition in inspiration. This supports the earlier hypothesis that the incrementing expiratory interneurones are inhibited during inspiration, and it is possible that there are two strong inputs that modulate their discharge pattern, an excitatory input causing the discharge and, an inhibitory input preventing discharge in inspiration.

A large group of interneurones were identified that displayed no appreciable modulation of their firing or membrane potential. These interneurones were included in the study for several reasons. Firstly under the experimental paradigm not all respiratory interneurones would be expected to receive a strong respiratory drive. Secondly the interneurones probably subserve several functions and may receive a respiratory input in behaviours in the awake animal. And thirdly as many of these were stable recordings they

were suitable for investigating with STA.

The majority of the interneurones could be antidromically identified from the caudal spinal stimulating electrodes. Only the non-respiratory category had a large proportion of interneurones which could not be antidromically activated; with only the expiratory interneurones being predominantly activated from one side of the cord, with the majority of the axons activated contralaterally. No overall pattern in the other categories can be identified. There are however certain technical problems associated with antidromic activation of descending projections. Firstly the position of the stimulating electrodes was only known approximately and may not result in the stimulation of the desired region. Secondly axons may be travelling in portions of the cord that the electrodes do not stimulate and thirdly the stimulating current may spread to the contralateral cord activating contralateral axons. These factors compromise the activation of axons within the cord. In this study however, as interneurones have been labelled the location of their axonal projection can be determined and this compared to the antidromic activation results (see Chapter 4.4.2).

From these data it can be concluded from their firing patterns that these interneurones represent examples of the same populations studied previously using extracellular recordings as their overall firing characteristics and axonal projections are the same as those previously identified. However in this study using intracellular recordings the interneurones can be classifies according to their CRDP and hence a new population is represented here that would not of been detected previously. Additionally, a population of thoracic interneurones

have been identified that do not show evidence of respiratory input. These intracellular recordings provide a population of interneurones in which STA can be performed to identify any connection from the EBSNs.

4.3.3. Spike-Triggered Averaging in Thoracic Interneurones.

The wholly negative results produced from STA indicate the absence of a descending connection to these thoracic interneurones. However, in drawing such conclusions one must consider a number of caveats. Although connections between EBSNs and inspiratory phased motoneurones have been demonstrated in Chapter 3, they were unexpected, and there is no reason to expect to see such connections to interneurones; with this in mind the sample size becomes very small, if all the inspiratory and the non-respiratory interneurones are excluded. The remaining sample then consists of 11 expiratory and 1 unclassifiable interneurones. Some of these penetrations were axonal, and although we believe that this should not always preclude STA, especially if the penetration is close to the soma, we have not as yet demonstrated averaged PSPs in axonal penetrations. Consequently, we must consider this to affect our sample. A feature of the interneurones is the high levels of noise seen in the penetrations when compared to motoneurones. This high level of noise may prevent the identification of small EPSPs. For expiratory interneurones that were discharging it was often difficult to get averages that were free from contamination with spikes; although no such averages have been included here it represents a technical difficulty preventing repeated

averages being made to identify consistent potentials. However one such consistent potential was seen for the interneurones illustrated in Figure 4.3.14 this potential is shown in Figure 4.2.8.A. A terminal potential can clearly be seen in both the intracellular and extracellular average at 7.1 ms after the trigger. Following this TP a positive deflection was consistently seen. However, the rise time is too long for reliable identification of a direct connection.

With these caveats taken into account it is not possible to draw firm conclusions about the connectivity of EBSNs and thoracic interneurones until the sample size is significantly increased and more averages from somatic penetrations are performed, as it is possible that inputs to the dendrites, especially the more distal dendrites are not seen in the axon. However it is known that the expiratory bulbospinal neurones are projecting to the regions of the cord in which the interneurones are located as EPSPs have been identified in motoneurones in the same region as the interneurones. For the expiratory phased neurones in which a connection from expiratory bulbospinals may expected to be most abundant the connection to motoneurones is much higher with 17/41 motoneurones having a connection compared to 0/17 interneurones.

4.3.4. Concluding Remarks.

The interneurones recorded in this study have similar firing patterns to those seen in previous studies interneurones (Kirkwood *et al.* 1988; Schmid *et al.* 1993), and can be concluded to be part of the same population. The firing patterns have previously been compared to the firing patterns of other

respiratory phased neurones within the medulla and spinal cord (Kirkwood *et al.* 1988) and it was suggested that some of the thoracic interneurones possessed *unique* firing characteristics. These unique firing patterns, being described as multiphasic, pump and post-inspiratory (Kirkwood *et al.* 1988), these activities however were not reported in the later study of Schmid *et al.* (1993) and with the exception of the post-inspiratory phased interneurones. However, in this study motoneurones with similar modulation have been identified (see Figure 3.2.5.) indicating that this discharge is not unique to the thoracic interneurones. Consequently, the thoracic interneurones can be considered to have firing patterns many with a similar phasing to other spinal and medullary neurones.

STA was subject to the technical difficulties of maintaining stable somatic penetrations for long durations in interneurones with good membrane potentials and a low level of background noise. With these difficulties taken into consideration and the small sample of expiratory interneurones no firm conclusions regarding the presence or absence of a bulbospinal input can be drawn.

4.4.1. Intracellular Labelling of Interneurones.

A total of 20 interneurones were iontophoretically injected with Neurobiotin, the duration of filling ranged from 5.4 to 116 nA.min (51.3 ± 29.1 mean and SD). The penetrations were believed to be somal for 7, axonal for 6, with the site of penetration being unclear for the remainder. Examples of identified axonal penetrations are shown in Figure 5.3.1.. In Figure 5.3.1.A. a

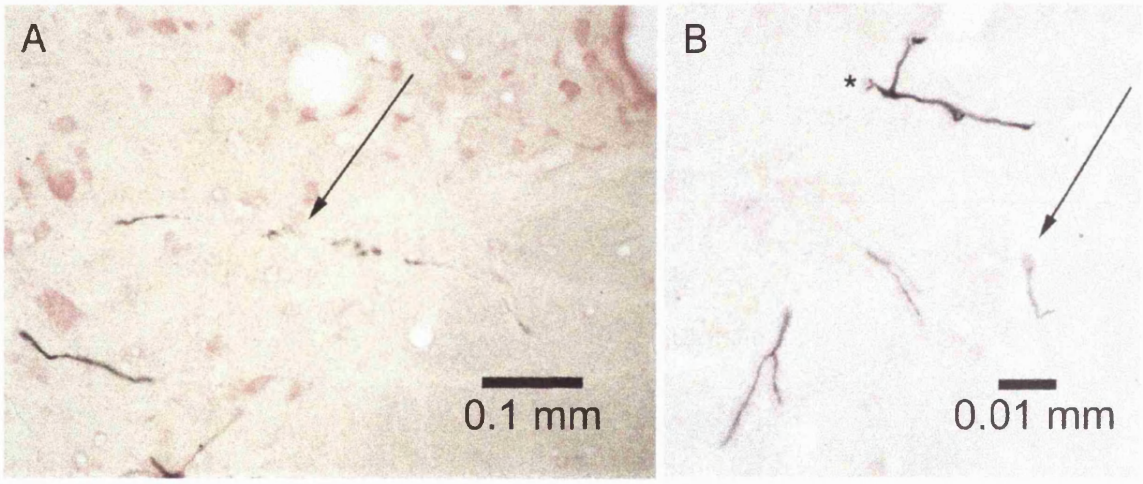

Figure 4.3.1. Photomicrographs of sites of presumed axonal penetration. A. Area of presumed axonal degeneration. Arrow indicates the site of presumed axonal penetration. B. Area of presumed axonal degeneration. Arrow indicates the most proximal piece of axon recovered. Asterisk indicates the origin of a second axon from a primary dendrite.

portion of axon (indicated by the arrow) is missing, and may have undergone degeneration, the Neurobiotin contained within this portion of the axon appears to have been taken up by glial like structures. It is believed that this probable degeneration is a direct consequence of intracellular labelling procedure. The soma of this neurone is shown in Figure 4.3.2.A. and is fully reconstructed in Figure 4.3.6. A further example of probable axonal degeneration is shown in Figure 5.3.1.B. For this neurone the proximal axon was not recovered, at the arrow an area of dilation in the axon can be seen and it is assumed that the proximal axon has degenerated. This interneurones is fully reconstructed in Figure 4.3.13. It is assumed that degeneration of the axon occurs to an equal extent either side of the site of penetration, therefore it is concluded that the axon shown in Figure 4.3.1.A. was penetrated 375 μm from the soma this being consistent with the micrometer readings. The axon in Figure 4.3.1.B. was penetrated 75 μm from the soma as deduced from electrode tracks and the micrometer readings.

A total of 10 interneurones were strongly labelled and full reconstruction of their dendritic trees was possible. A further 5 interneurone somata were recovered that were not well enough stained to allow full reconstruction an example is shown in Figure 4.3.3.F where the soma is lightly stained; this was due to alternate sections (that were reacted separately) having markedly different intensities of staining. Another 3 interneurones had only their axons stained and no evidence of a soma, 2 interneurones were not recovered.

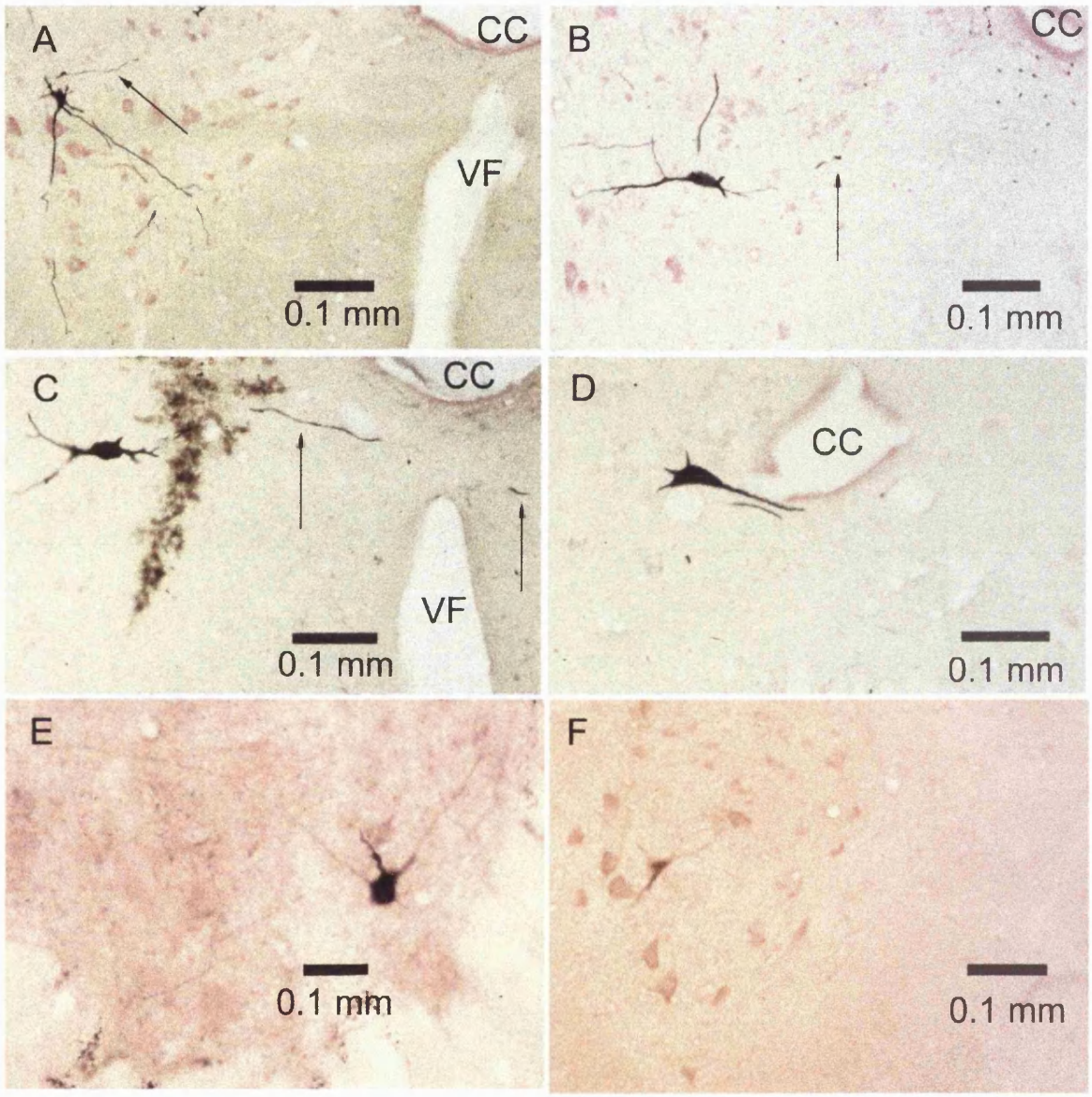

Figure 4.3.2. Photomicrographs of interneuronal somata. A & C. Interneurones in lamina VII. B. An interneurone in lamina VIII. D. An interneurone in lamina X. E & F. Interneurones in lamina IX. Arrows indicate the axon. CC, central canal. VF, ventral fissure.

For the recovered interneurones total of 6 were inspiratory, 3 expiratory and 6 non-respiratory.

4.4.2. Location of the Interneurones.

For the interneurones that had an identifiable soma, the soma lay in segments; T5 (n=3), T6 (n=3), T7 (n=2) or T8 (n=7). The soma were located throughout the ventral horn and intermediate zone; 8 in lamina, 4 in lamina VIII, 2 in lamina IX and 1 in lamina X. Examples of the location of the somata are shown in Figure 4.3.2 and are described schematically in Figure 4.3.16.

4.4.3. Morphology of the Interneurones.

The morphologies of the interneurone somata were diverse but can be considered to be predominantly oval, with the mean soma diameter estimated to be between 21–38 μm (30 ± 5.8 mean ± SD) for the neurones with a section containing a portion of the soma missing (this section being used for immunohistichemical staining for transmitters) and 20-46 μm (26 ± 9.3 mean ± SD) for complete neurones. The interneurones possessed between 5-11 dendrites (7 ± 2.2 mean ± SD n=12). The dendrites were typically tapered, reaching a constant diameter proximal to the first branch point, where the diameter was 5 ± 2.5 μm (mean ± SD). Beaded dendrites (Lipski & Martin-Body 1987) were evident in some interneurones, however they were rarely seen and were not a characteristic feature. The primary dendrites gave rise to between 0 to 4 secondary dendrites (2.2 ± 0.9 mean ± SD) and prior to branching the

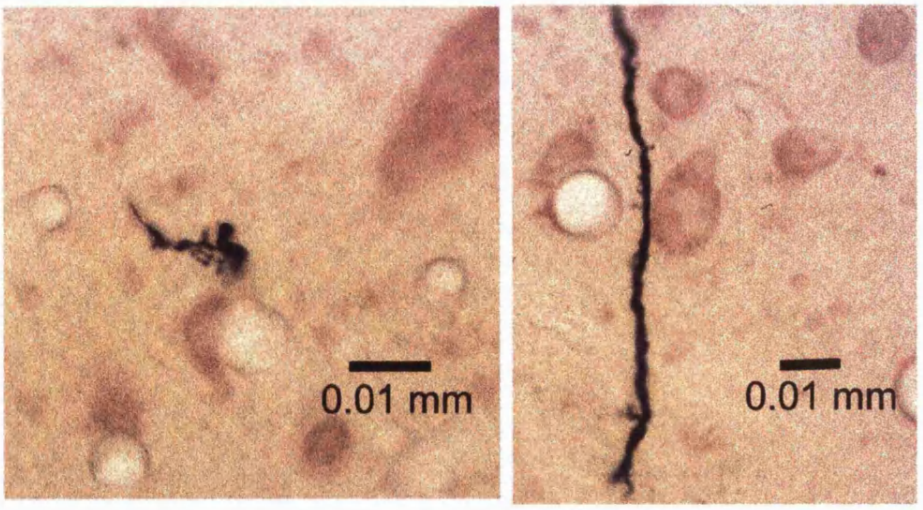

Figure 4.3.3. Examples of spined dendrites.

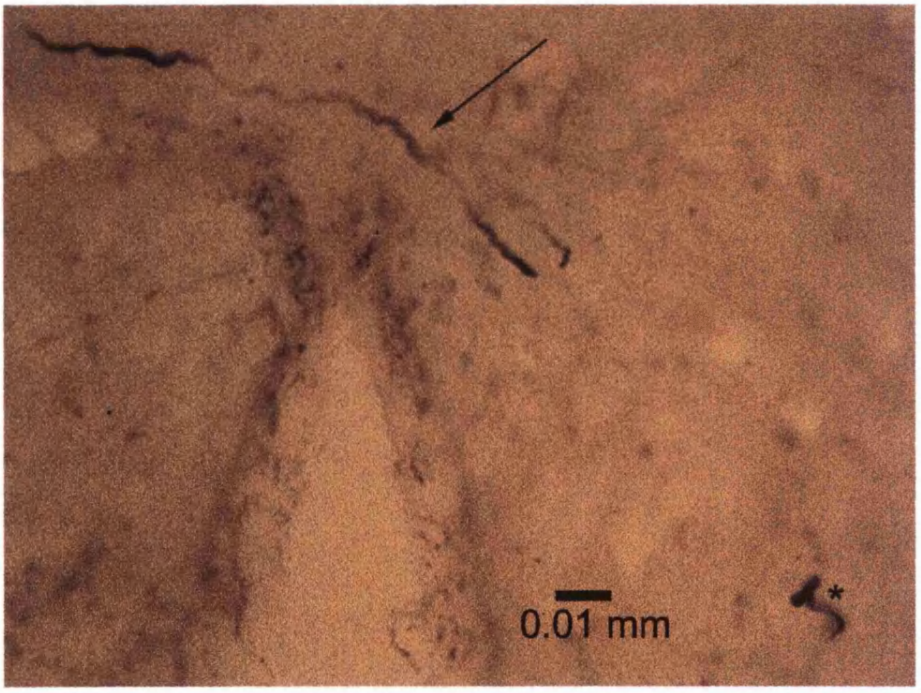

Figure 4.3.4. Photomictograph of a crossing axon. Axon (Arrow) crosses to the contralateral cord and bifurcates into a rostral and caudal running branch. Bifurcation is indicated by the asterisk.

diameter of the dendrite increased. Although occasionally unbranched microdendrites were seen (Lipski & Martin-Body 1987) with diameters of less than 1 μm. The tapered dendrites were highly branched and projected throughout all of the laminae of the ventral horn, examples of which can be seen in Figures 4.3.7–4.3.15 where the entire dendritic projections have been reconstructed. The dendrites were typically devoid of spines and where present the spines tended to be sparse, examples of spines are shown in Figure 4.3.3.. On one occasion, as shown in Figure 4.3.7 dendrites were seen to have a contralateral projection. Over all the dendrites tended to project in the rostro-caudal direction for up to 1250 μm (817 ± 227 mean ± SD) rostral and up to 1500 μm caudally (712 ± 350 mean ± SD) frequently entering the white matter as seen in Figure 4.3.6 and Figure 4.3.14

4.4.4. Axonal Projection of the Interneurones.

The axons were found to arise from the soma (n=7) or dendrites (n=4). However it was impossible to identify the axonal origin for 4 interneurones due to the origin being located in the missing section, poor staining or presumed degeneration of the proximal axon around the site of penetration. In total 11 had contralaterally projecting axons, 2 ipsilaterally projecting axons and 1 bilaterally projecting axons. The contralateral axons predominantly looped rostral from the soma (n=9), moving medially toward the midline and crossing between 1500 μm rostral and 720 μm caudal (511 ± 209 μm mean + SD) to the soma. The majority of the contralateral axons projected caudally (n=8) with 1 projecting only rostrally and 2 having a bifurcating axon that projected both

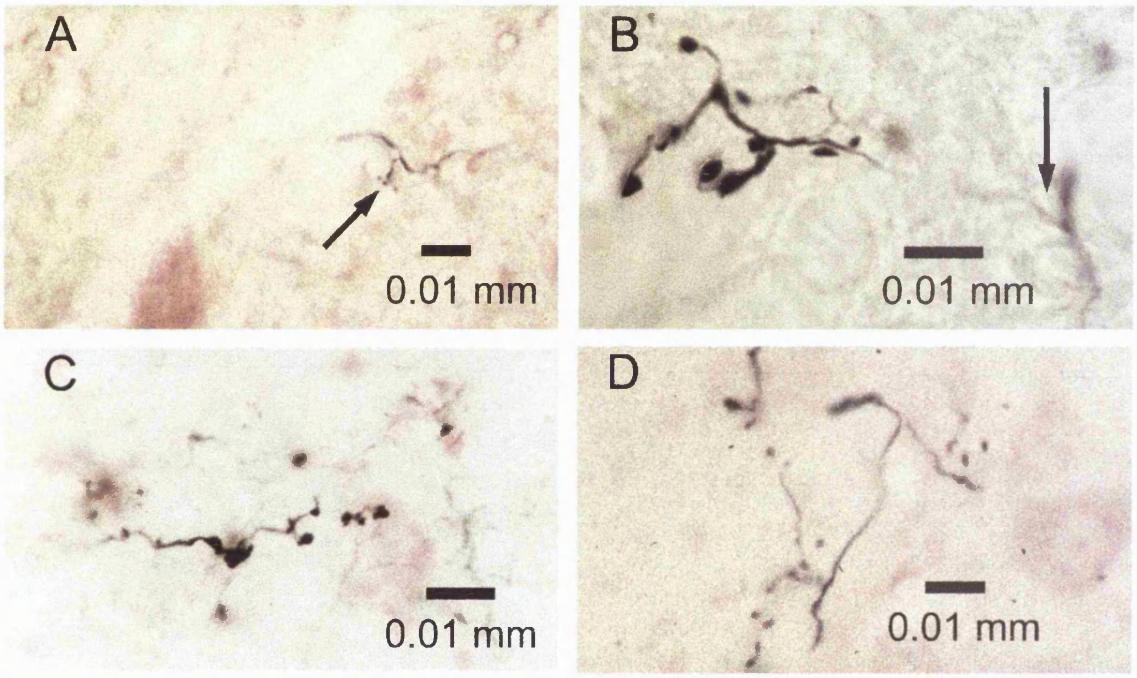

Figure 4.3.5. Photomicrographs of portions of the terminal fields of the interneurones. A. Contralateral collateral branch and small presumed boutons (arrow) of a phasic expiratory interneurone. B. Collateral branch of a non-respiratory interneurone. The arrow indicates the origin of the collateral from the stem axon. C. Part of the terminal field of a non-respiratory interneurone. D. A portion of an ipsilateral collateral from a phasic inspiratory interneurone.

rostrally and caudally. The bifurcation points of the axons are illustrated in Figure 4.3.4 and 4.3.8. After crossing the midline the contralateral axons ran in the medial funiculus and tended to gradually migrate ventral toward the ventral funiculus. The ipsilateral axons projected solely caudally for one interneurone and in both directions for the other, with the axons running in either the medial or ventral funiculus. One interneurone possessed both an ipsilateral and a contralateral axon. For this interneurone the ipsilateral axon projected rostrocaudally in the ventral funiculus and the contralateral axon projected caudally in the medial funiculus, this interneurone is illustrated in Figure 4.3.13. No axon was traced to its terminal arbourisation. The projection of the axons is represented schematically in Figure 4.3.16.

The diameter of the axons measured at a point close to the soma ranged from 2-3.5 μm (2.6 ± 0.6 mean and SD). However, a characteristic feature of the axons was their irregular nature, having a wide variation in their diameter throughout their course. An example of the irregularity is shown in Figure 4.3.4. and can be seen in the reconstructions shown in Figures 4.3.7. - 4.3.10 and also in Figures 4.3.12 and 4.3.14.

Comparison of the projections deduced from antidromic activation with the histologically confirmed axonal projection allows an estimation of the reliability of antidromic axonal identification to be made. For the interneurones with a histologically identified axonal projection 8/14 could be antidromically activated from the caudal spinal electrodes, indicating a descending axonal projection of at least two segments. For the 13 interneurones with a confirmed

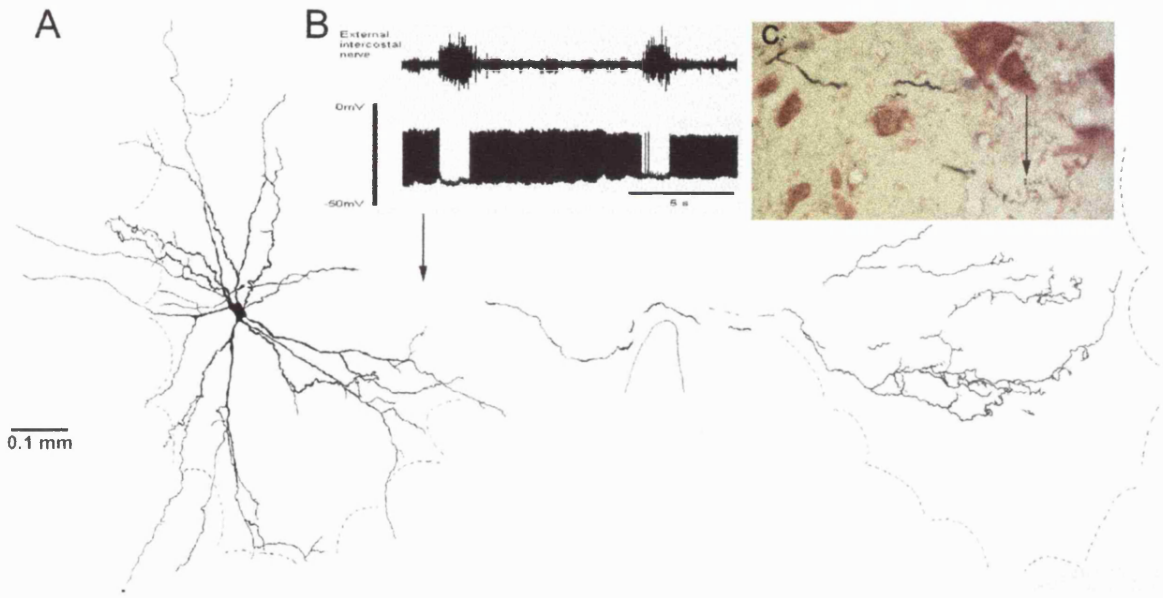

Figure 4.3.6. Reconstruction of a phasic expiratory interneurone and axonal projection. A. Reconstruction of interneurone. Arrow indicates presumed site of penetration B. Firing pattern of the interneurone. C. Photomicrograph of a section of the collateral. Arrow indicates boutons in the region of presumed motoneurone somata

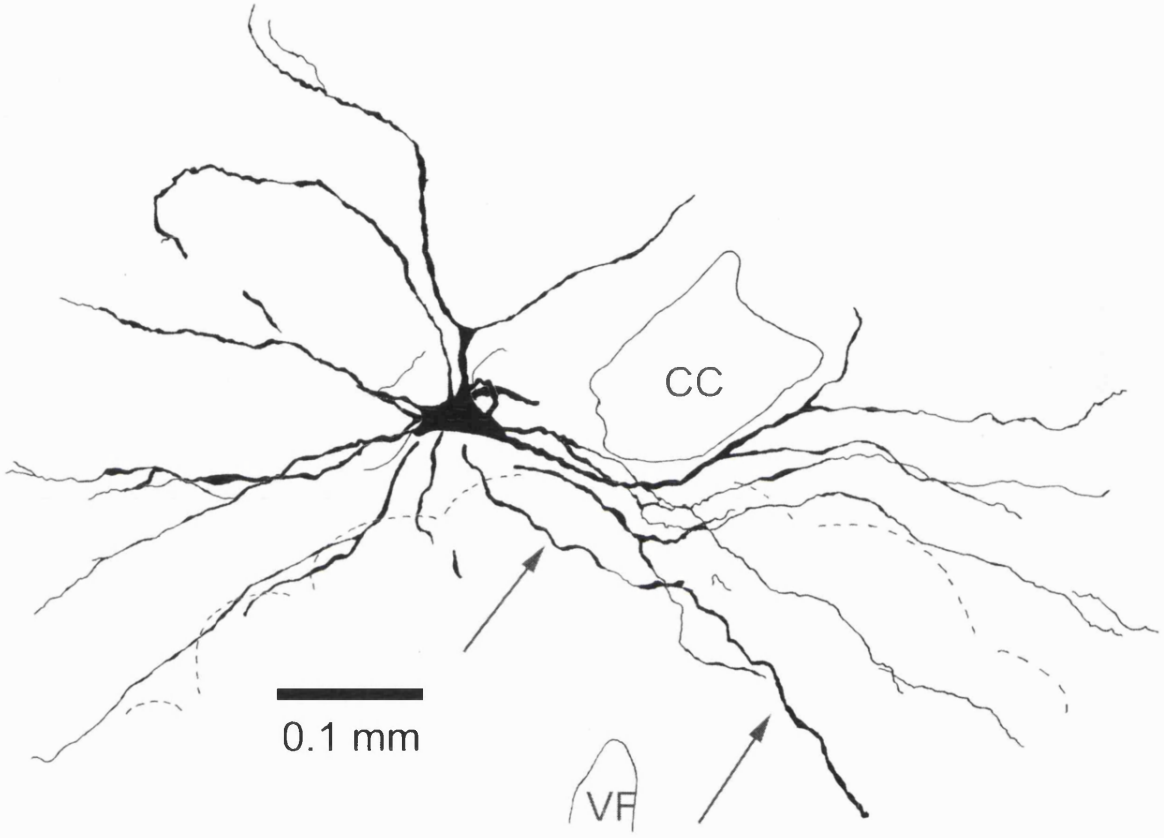

Figure 4.3.7. Reconstruction of a tonic inspiritory interneurone. Arrow indicates the course of the axon. CC, central canal VF, ventral fissure.

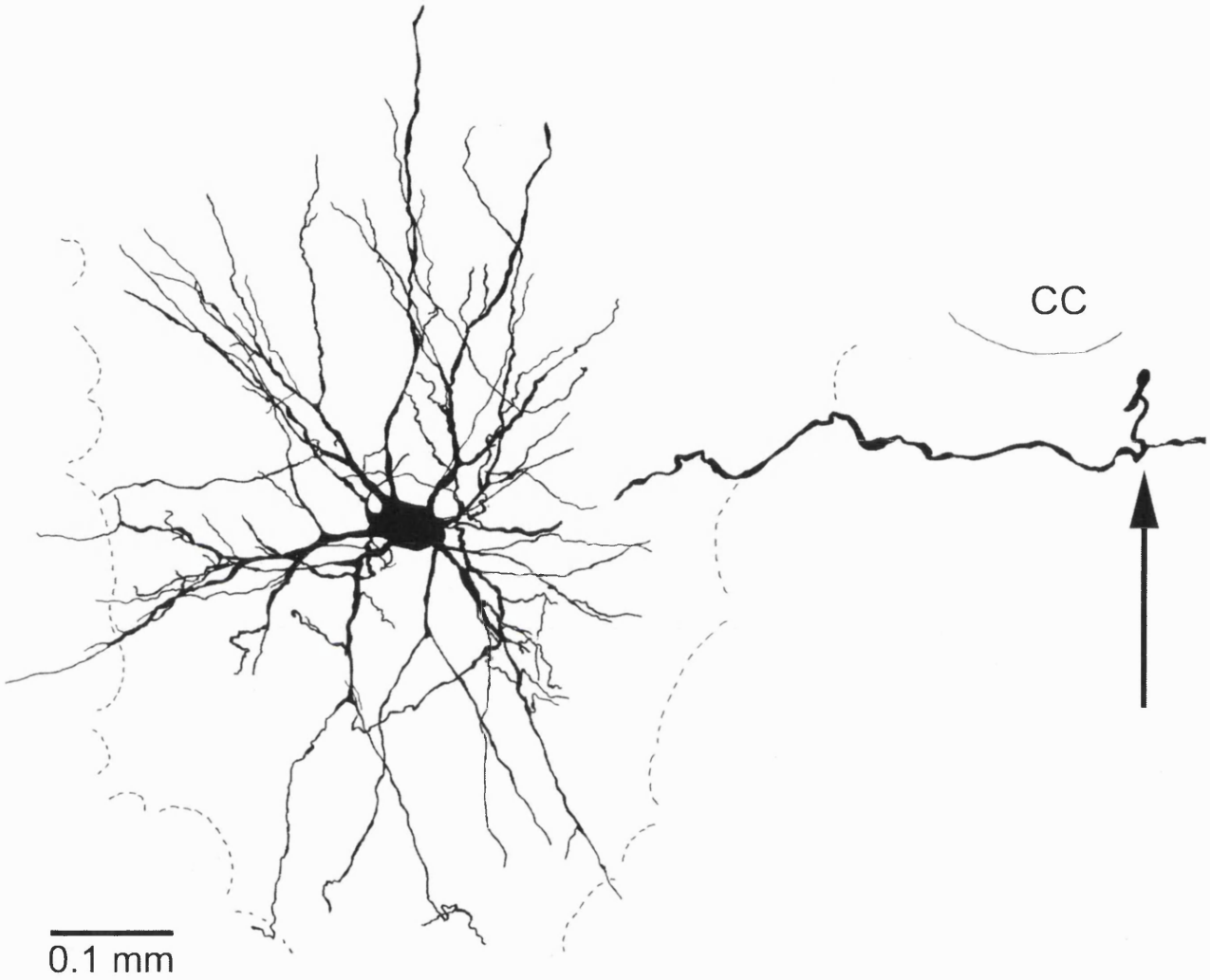

Figure 4.3.8. Reconstruction of a non- respiratory interneurone. Arrow indicates the bifurcation of the axon into rostral and caudal running branches. CC, central cannal

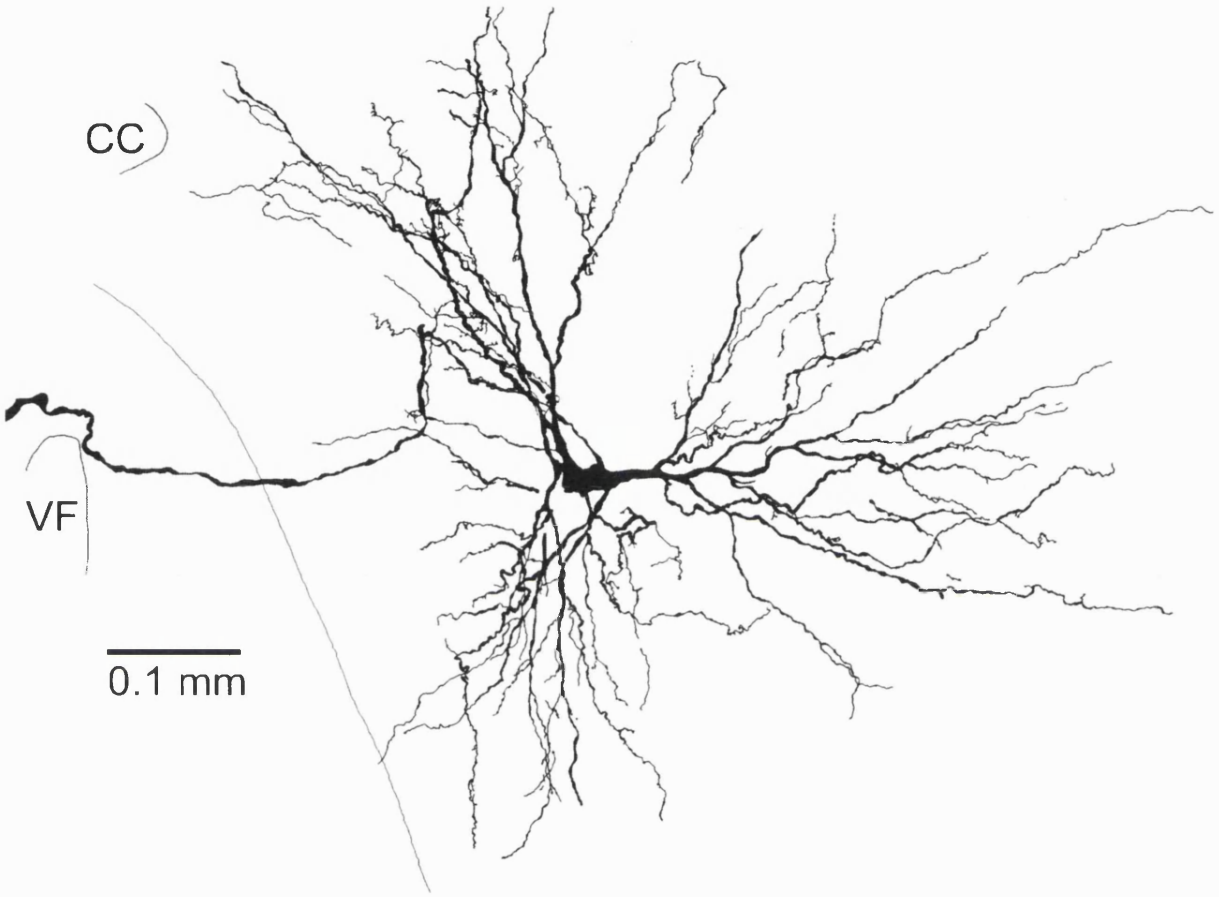

Figure 4.3.9. Reconstruction of an intra-axonally labelled Interneurone. The microelectrode penetration was contralateral to the soma. CC, central canal. VF, ventral fissure.

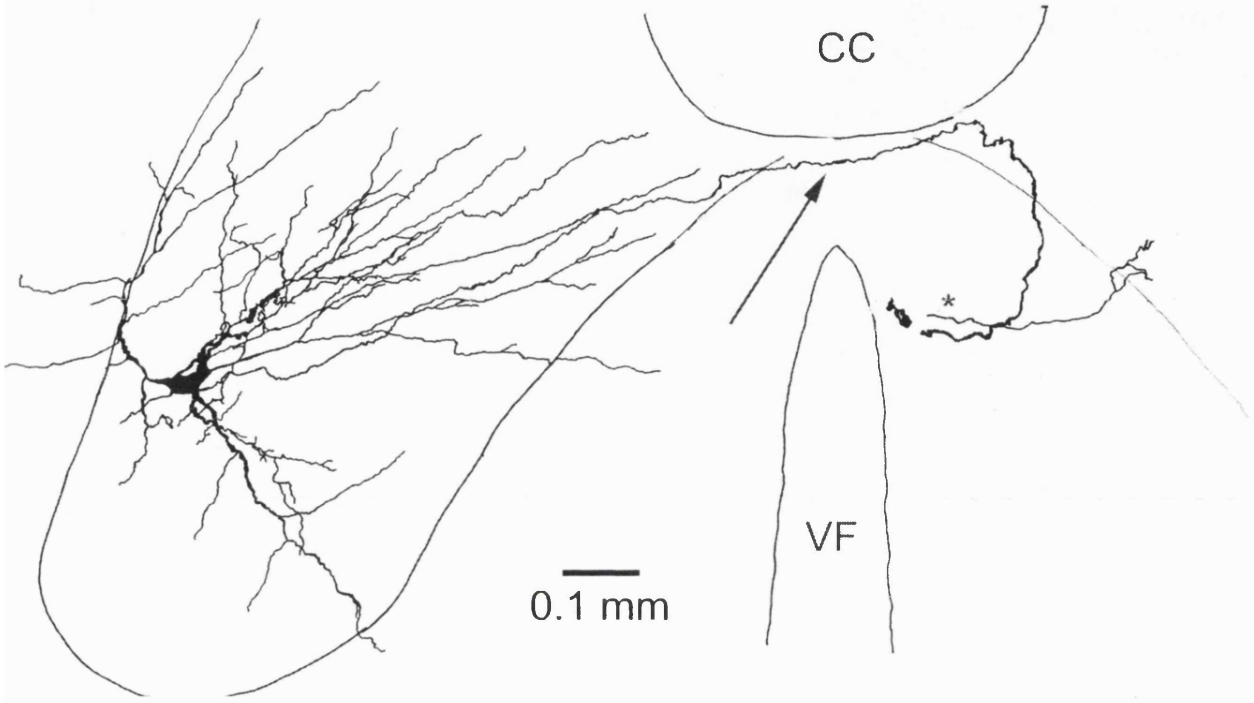

Figure 4.3.10.Reconstruction of a non- respiratory interneurone and its contralaterally projecting axon and collateral branch. CC, central canal. VF, ventral fissure. Arrow indicates axon. Asterisk indicates collateral branch.

descending contralateral axon; 4 were activated contralaterally, 3 ipsilaterally with 1 not being activated at all. Similarly, for the 2 axons descending ipsilaterally; 1 was activated ipsilaterally with the other not being activated at all.

4.4.5. Collateral Projections of the Interneurones.

A total of 14 interneurones and 2 of the 3 axons for which no soma was recovered were considered well enough stained to reveal the existence of collateral branches. Collateral branches were identified in 13 of the recovered interneurones and both of the well stained axons, with a maximum of 4 separate collaterals identified in one neurone. The projection of the collaterals was limited to the side of the cord from which they originated with one exception, where the collateral originated close to the midline and branched profusely bilaterally as illustrated in Figure 4.3.12. No ipsilateral collaterals were seen to arise from axons that crossed to the contralateral cord. The collaterals projected throughout the ventral horn with no projection identified in the dorsal horn. The regions to which the interneurones project is represented schematically in Figure 4.2.17. and examples of individual collaterals are shown in Figure 4.3.5. with reconstructed collaterals shown in Figures 4.3.6, 4.3.10, 4.3.11,4.3.12, 4.3.13, 4.3.14 and 4.3.15.

The collaterals originated between 1.9 mm rostral and 7.1 mm caudal to the soma with the first collateral originating 426 ± 671 μm caudal to the soma. The site of origin of the collaterals is represented schematically in Figure 4.3.16. The collaterals projected laterally and dorsally into the ventral horn and

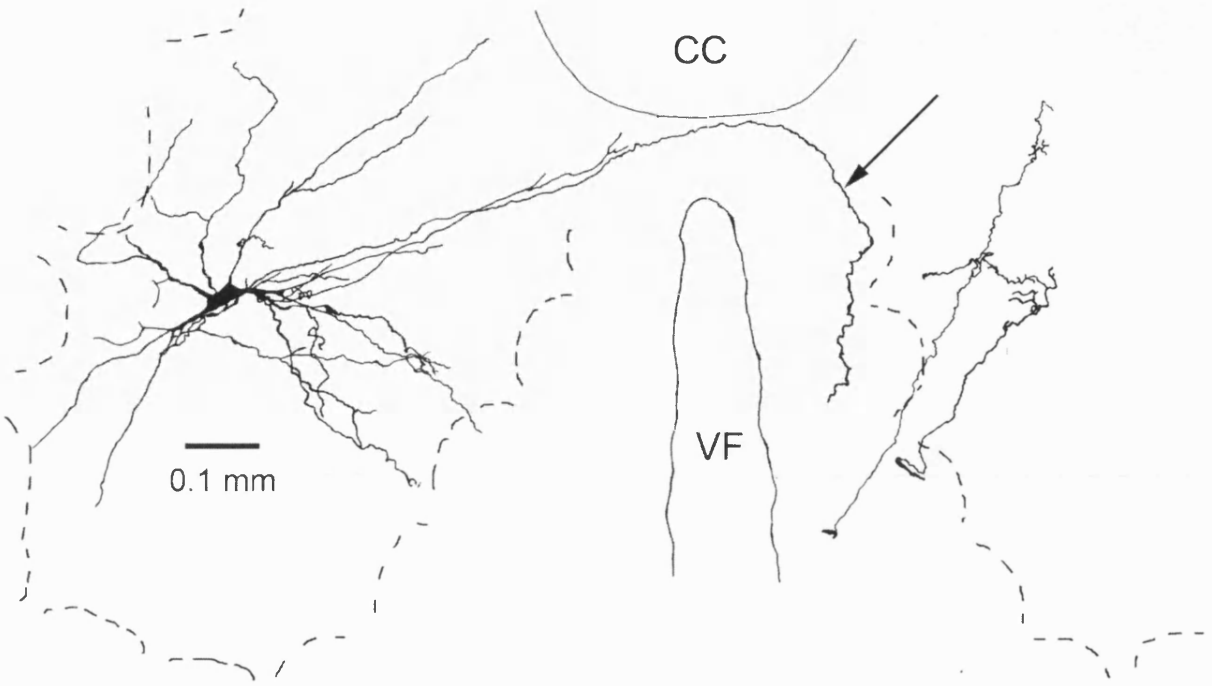

Figure 4.3.11. Reconstruction of a T8 interneurone and its axonal projection with two collateral branches originating 0.5 mm apart Arrow indicated the axon. CC, central canal.
VF, Ventral fissure

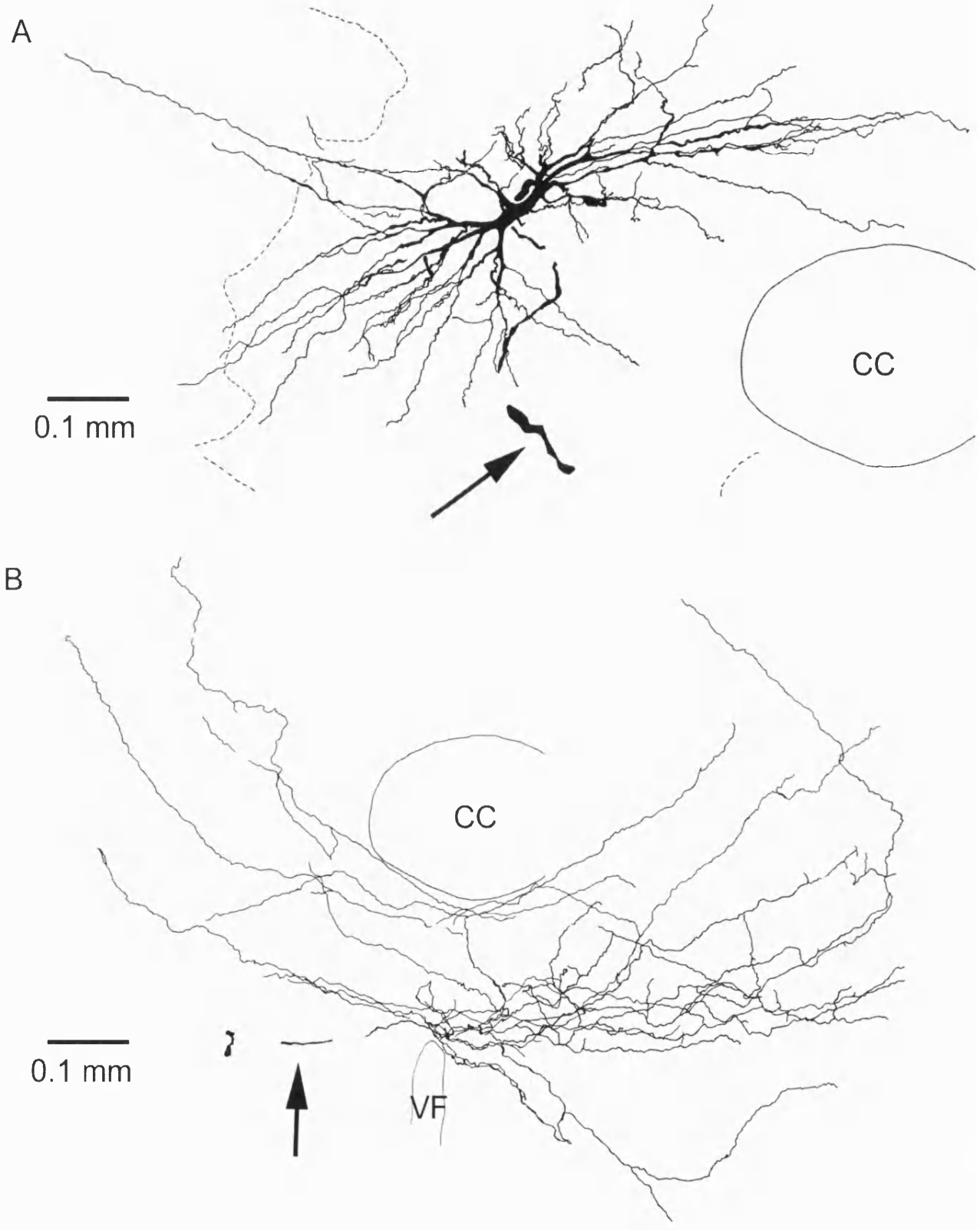

Figure 4.3.12. Reconstruction of a respiratory interneurone.
A. Reconstruction of the interneurone, Arrow indicates the axon.
B. Reconstruction of the collateral. Arrow indicates the stem collateral. CC, Central canal. VF, Ventral fissure.

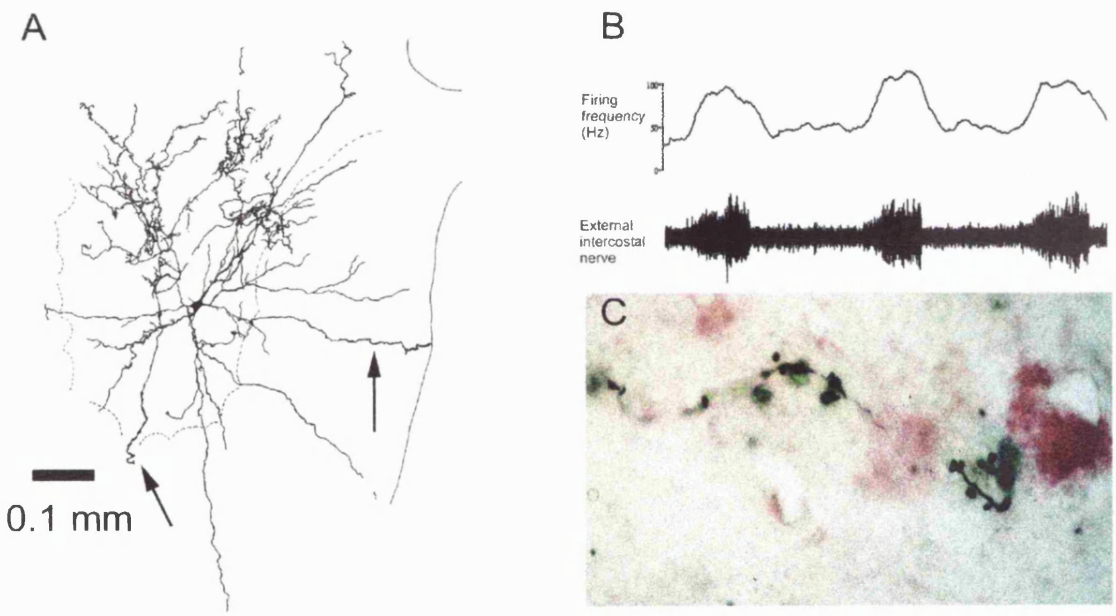

Figure 4.3.13. Reconstruction of a bilaterally projecting inspiratory interneurone. A reconstriuction of interneurone and ipsialteral collateral. Arrows indicate axons. B. Firing pattern of the interneurone. C. Photomicrograph of a portion of the ipsilateral collateral.

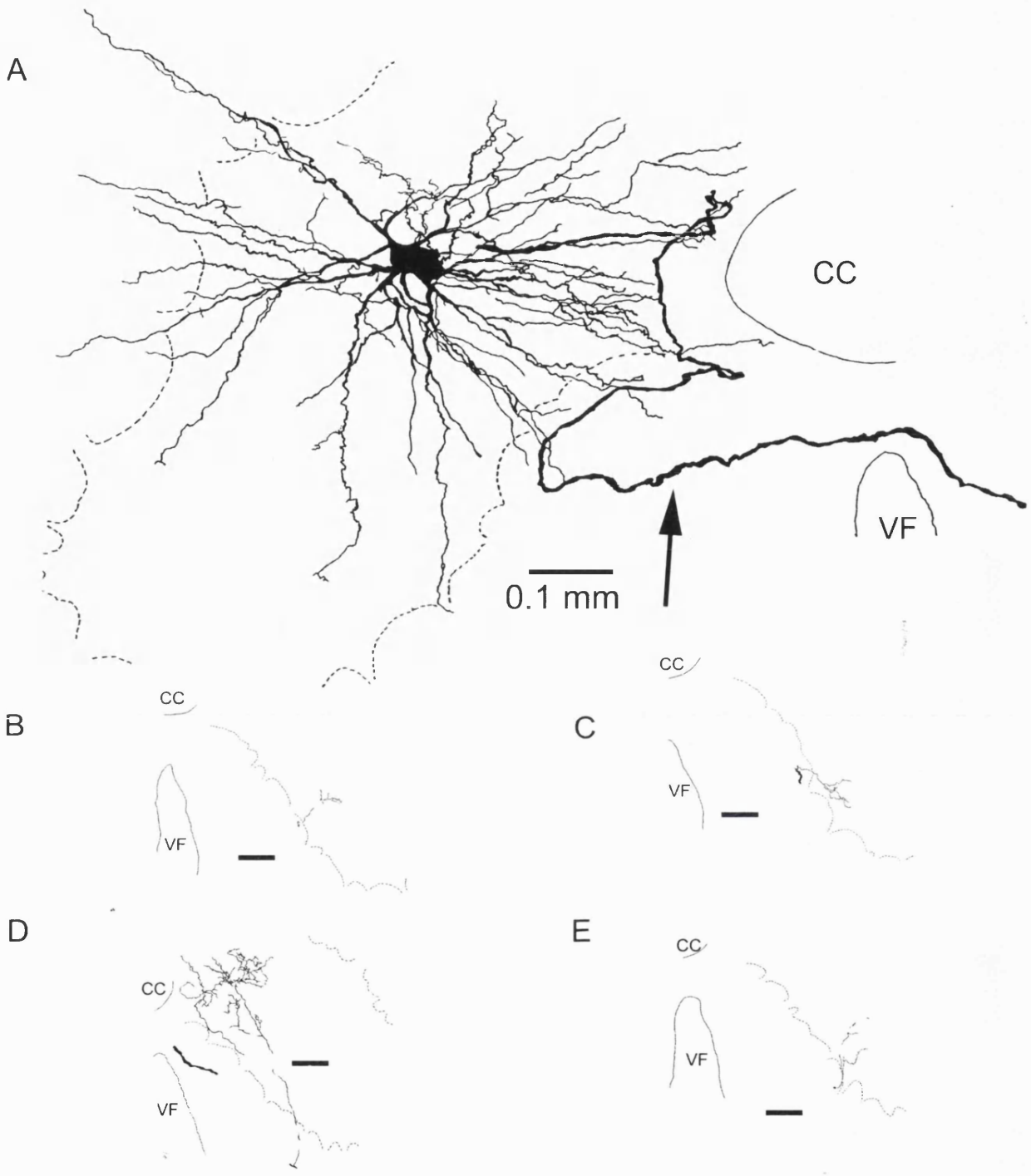

Figure 4.3.14. Reconstruction of a T8 lamina VII interneurone and its contralateral projections. A. Reconstruction of the Interneurone. Arrow indicates the axon. B-D. Reconstructions of four contralateral collaterals. Bars = 0.1 mm. CC, Central canal. VF, Ventral Fissure.

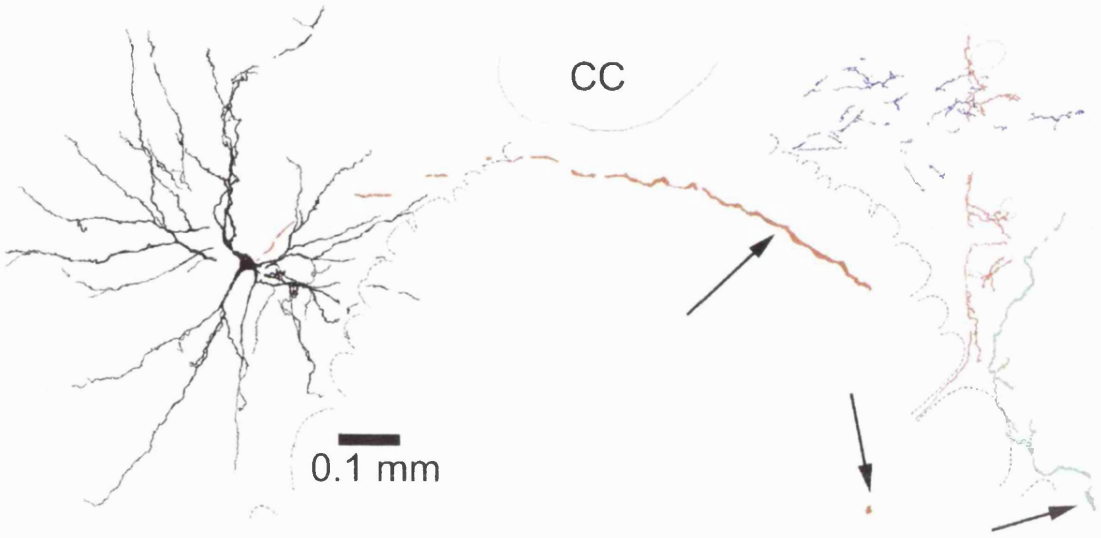

Figure 4.3.15. Reconstruction of an interneurone and its contralateral projection. Arrows indicate the course of the axon. Individual collaterals are coloured blue, red and green and originate in that order. CC, central canal

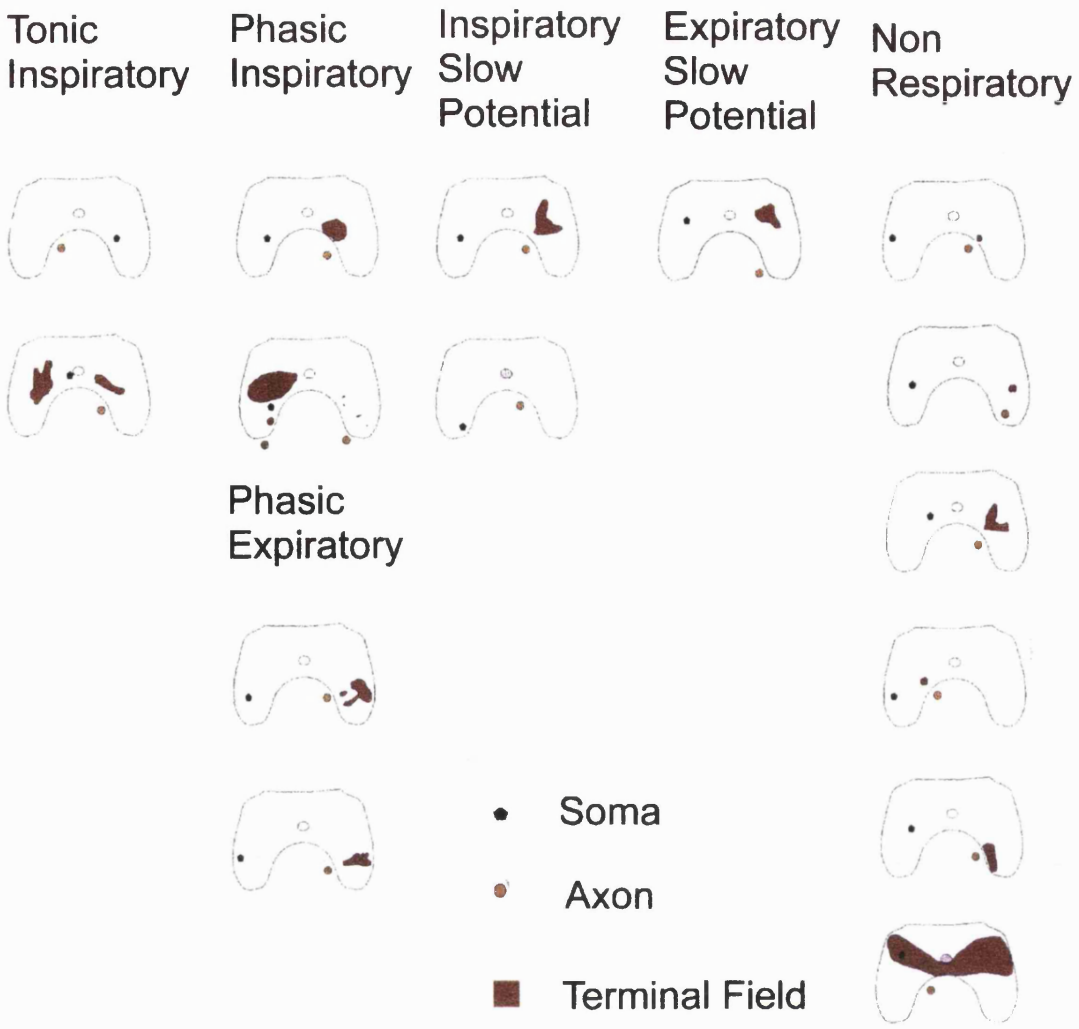

Figure 4.3.16. Schematic showing the relationship between soma location, axon projection and terminal field in the transverse plane. The intereurones are divided according to their respiratory modulation. Note the very small terminal fields contralatrally for the second phasic inspiritory neurone also the first, second and fourth non-respiratory neurones.

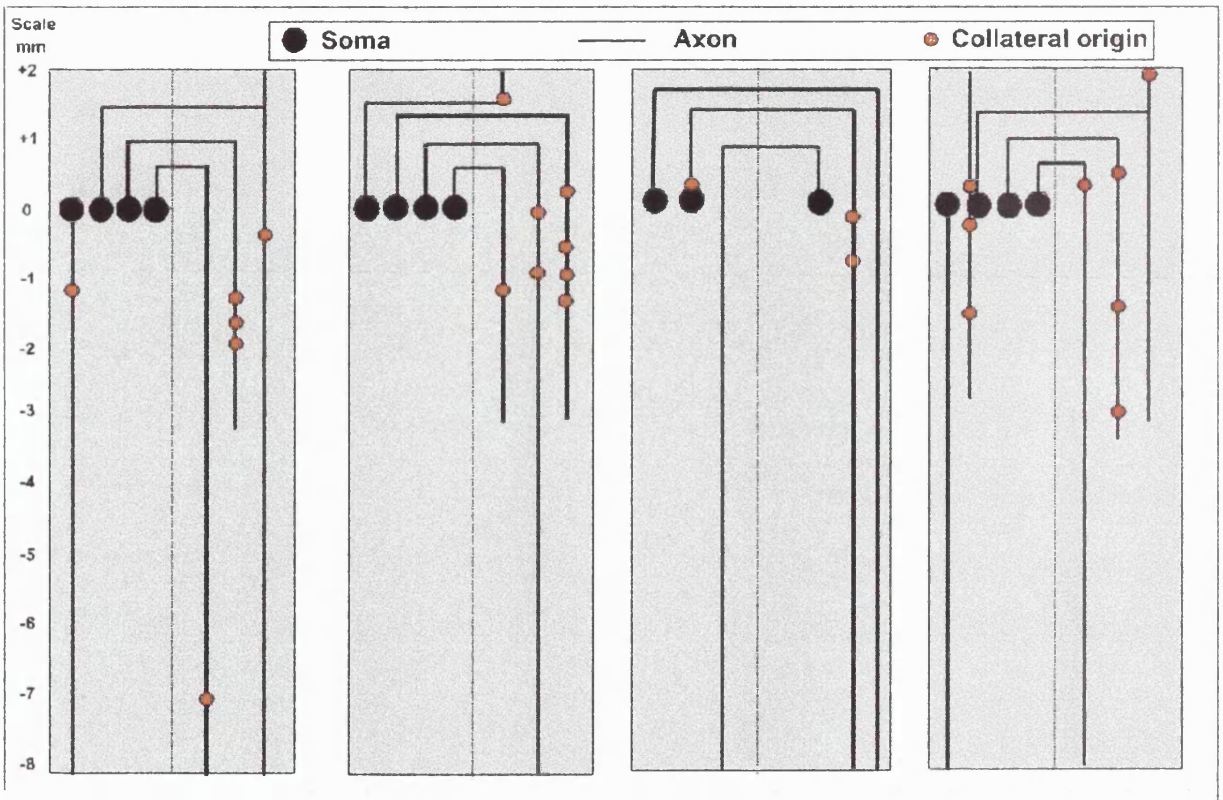

Figure 4.3.17. Schematic diagram illustrating the axonal trajectory and the collateral origins in relation to the soma.

began to branch close to their origins and project rostrocaudally. The collaterals projected principally within lamina VII and VIII, occasionally collaterals projected into lamina IX and X. The collaterals tended to run in a rostrocaudal direction throughout the ventral horn and possessed terminal fields that projected up to 1250 μm in a rostrocaudal direction. The collateral branches were also widely spaced with no collateral projections overlapping each other rostrocaudally.

The collateral branches were characteristically fine and possessed presumed *en passent* and *terminaux* boutons. These boutons were generally sparse and small with diameters ranging between <1 to 7.5μm. One interneurone did however have uncharacteristically large boutons and these are represented in Figure 4.3.5.B. The boutons were occasionally seen to appear to abut counterstained neurones, examples of the boutons are shown in Figure 4.3.5.

One feature of these interneurones is that the more dorsally located neurones tend to project to the same lamina that the soma are located in, whether the projection is ipsilateral or contralateral. This relationship can be seen schematically in Figure 4.3.17. where the area of the collateral projection illustrated in red can be seen to project through a similar portion of the ventral horn and intermediate zone that the soma is located in. This can also be seen in the reconstructions in Figures 4.3.6, 4.3.10-4.3.12 and 4.3.14-4.3.15.

4.4.6. Immunohistochemistry and Confocal Microscopy.

In total the terminal fields of three interneurones were selected for immunohistochemical staining with fluorescent markers. One of these interneurones was a phasic inspiratory interneurone with the other two having little or no respiratory modulation. The collateral projected ipsilaterally for the inspiratory interneurones and contralaterally for the other two, with all the collaterals projecting in lamina VII.

For the collateral of the inspiratory phased interneurone the confocal images of the collateral are shown in Figures 4.4.1 and 4.4.3. In Figure 4.4.1.1-9 the collateral (coloured green) is shown in serial 1 μm thick confocal images. An additional overlay of all 9 serial images (collateral label only) to show the extent of the collateral is shown in Figure 4.4.1.10. Regions of the collateral thought to be boutons are indicated with arrows and can be seen to closely abut gephyrin punctae shown as red, with the close opposition showing as yellow. The collateral does not co-localise with GAD shown in blue and consequently the interneurone can be concluded to be inhibitory with glycine as the transmitter. The likely targets of this collateral are unknown. However, in Figure 4.4.3. a neurone can be seen to be stained blue with the exception of the nucleus indicated by an asterisk. Another portion of a collateral from the same neurone as in Figure 4.4.1 having two terminal boutons, can be seen to make presumed synaptic contacts on the proximal dendrite of the neurone. The identity of this neurone is unknown. However, due to the proximal location of the synapse the inhibitory input from the interneurone is probably

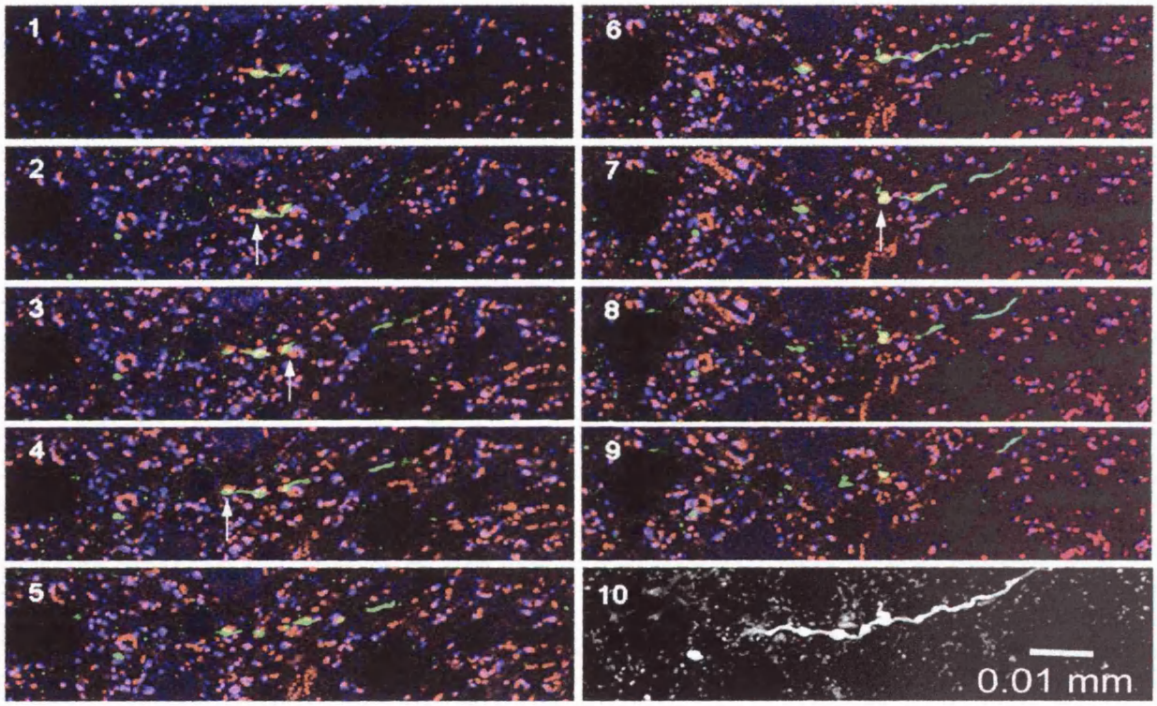

Figure 4.4.1. Confocal images of part of a collateral of a phasic inspiratory interneurone. Serial confocal images (1-9) of a collateral (green) showing boutons (arrow) apposed to gephyrin puncta (red) and not co-localised with GAD (blue). Superimposition (10) of the images to show the extent of the collateral.

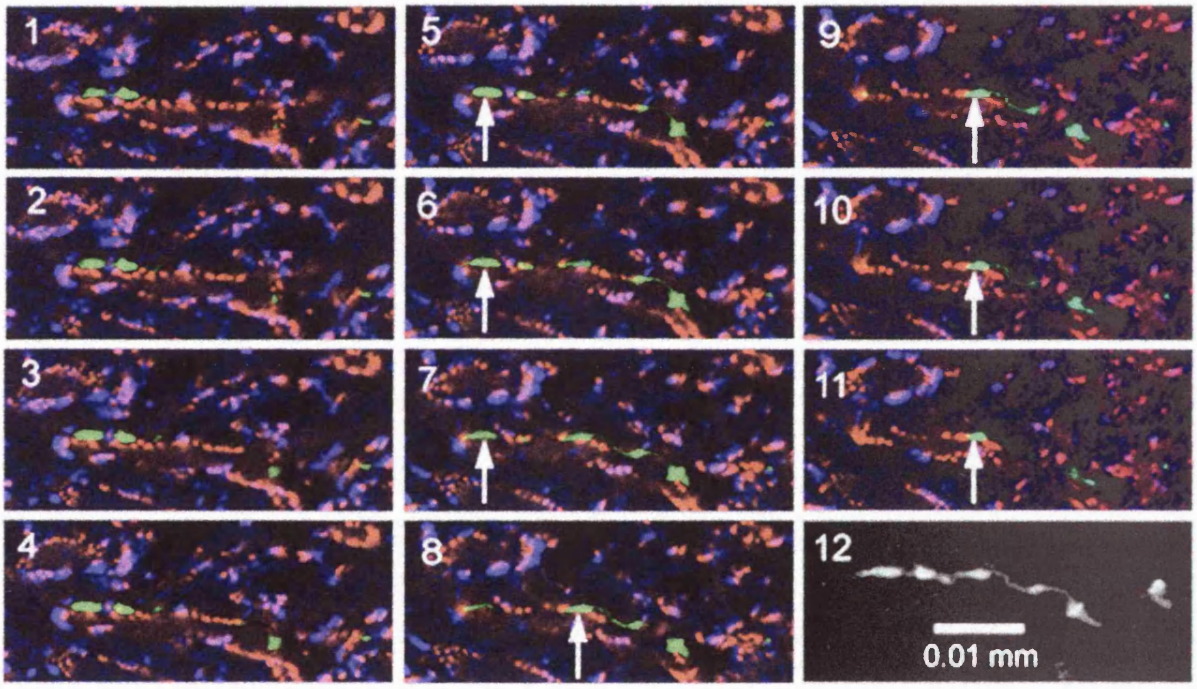

Figure 4.4.2. Confocal images of part of a collateral from a non- respiratory interneurone. Serial confocal images (1-11) of a collateral (green) showing boutons (arrows) not apposed to gephyrin (red) and not co-localized with GAD (blue). Superimposition (12) of the images to show the extent of the collateral.

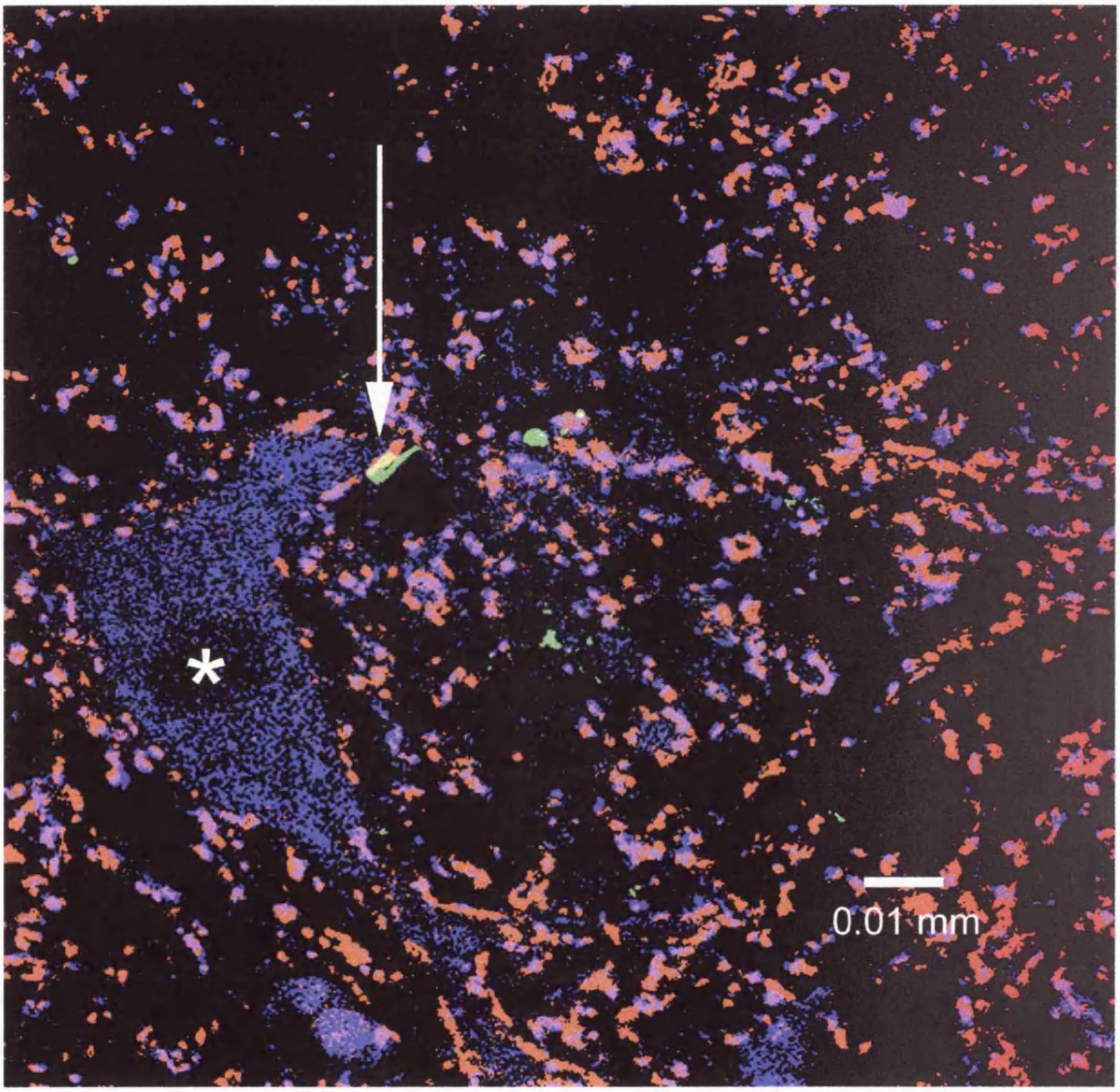

Figure 4.4.3.A single confocal image of part of a collateral of an inspiratory interneurone. Confocal images of a collateral (green) showing boutons (arrow) apposed to gephyrin (red) on a proximal dendrite and not co-localized with GAD (blue). The target neurone can be seen as blue with the exception of the nucleus shown by an asterisk.

strongly inhibitory.

Confocal images from a portion of collateral of a non-respiratory interneurone are shown in Figure 4.4.2, where the collateral is again coloured green. Presumed boutons are indicated by the arrows and are not opposed to gephyrin (red), and any partial appositions did not occur with a greater frequency than that which would be expected to arise by chance. The boutons also do not co-localise with GAD (coloured blue) and consequently this interneurone is unlikely to be inhibitory.

4.5.1. Discussion Relating to the Morphology of the Interneurones.

For the group of interneurones labelled here comparison needs to be made between the population of thoracic interneurones previously described, to see if the interneurones in this study can be considered as part of the same population. Firstly the selection of these neurones and any sampling bias introduced due to the methodology needs to be considered. Secondly, the anatomical data in this study needs to be compared with the location and projections deduced from physiological recordings.

One final issue is whether the thoracic interneurones located in the ventral horn have unique morphological characteristics or are they part of a much larger population of spinal or bulbospinal interneurones that become functionally specialised according to their location as hypothesised by Kirkwood, Schmid & Sears (1993). If this were so one would expect to see

many morphological similarities between the neurones at these locations (see Chapter 4.5.7).

4.5.2. Methodological Considerations.

An important consideration, for any study involving intracellular recordings, is, the sampling bias toward penetrating larger neurones, as these neurones would be expected to be easier to penetrate and be more stable. This is certainly the case when comparing the interneurones with thoracic motoneurones, in which, stable, long lasting penetrations can be achieved with relative ease. In this study we have undoubtedly introduced to some extent a bias toward somal penetrations in larger neurones, that in some cases have dimensions comparable to thoracic motoneurones (Lipski & Martin-Body 1987) with no interneurones labelled with somal diameters as small as 10 μm such as those reported by Schmid *et al.* (1993), although the retrograde labelling probably underestimated the size of the neurones and no counterstaining was used. A significant proportion of the interneurones labelled here have been penetrated axonally, and if the diameter of the axon is proportional to the size of the soma, these penetrations will also be biased toward larger interneurones. The diameters of the axons, however, showed great variation along their courses, in some cases reaching large diameters for relatively small neurones. This variation in diameter may be due to the effects of the labelling, and this will be considered below. We feel however, that axonal penetrations have reduced the sampling bias, as axons with relatively small diameters have been penetrated, the diameter of the axons having been accurately estimated at a

region close to the known site of penetration (see Chapter 4.4.1). Axonal penetrations have also been found to be more stable than somal penetrations and they have significantly increased the sample size.

A further issue that needs to be considered when labelling neurones intracellularly is the toxic effects of the label used. Any toxic effect could cause morphological changes or deterioration of the neurone. It has been shown that in axonal penetrations, deterioration of the axon occurs around the site of penetration, however, it is not known if this is a response to the presence of the label, the effects of sustained current passage or an injury response due to penetration with the microelectrode. What appears to be degradation of the Neurobiotin or possibly degeneration of the neurone occurring in a somal penetration has also been demonstrated (See next chapter). Such responses may account for the complete or partial failure to recover some interneurones. Similarly, degenerative responses may account for the variation in diameter seen in the axons and the occasional beading of dendrites. Although these processes and responses are speculative, they must be considered. However, as these morphological characteristics are not seen to be widespread i.e. only small areas of axon degenerate and widespread beading never occurred and does not represent a significant observation for the overall characterisation of the interneurones.

A large variability in the intensity of staining was evident in many neurones, this variability ranged from very intensely stained neurones to intensities that can barely be detected under the microscope. There are a

number of possibilities that may account for this, but generally fall into two categories; those involving the concentration of Neurobiotin within the neurone and the success of the reaction.

For iontophoretic injections the amount of injected material is never accurately known, this being due to a number of factors, for example, variability in the resistance to passage of the material at the electrode tip (Stone 1985). For the neurones labelled here there is no correlation between the intensity of staining and the duration of the filling, in fact, many motoneurones have been well labelled during penetrations when STA was being performed and no current was passed. Once the Neurobiotin has been injected into the neurone its concentration is affected by many factors, these include, the size of the neurone, the extent of the dispersion of the Neurobiotin and any metabolism that may occur. It has not been observed that smaller interneurones become more intensely stained than larger ones The survival period of the animal after the injection, which will affect the dispersion and metabolism, has however, in some cases appeared to be an important factor. In some animals where long survival times occurred it was more common not to recover the interneurones, and in some cases where multiple interneurones have been labelled the interneurones with the longest survival time were the most poorly labelled, unlike in the study of Lipski *et al.* (1993) where long survival times were said to result in extensive staining . One further observation regarding the transport of label is that for axonally filled interneurones, the somata tend to be well labelled, whereas for somally filled interneurones the axons tend to be most intensely labelled, this suggests that the Neurobiotin is rapidly transported away

from the sight of injection. The above factors are discussed in detail by Stone (1985).

The factor that most profoundly effects the intensity of the staining appears to be reaction with DAB. This is believed to be so for the following reasons. A great variability in the intensity of the reactions was seen between adjacent sections that had been reacted separately. This variation in intensity cannot be accounted for by an uneven distribution of Neurobiotin, as the neuronal structures in each section were microns apart in the intact tissue. The separate reactions used exactly the same reagents at the same concentrations and the reactions were conducted under the same conditions. Despite this, the sections stained differently. There was however one variable factor that may account for some of the variation, this being that the incubation periods varied, with one batch of sections being to left incubate overnight in the avidin solution. Retrospectively, it is not known whether there was any consistency as to which batch of sections, long or short incubation, stained more strongly.

4.4.3. Location of the Interneurones.

The interneurones were present in all the segments from T5 to T8, and although they appeared to be most abundant in T8 this is not necessarily the case as the majority of the experiments preferentially used this segment. The somata of the interneurones appear evenly distributed in the transverse plane throughout the ventral horn, with no preference for a medial location as described by Schmid *et al.* (1993). Similarly, the ipsilaterally projecting

interneurones were not confined to the lateral ventral horn as previously described, although few ipsilaterally projecting interneurones have been stained. Interneurones have here been described in all the laminae of the ventral horn including within the motoneurone pools toward the tip of the ventral horn.

4.5.4. The Morphology of the Interneurones.

The interneurones possessed a range of somal morphologies, although the somata were mostly round or oval. However, all the interneurones possessed dendrites that projected in all directions and they are thus best considered as being multipolar neurones. The shape of the soma found in this study are similar to those described by Schmid *et al.* (1993), but with no spindle shaped cells seen among this population. The mean diameter of the interneurones is less than that described for thoracic motoneurones (Lipski & Martin-Body 1987). Some of the interneurones however have a soma of a size comparable to that of motoneurones; for example, the cell shown in Figure 4.3.2., this cell is also located in lamina IX the location of the motoneurone pools. This cell is not however a motoneurone, as it has a crossing contralateral axon. As mentioned earlier in this chapter, on occasions motoneurones were unintentionally labelled whilst performing intracellular STA. It was observed that many of these motoneurones had somal diameters that lay within the range of that for interneurones. Consequently, it is felt that identifying motoneurones anatomically on the basis of size is unsafe at least in the thoracic cord unless they are very large.

The interneurones have extensive dendritic trees with numbers and types of dendrites comparable to those demonstrated for thoracic motoneurones (Lipski & Martin-Body 1987), the dendrites tapering to a constant diameter proximal to the first branch point. At the branch point the diameter of the dendrite increases as they do in thoracic motoneurones (Lipski & Martin-Body 1987). The diameter and number of secondary dendrites is also comparable to that seen in motoneurones. Though the dendrites project into all laminae of the spinal cord, they appear to project into laminae IX to a lesser extent than the other laminae of the ventral horn (unless of course this is the location of the soma). The fact that the dendrites are seen to cross the midline to project into the contralateral cord has functional implications regarding the size of any descending input as input may be received bilaterally; a similar projection is also evident in thoracic motoneurones (Lipski & Martin-Body 1987). The predominant orientation of the dendrites was seen to be rostrocaudal, however the projection is not as extensive as that seen in thoracic motoneurones (Lipski & Martin-Body 1987) and the dendrites conformed less well to the grey white border as they frequently entered the white matter. The extent of the rostrocaudal projection does however allow for a large amount of descending input to be received from rostrocaudally running bulbospinal collaterals as described by Ford *et al.* (1997). The interneuronal dendrites were characteristically unspined, with spines, when seen, being located on predominantly the mid to distal dendrites; these spines are presumed to be sites of synaptic contact.

Another similarity between the dendrites of interneurones and motoneurones is the presence of microdendrites. These microdendrites do not branch or taper, and are unlikely to be axons as the diameter is very small, with the characteristic 'halo' effect seen around axons due to the myelin sheath being absent. The functional significance of these microdendrites remains obscure. It can only be concluded that their significance is probably minor as they are, due to their size, unlikely to receive a strong synaptic input from other neurones.

The thoracic interneurone is thus widely distributed throughout the ventral horn and as far as morphological differences are concerned they represent a heterogeneous population, with the functional significance of their anatomy probably related to variations in their collateral projections.

4.5.5. Axonal Projections of the Interneurones.

The caudal axonal projections of respiratory interneurones has been deduced from electrophysiological stimulation to be predominantly contralateral (Kirkwood *et al.* 1988; Schmid *et al.* 1993). Most of the interneurones identified in this study also have a contralaterally projecting axon. The crossing axons tend to loop rostrally before crossing the midline following which they run in the medial funiculus or the medial portion of the ventral funiculus. This predominance of crossing axons and the consistent projection of their axons may represent a spinal interneuronal tract. These interneurones may project many segments, although, intracellular labelling is unable to stain them over

many segments. Some of these interneurones also have an additional rostral projection, although this projection is not as abundant as the caudal projection. From the evidence of collateral branching, the targets of this projection lie in the spinal cord. However, targets in the brain itself cannot be excluded. A smaller portion of interneurones were also identified as having an ipsilateral projection, this agrees with the electrophysiologically identified ipsilateral projection (Kirkwood *et al.* 1988).

4.5.6. The Collateral Projection Patterns.

The interneurones in all but two cases can be seen to have inputs to other neurones within the spinal cord as shown by the existence of collateral branches. These projections are mainly to the contralateral cord indicating that these neurones may have some role in co-ordinating the activity of the two sided of the cord. The collaterals are fine with small boutons similar to those seen in the inspiratory interneurones in the cervical cord of the rat (Lipski *et al.* 1993). One consistent observation in the projection patterns of the collaterals is that the collaterals project to the same regions as the soma is located in, with the interneurones with the strongest respiratory modulation i.e. phasically firing interneurones located more ventrally than less strongly modulated interneurones. This is consistent with the theory of Kirkwood, Schmid and Sears (1993) that the strongly modulated phasic interneurones project ventrally toward the motoneurones providing a powerful inhibitory drive, whereas the weekly modulated interneurones provide a tonic excitatory drive to the distal dendrites. Immunohistochemical evidence also supports this with the dorsally

located collateral branches from the two non-respiratory interneurones showing no evidence of inhibitory transmitters, whereas the phasically active interneurone with a more ventral projection having glycine as a neurotransmitter.

4.5.7. Morphological Comparison of the Thoracic Interneurones with other Spinal and Bulbospinal Interneurones.

Many different classes of interneurones have been described in the spinal cord (for review see Jankowska 1975; McCrea 1992; Jankowska 1993), and have largely been identified physiologically. Similarly, within the medulla there is a large population of respiratory neurones with descending axons. These neurones can then be compared with the thoracic interneurones in two ways; either the projections of the neurones identified by antidromic activation can be compared, or direct morphological comparison can be made for neurones that have been intracellularly labelled.

Intracellular labelling of neurones provides much information about the morphology and projection of the axon and collateral branches. The limitation of this technique is that the axonal projection can only be traced for relatively short distances, hence longer axonal projections have to be determined electrophysiologically.

The respiratory neurones in the medulla have a diverse range of firing

patterns as described in Chapter 1; however, a common feature of these neurones that is independent of their physiology is the presence of a long descending axonal projection that predominantly descends in the contralateral spinal cord.

Antidromic activation of the descending axons has identified, with the axons of the respiratory DRG neurones descending contralaterally (Bianchi 1971;1974; Von Euler *et al.* 1973a,b; Berger 1977; Davies *et al.* 1985) in the lateral funiculus, the cVRG neurones descending contralateral (Merrill 1970; Bianchi 1971; 74; Davies *et al.* 1985; Arita, Kogo & Koshiya 1987; Kirkwood, Schmid & Sears 1993; Kirkwood 1995), in the ventral funiculus and the Böt C neurones descending predominantly contralaterally (Kalia, Feldman & Cohen 1979, Lipski & Merrill 1980; Merrill & Fedorko 1984), with only a small ipsilateral projection (Bianchi & Barillot 1982). The neurones of the rVRG have a more diverse projection pattern with ipsilateral and contralaterally projecting axons (Merrill 1970; Bianchi 1971;1974).

Within the cervical cord respiratory phased interneurones have been identified and the descending projection of these neurones have been shown to be ipsilateral (Lipski & Duffin 1987; Hoskin, Fedorko & Duffin 1988; Douse & Duffin 1993).

Intracellular labelling has accurately described the morphology of neurones. The mean somal diameters of intracellularly labelled neurones have been shown to be around 40 μm for the DRG (Berger, Averill & Cameron

1984), 55 μm for the cVRG (Arita, Kogo & Koshiya 1987), 36 μm for the rVRG neurones (Sasaki *et al.* 1989) and 36 to 39 μm for the Böt C neurones (Otake *et al.* 1987).

The number of dendrites the bulbospinal neurones posses ranges from 4-10 for the DRG (Berger, Averill & Cameron 1984), 4-6 for the cVRG (Arita, Kogo & Koshiya 1987). The dendrites project up to 1 mm for the DRG neurones (Berger, Averill & Cameron 1984), 0.9 mm for the cVRG neurones (Arita, Kogo & Koshiya 1987) and 0.6 mm for the Böt C neurones (Otake *et al.* 1987).

The origin of the axon has been identified as either the soma or the dendrite in all of the intracellular labelling studies in respiratory bulbospinal neurones. The axons that cross the midline loop rostrally and cross the midline at the level of the soma (Arita, Kogo & Koshiya 1987; Sasaki *et al.* 1989; Otake *et al.* 1987) or slightly rostral to the soma (Otake *et al.* 1987).

Many similarities between the interneurones characterised in this study and bulbospinal neurons can be seen. The size of the soma, number of dendrites and dendritic projections of these interneurones are within a similar range to the bulbospinal neurones. Also there are similarities in the axonal projection, as the axon arises from either the soma or a dendrite and tends to loop rostrally with the majority of the axons projecting to the contralateral cord.

For the respiratory interneurones in the upper and lower cervical

segments, to date no intracellular labelling data has been published except in the rat (Lipski, Duffin, Kruszewska & Zhang 1993). However, in this study the sample size was very small, and the neurones described had somal diameters between 9 to 25 μm with 3 to 5 dendrites that projected for up to 1 mm. There is thus little similarity between the size or projection these cervical interneurones and the thoracic interneurones described here, however this may be due to interspecies variation.

Neurones of the ventral spinocerebellar tract have been intracellularly labelled in the lumbar segments (Bras, Cavallari & Jankowska 1988). These neurones are located in lamina VII and are larger than the interneurones described here. However they have a similar dendritic projection throughout the ventral horn and also a similar initial axonal projection to the contralateral cord with a collaterals projecting to a similar location to that of the soma in the contralateral cord. It is possible that there was a sample bias in this study toward larger neurones and that the neurone labelled with an ascending axon in this study is part of a similar population of ascending neurones to those described by Bras, Cavallari & Jankowska (1988) and those identified by Tanaka & Hirai (1994).

Interneurones with a group II input have also been stained in lamina VII (Bras *et al.* 1989) and have large soma with dendrites projecting thorough the ventral horn similarly to the interneurones in this study. The axons project both ipsilaterally and contralaterally, but no contralateral axons had a caudal projection. The only caudal projection from these neurones located in the

ventral horn were from ipsilaterally projecting neurones that had an additional rostral branch. This arrangement was seen for one of the neurones in this study and thus may be part of a similar population to that described by Bras *et al.* (1989).

The interneurones described in this thesis can be seen to have many common features with other interneurones within the medulla and spinal cord however it is not yet clear if there is a common organisation of interneuronal types or projections at different levels of the neuraxis.

4.5.8. Summary.

Intracellular recordings have been made from thoracic interneurones penetrated both somally and axonally. Many of these interneurones displayed a respiratory modulation of their membrane potential or firing pattern and the firing patterns seen were diverse in nature. Spike-triggered averaging of the membrane potential failed to identify direct connections from EBSNs.

Intracellular labelling identified interneurones with somata located in all laminae of the ventral and intermediate horn. The somata were typically multipolar and usually possessed tapered dendrites that projected throughout the ventral and intermediate horn. The axons of these interneurones projected predominantly to the contralateral cord crossing the midline close to the somata, with the majority then projecting caudally. A smaller number of interneurones with ipsilateral, bilateral and rostral going projections were also

identified. The axons gave off fine collaterals that projected within the ventral and intermediate horn. These collaterals possessed both *en passent* and terminal boutons that were typically small. Immunohistochemical staining indicated that they possessed either inhibitory or excitatory neurotransmitters.

Chapter 5. The Thoracic Respiratory Renshaw cell.

5.1.1. The Renshaw Cell.

Renshaw (1941) observed that antidromic stimulation of lumbar efferent nerves inhibited the discharge of motoneurones in adjacent nerve branches, initiated by stimulation of the dorsal columns. The magnitude of this inhibition depended on the temporal relationship of the evoked impulses within the cord. It was concluded that motoneurones may exert an inhibitory effect on neighbouring motoneurones, and it was postulated (Renshaw 1941) that this inhibition may be mediated by interneurones excited by motoneurone axon collaterals (Ramón y Cajal 1911). Subsequently, in the lumbar segments of the deafferented cat and rabbit, antidromic efferent stimulation was shown to induce extracellular action potentials of a regular but decreasing frequency (Renshaw 1946). These action potentials were attributed to the somal discharge of interneurones in the ventral horn (as defined by motoneurone field potentials), occurring with a minimum latency of 0.6-0.7 i.e. equivalent to one synaptic delay. These data thus supporting the hypothesis that motoneurone axon collaterals activate interneurones that inhibit adjacent motoneurones (Renshaw 1946).

Further investigation of these cells employing intracellular recordings were performed by Eccles Fatt & Koketsu (1954). Inhibitory post-synaptic potentials (IPSPs) were identified in motoneurones in response to antidromic

stimulation in deafferented cats, and occurred at around an appropriate latency to be consistent with an input from the cells identified by Renshaw. It was further observed, that within the trajectory of the IPSP there were incremental steps that appeared to be of the appropriate frequency range of observed interneurone discharge. Consequently, it was concluded that the increment of discharge frequency, duration and often decrease in onset latency with increased stimulus intensity was consistent with these cells, posthumously named Renshaw cells receiving innervation from several motoneurone collaterals.

The first intracellular recording from a Renshaw cell (Eccles, Fatt & Koketsu 1954) gave anecdotal evidence of an excitatory post-synaptic potential (EPSP) induced from antidromic motoneurone activation. Subsequently, EPSPs with fast and slow time courses were recorded in Renshaw cells stimulated via antidromic ventral root stimulation (Eccles *et al.* 1961a). Latterly, a direct connection between Renshaw cell and motoneurone was demonstrated by Van Keulen (1981), by a combination of extracellular recording from Renshaw cells and intracellular STA in motoneurones, at the same rostrocaudal location. This connection was shown to be autogenic, i.e. the inhibition acting back on the motoneurone that induced the inhibition, and non-autogenic where the inhibition affects other neurones. A direct connection between motoneurones and Renshaw cells has also been demonstrated by Hamm *et al.* (1987), by averaging the membrane potential of the motoneurones after stimulation of single motoneurone axons.

The input to Renshaw cells is not solely segmental as there is evidence of a descending input to Renshaw cells located in the cervical cord (Hilaire, Khatib & Monteau 1986). Renshaw cells showed respiratory modulation, and increasing the central respiratory drive (CRD) by tracheal occlusion, 'enhanced Renshaw cell reactivity'. However, this could either be due to increased activity in the phrenic motoneurones or greater CRD acting on the Renshaw cells. The intravenous administration of mecamylamine, a nicotinic acetylcholine antagonist (Hilaire, Khatib & Monteau 1986) had no persistent effect on the modulation, suggesting the modulation was not due to increased motoneurone input. Also, the observation that maximum responses to stimulation were seen during the transition between expiration to inspiration when the phrenic motoneurones are not active supports a CRD acting on the Renshaw cells.

Pharmacological investigations of Renshaw cell activity were performed by Eccles Fatt & Koketsu (1954). The systemic administration of nicotinic acetylcholine antagonists and anticholinestreases produced a depression and potentiation of Renshaw cell discharges respectively. It was postulated that Renshaw cells were excited cholinergically via motoneurone collaterals. Administration of strychnine was shown to decrease the size of the IPSP in the motoneurone in a dose dependent manner, implying that glycine was a likely transmitter at these synapses (Eccles Fatt & Koketsu 1954). Similarly, strychnine was shown to completely abolish the motoneuronal IPSP in some neurones, while in others, a residual strychnine insensitive inhibition having a central latency typical of a disynaptic input remained, but was abolished by bicuculine and picrotoxin. Application of both antagonists (Cullheim & Kellerth

1981) completely abolished the IPSP indicating co-transmission at some Renshaw cell synapses. This is consistent with the possibility of a proportion of Renshaw cell IPSPs having two components (Hamm *et al.* 1987).

The extent of the recurrent inhibition seen in motoneurones is dependent on the distance of the motoneurone soma from the stimulated motor group (Eccles *et al.* 1961b; Hamm *et al.* 1987b). Similarly, peri-stimulus time histograms (PSTHs) of motoneurone discharges, expressed as cumulative sums (CUSUMs) (Ellaway, 1971) have shown an intersegmental decline in the strength of recurrent inhibition in the thoracic segments (Kirkwood, Sears & Westgaard 1981), and between adjacent segments in phrenic motoneurones (Lipski, Fyffe & Jodowski 1985), where the CUSUM showed a differential inhibition between segments. However, in the nerves supplying neck muscles the relationship between the proximity of the motoneurone and the strength of the recurrent inhibition is less clear (Brink and Suzuki 1987), with the strength of the recurrent inhibition in C4 being greater than in C3, when the C3 nerve is stimulated. Recurrent inhibition, with one exception always occurs ipsilaterally; the exception being the crossed recurrent inhibition demonstrated in the sacral cord for nerves innervating the tail muscles (Jankowska, Padel & Zarzecki 1978). Overall it appears that there is a powerful topographic distribution of recurrent inhibition and that the action of Renshaw cells is most profound close to the motoneurone that stimulates them (Eccles *et al.* 1961b; Kirkwood, Sears & Westgaard 1981; Hamm *et al.* 1987b; Lipski, Fyffe & Jodowski 1985) than in more distant segments.

Recurrent inhibition is not only limited to α-motoneurones. Recurrent inhibition has been identified in group Ia interneurones identified close to but outside the motor nucleus (Hultborn, Jankowska & Lindström 1968), although restricted to the interneurones with a more ventral location (Hultborn, Jankowska & Lindström 1971b), Renshaw cells (Ryall, Piercey & Polosa 1971) and γ-motoneurones (Ellaway 1971).

Renshaw cells can be defined by their firing characteristics as well as by the identification of a recurrent EPSP (Renshaw 1946, Eccles Fatt & Koketsu 1954, Eccles *et al.* 1961a). Renshaw cells exhibit an initial high frequency decrementing discharge in response to antidromic stimulation of motoneurone axons and it has been hypothesised (Ryall 1970), that the decrementing portion of the discharge is due to the activation of muscarinic acetylcholine receptors. This characteristic discharge, however, was not seen to occur spontaneously in the lumbosacral cord in anaesthetized or decerebrate preparations (Renshaw 1946, Eccles Fatt & Koketsu 1954, Eccles *et al.* 1961), thoracic Renshaw cells (Kirkwood, Sears & Westgaard 1981), cervical Renshaw cells innervating the neck muscles (Brink and Suzuki 1987), or phrenic motoneurones (Lipski, Fyffe & Jodowski 1985) hence the functional significance of the discharge is questionable and may merely be a consequence of the stimulation paradigm.

Increasing the antidromic nerve stimulus strength causes Renshaw cells to fire a higher frequency longer discharge (Brink and Suzuki 1987), this being a consequence of the recruitment of greater numbers of motoneurones at higher stimuli strengths thus producing a stronger input to Renshaw cells. The

likelihood of such a powerful input to Renshaw cells occurring during non-tetanic movements is thus questionable. It is however possible, that the anaesthetic protocol used suppresses the spontaneous activity of Renshaw cells (Renshaw 1946; Eccles Fatt & Koketsu 1954; Hamm *et al.* 1987). Similarly, paralysis may decrease Renshaw cell excitability (Kirkwood, Sears & Westgaard 1981).

Spontaneous Renshaw cell discharges have however been described in the majority (18/33) of cervical Renshaw cells stimulated by phrenic motoneurones (Hilaire, Khatib & Monteau 1986) in heavily barbiturate anaesthetised animals with a caudal spinal section. This would suggest that the use of anaesthetic does not prevent activity occurring spontaneously in these Renshaw cells, as under anaesthesia breathing is principally diaphragmatic and hence retains its functional integrity.

Initially, the distribution of Renshaw cells was considered to be limited to the lumbar spinal cord (Renshaw 1946) and not seen in other regions of the spinal cord or brainstem. However, neurones with characteristic Renshaw cell activities have since been identified in the cervical (Lipski, Fyffe & Jodowski 1935; Hilaire, Khatib & Monteau 1986; Brink and Suzuki 1987), thoracic (Kirkwood, Sears & Westgaard 1981) and sacral cord (Jankowska, Padel & Zarzecki 1978). Renshaw cell mediated recurrent inhibition thus appears to be a widespread phenomenon affecting motoneurones within the spinal cord with perhaps the exemption of some muscle groups with no antagonists (Mackel 1979), although this is not supported in the case of the diaphragm (Lipski, Fyffe

& Jodowski 1985).

From early electrophysiological recordings (Renshaw 1946; Eccles, Fatt & Koketsu 1954) the location of Renshaw cells somata was deduced to be in the ventromedial ventral horn. Subsequent lesions (Willis & Willis 1964), dye injection (Thomas & Wilson 1965) and finally intracellular labelling (Jankowska & Lindström 1971) identified Renshaw cells as lying in ventromedial lamina VII in the region of motoneurone collaterals (Ramón y Cajal 1911).

Anatomical characterisation of physiologically identified Renshaw cells, by intracellular labelling with procion yellow (Jankowska & Lindström, 1971), revealed cells with somal diameters of 10-15 μm with evidence of funicular axons. Subsequently, intracellular Labelling with HRP has revealed that Renshaw cell somata are located ventromedially in laminae VII (Van Keulen 1971; Largerbäck & Kellerth 1985; Fyffe 1990; 1991), although one cell was identified as being more ventrolateral (Fyffe 1990; Jankowska, Padel & Zarzecki 1978). Typically larger somal diameters were seen than in the Jankowska & Lindström study having somal diameters of about 20x26 μm (Van Keulen 1979) and mean diameters of 21-33μm in presumed Renshaw cells (Largerbäck & Ronnevi 1982a) and 29.4 μm (Largerbäck & Kellerth 1985), 40.5 μm (Fyffe 1990) in identified Renshaw cells. The smaller sizes in the Jankowska & Lindström, study may be due to cytotoxicity of procion yellow (Largerbäck & Ronnevi 1982a).

The morphology of the soma has been described as spherical

(Largerbäck & Kellerth 1985), elongated (Largerbäck & Ronnevi 1982a; Fyffe 1990), ovoid, irregular or fusiform (Fyffe 1990). It was thus proposed (Fyffe 1990) that there were two distinct morphological types of Renshaw cells (multipolar and fusiform) and they may represent functionally distinct classes of Renshaw cells (Fyffe 1990) having different pharmacologies (Cullheim & Kellerth 1981). There is however as yet no direct pharmacological or indirect immunohistochemical data to support subpopulations of Renshaw cells with different transmitter systems. There being no difference in somal diameters between the proposed populations, the fusiform cells may merely be natural variants.

Renshaw cells have been shown to have 4-8 (Van Keulen 1979; Largerbäck & Kellerth 1985) or 3-7 (Largerbäck & Ronnevi 1982a; Fyffe 1990) dendrites. The dendrites have been shown to project 0.7 mm within laminae IX, VIII and throughout laminae VII, exclusively ipsilaterally (Largerbäck & Kellerth 1985; Fyffe 1990), occasionally entering the ventral white matter (Largerbäck & Kellerth 1985). The dendrites were generally sparsely branched. Some were unbranched while others bifurcated (Largerbäck & Kellerth 1985; Fyffe 1990) although one trifurcation could not be excluded (Largerbäck & Kellerth 1985a).

The origin of the axon has been identified as occurring at both somatic and dendritic locations (Largerbäck & Ronnevi 1982b; Largerbäck & Kellerth 1985; Fyffe 1990). Intracellular Labelling has identified axons stained for 3 mm (Van Keulen 1979) and 2.7 mm (Largerbäck & Kellerth 1985). All Renshaw cells have axons that run in the ventral funiculus (Jankowska & Lindström 1971;

Jankowska & Smith 1973; Van Keulen 1979; Largerbäck & Kellerth 1985; Fyffe 1990;1991) ipsilaterally with the exemption of the one Renshaw cell stained in the sacral cord (Jankowska, Padel & Zarzecki 1978) that had a contralaterally projecting axon. The axons have diameters ranging between 2.1 and 10μm (Largerbäck & Kellerth 1985a) and there was much variation of individual axonal diameters. The axons were shown to project both rostrally and caudally (Van Keulen 1979; Largerbäck & Kellerth 1985a; Fyffe 1991), although some axons were reported to only have a rostral projection (Largerbäck & Kellerth 1985a). However, in the absence tests for caudal antidromic activation, and with the possibility that penetrations were axonal and rostral to the soma, caudal axons in all Renshaw cells cannot be excluded, as the label may not have been adequately retrogradely transported.

In Van Keulen's (1979) study collateral branches have been demonstrated in lamina IX and also in lamina VII and VIII caudally. Although boutons were not clearly demonstrated in this study, the collateral branches were more extensive proximally and focal and less complex distally both rostrally and caudally. Subsequently, the number of first order collaterals per 100 μm has been shown in the lumbosacral cord to vary between 0.12-0.47 mm with collateral spans between 115-1,200 μm, occasionally overlapping (Largerbäck & Kellerth 1985a). Examination under the electron microscope (Fyffe 1991) suggested that the Renshaw cell collaterals are myelinated up to the boutons, the boutons having a mean size of 1.54 x 0.96 μm in lamina IX where 87% of the boutons were found, these being both *en passant* and *terminaux*. Similarly, presumed boutons have been reported consisting of 59%

en passant and 41% terminal boutons (Largerbäck & Kellerth 1985a), with between 25 and 1278 boutons associated with a single collateral branch with no apparent correlation between distance of the collateral from the soma and the number of boutons per collateral. The total number of boutons however, has been shown to decrease with distance from the soma (Fyffe 1991), and appears not to be due to limited transport of label. Boutons have been seen in close opposition to presumed Nissl stained motoneurones in lamina IX (Fyffe 1991). Double Labelling of motoneurones and Renshaw cells (Fyffe 1991) revealed Renshaw cell boutons synapsing on motoneurone dendrites and not the soma. The presence of synaptic contacts was confirmed by electron microscopy and it was concluded that the input was within an appropriate distance from the soma for the space constant to represent a significant input.

Using immunoflurecence for gephyrin (Alvarez *et al.* 1997) a post-synaptic protein associated with the glycine receptors, differential post-synaptic distributions were demonstrated in neurones that receive recurrent inhibition. alpha-Motoneurones and Ia interneurones demonstrated an increasing gephyrin cluster size and complexity in the more distal dendrites than on the soma or proximal dendrites whereas the opposite was the case for γ-motoneurones. Renshaw cells, however, had a large complex clusters on their soma and proximal dendrites. This agrees with the site of input to motoneurones identified from double labelling (Fyffe 1991).

Renshaw cells have thus been extensively characterised in terms of physiology, pharmacology and anatomy. However, the function or functions of

Renshaw cells remains a matter of conjecture with many possible functions being advanced, and have been extensively reviewed (Illert & Wietelmann, 1989; Hultborn, 1989; Windhorst 1989). Whatever the function of the Renshaw cell, it involves inhibition in a wide variety of spinal neurones at proximal electronic sites. This inhibition is most powerful close to the motoneurone pools that innervate the Renshaw cell.

5.2.1. Results.

5.2.2. Intracellular Labelling.

Four Renshaw cells were injected with Neurobiotin, with filling periods between 26-73 nA.min. The penetrations were axonal for 3 and somatic for the other. Three of the Renshaw cells were located in T7 with the other in T8. For three Renshaw cells the dorsal roots were sectioned, allowing positive identification of recurrent inhibition from stimulation of a thoracic nerve, whereas the other was identified only by its characteristic firing pattern as a result of peripheral nerve stimulation. Three of these were antidromically activated from the caudal stimulating electrodes located between 27-36 mm caudal, with the other remaining untested. All of the Renshaw cells showed respiratory modulation with their excitability to nerve stimulation being greater in expiration for three Renshaw cells and inspiration for the other. Examples of the activity are shown in Figure 5.2.1. and Figure 5.2.2.

A survival period of 2-3 hours was allowed for distribution of the label

before perfusion with fixative. The tissue was sectioned at between 30-50 μm, parasagitally for 3 Renshaw cells and transversely for the other, and reacted in separate alternate series as for the other interneurones. As either glycine or GABA are thought to be transmitters present in Renshaw cells an un-reacted section containing a portion of the soma was set aside for labelling with antibodies to glycine or GABA (with either DAB or silver intensified immunogold (SIG) visualisation) in the laboratory of Dr. A. Todd (Glasgow) as for the other interneurones. None of these attempts at this staining was successful, for a variety of reasons. All 4 injected Renshaw cells were recovered with the Neurobiotin reaction and 3 were well stained, with the soma of the other cell showing inconsistent granular staining, accompanied by poor staining of the dendrites; the axon and collateral branches however, were well stained.

5.2.2. Location and Morphology of Thoracic Renshaw Cells.

All of the somata were located ventrolaterally in the ventral horn in the rostral third of the segment as defined by the dorsal roots. The somata were oval for three and spindle shaped for the other, with diameters between 37.5 and 20 μm for the maximum and 25 and 15 μm for the minimum diameter; examples are shown in Figure 5.2.2. and Figure 5.2.3. and a partially reconstructed example in Figure 5.2.4. For three of the Renshaw cells the dendritic projections could be identified, with the inconsistent granularly stained cell not having clearly identifiable dendrites. The cells had between 3 and 5 primary dendrites that were predominantly tapered, with only one fine microdendrite seen, this dendrite is drawn in Figure 5.2.4. In one cell beading of

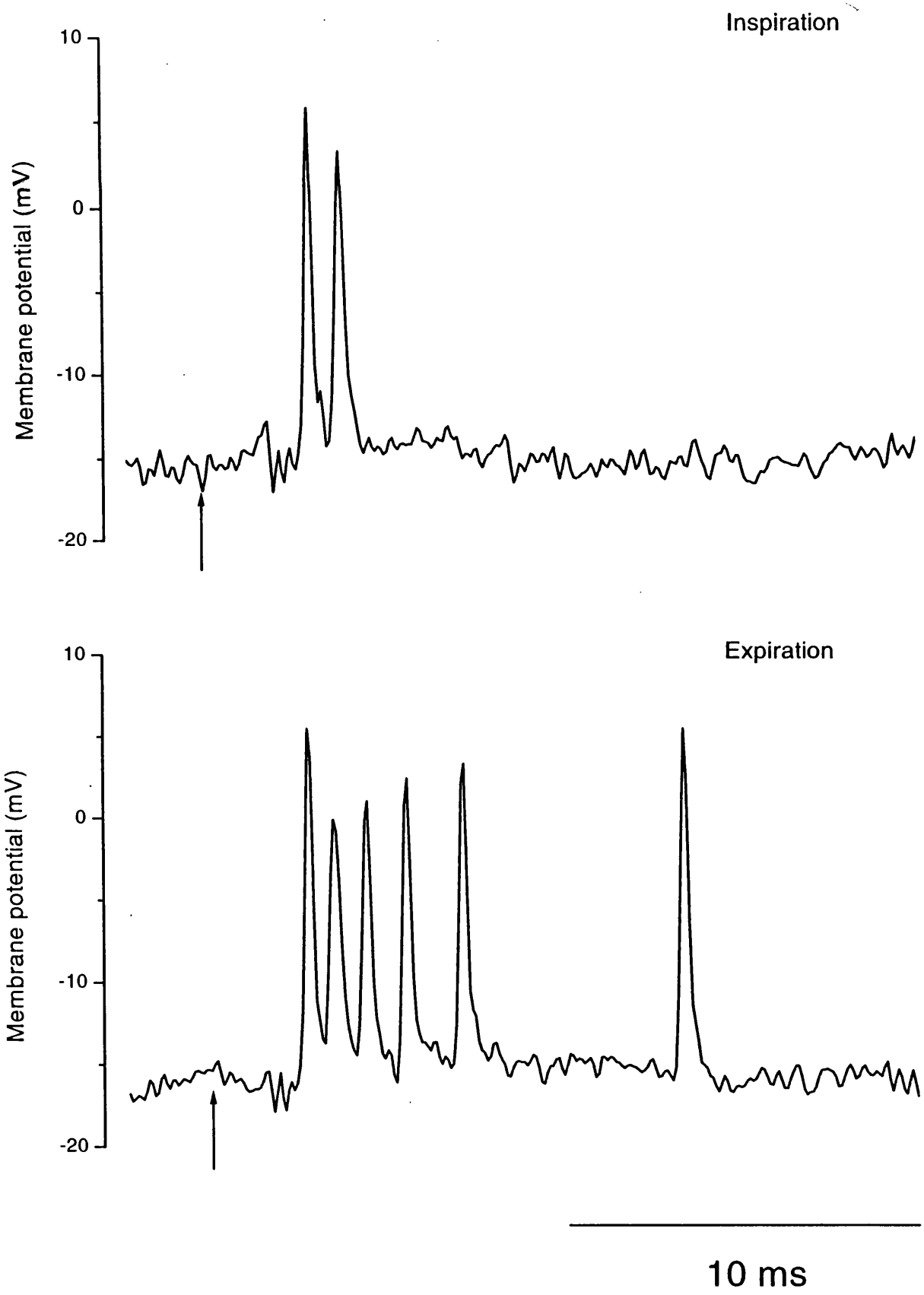

Figure 5.2.1. Respiratory Modulation of Renshaw Cell Discharge. Axonal recording showing response to the stimulation (arrows) of the internal intercostal nerve (5xT)

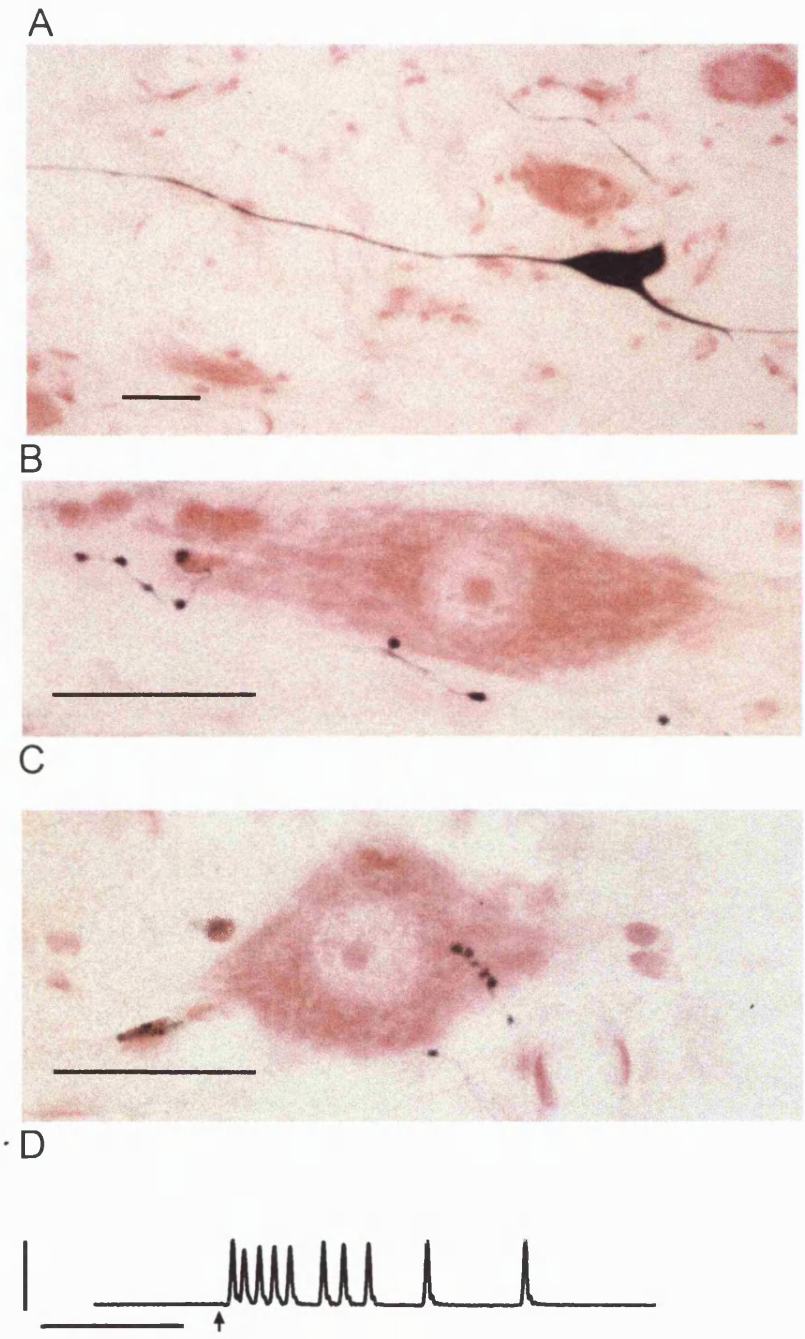

Figure 5.2.2. Photomicrographs of a Renshaw cell. A. Soma. B and C. Boutons in close proximity to somata. D. Electrophysiological identification. Calibrations, 50μ, 50mV and 10 ms.

distal dendrites was seen. The dendrites were mainly unbranched, and if branching occurred, the secondary dendrites were typically fine. The diameter of the primary dendrites was between 10 and 1 μm, with the microdendrite having a diameter of less than 1μm. The dendrites projected in a rostrocaudal direction, in one case for up to 700 μm rostrally and 500 μm caudally, for the remaining two Renshaw cells for which dendrites were clearly evident the rostrocaudal projection could not be unequivocally measured due to confusion of their distal dendrites with those of up to 3 labelled motoneurones. Little mediolateral dendritic projections were seen and no projections into the white matter, the dendrites being limited to laminae VIII and IX.

5.2.3. Axonal Projections of the Renshaw Cells.

All the axons ran in the ventrolateral funiculus close to the tip of the ventral horn, and could be identified for up to 9 mm rostrally and 9.5 mm caudally. The diameter of the axons ranged between 2.5 and 5 μm with little variation in their diameter in contrast to the interneurones described in

Chapter 4. For one interneurone the bifurcation point of the axon could be seen and is shown in Figure 5.2.4.C where the stem axon can be seen to narrow to two rostral and caudal branches. Extensive collateral branching was evident within laminae VIII and IX, examples of which are shown in Figure 5.2.2-5.2.4 and are drawn from one section in Figure 5.2.5 The collaterals projected dorsally and laterally into the ventral horn and possessed both *en passant* and *terminaux* boutons having diameters between <1 and 3.5μm. Examples are shown in Figure 5.2.2 and Figure 5.2.4 where boutons can be

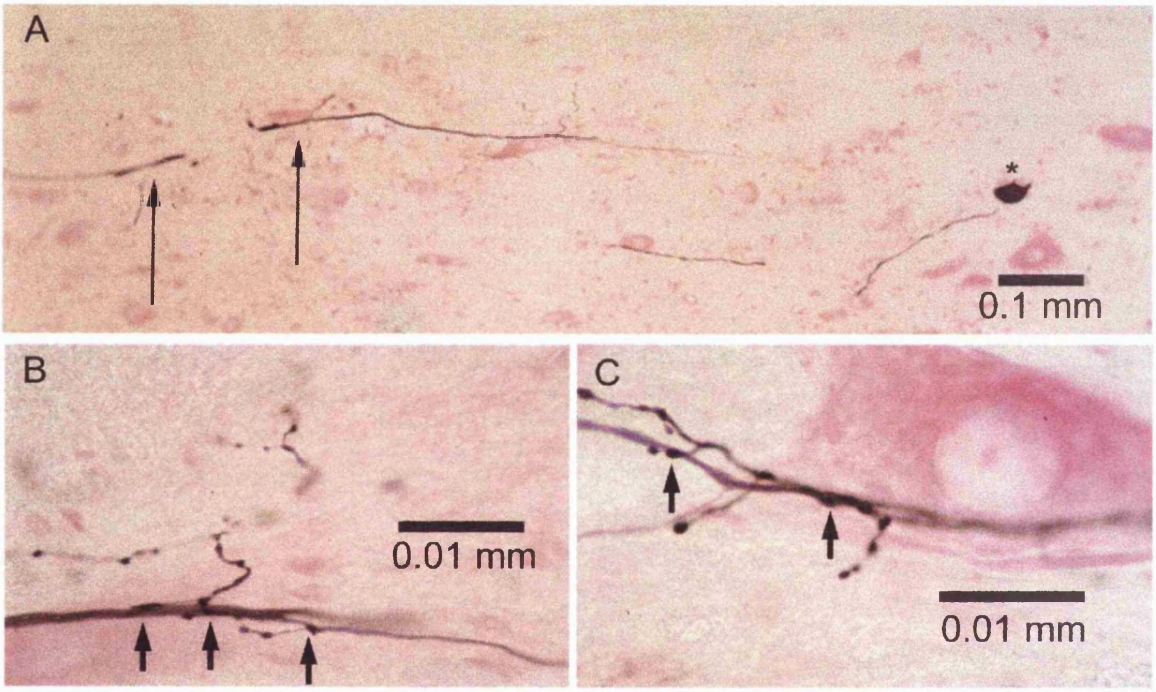

Figure 5.2.3. Photographs of a labelled motoneurone and Renshaw cell. A Dendrites of a motoneurone (Arrows) and the soma of a Renshaw cell (Asterisk). B. Detail from A showing presumed synaptic contacts from the Renshaw cell with the motoneurone dendrites. C. Further examples of presumed synaptic contacts. Presumed contacts are indicated with arrows

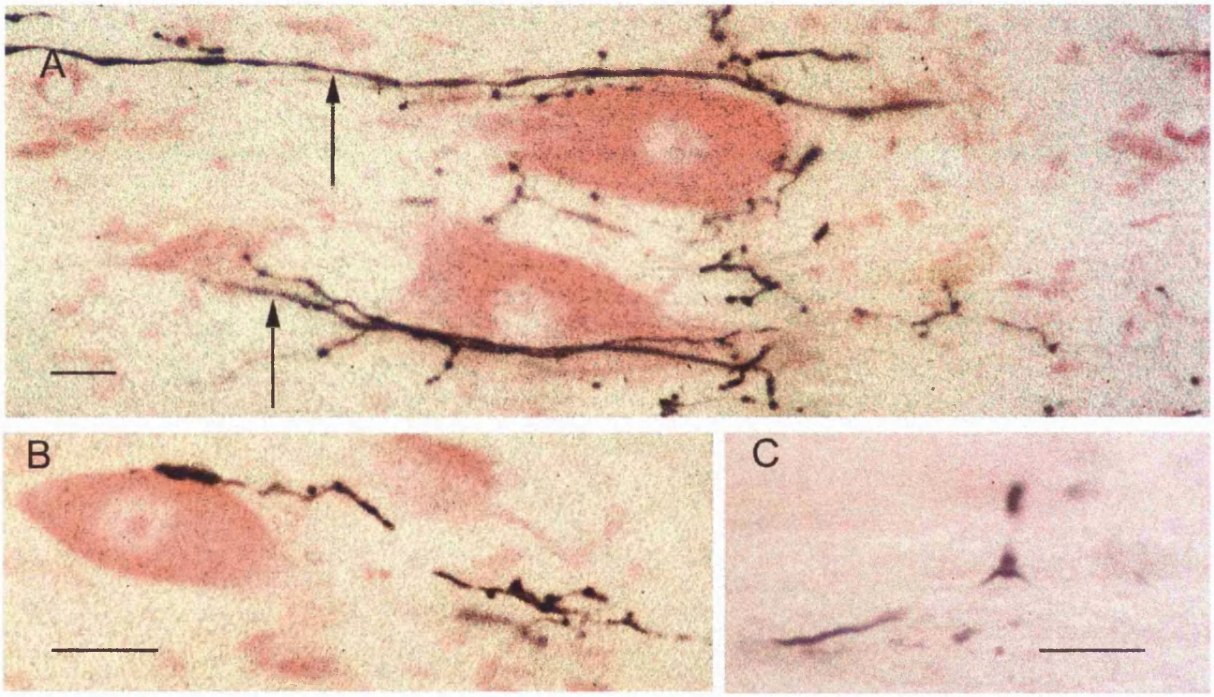

Figure 5.2.4. Photomicrographs of the axon and terminal field of a Renshaw cell. A. Boutons in close opposition to counterstained neuronal soma and intracellularly labelled motoneurone dendrites (arrowed). B. A cluster of boutons making apparent contact with a neurone.C.The axon bifurcation point. Scale bars are 25 microns.

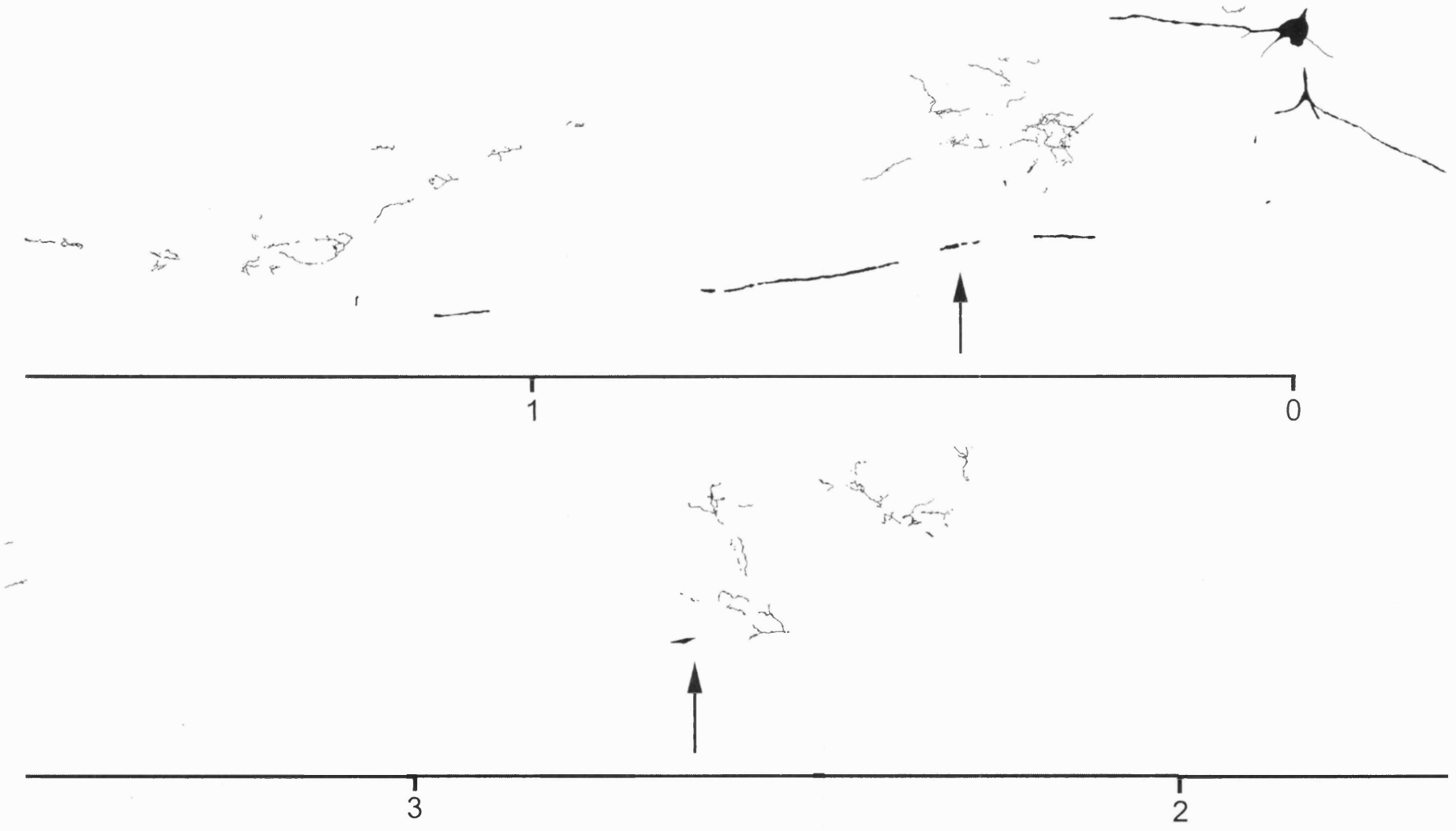

Figure 5.2.5. Drawing of a Renshaw cell and its projections from one parasagital section. The scale bar is in millimeters and represents the distance from the soma in the rostrocaudal direction. The arrow indicated the axon and the most distal projection is illustrated over the page.

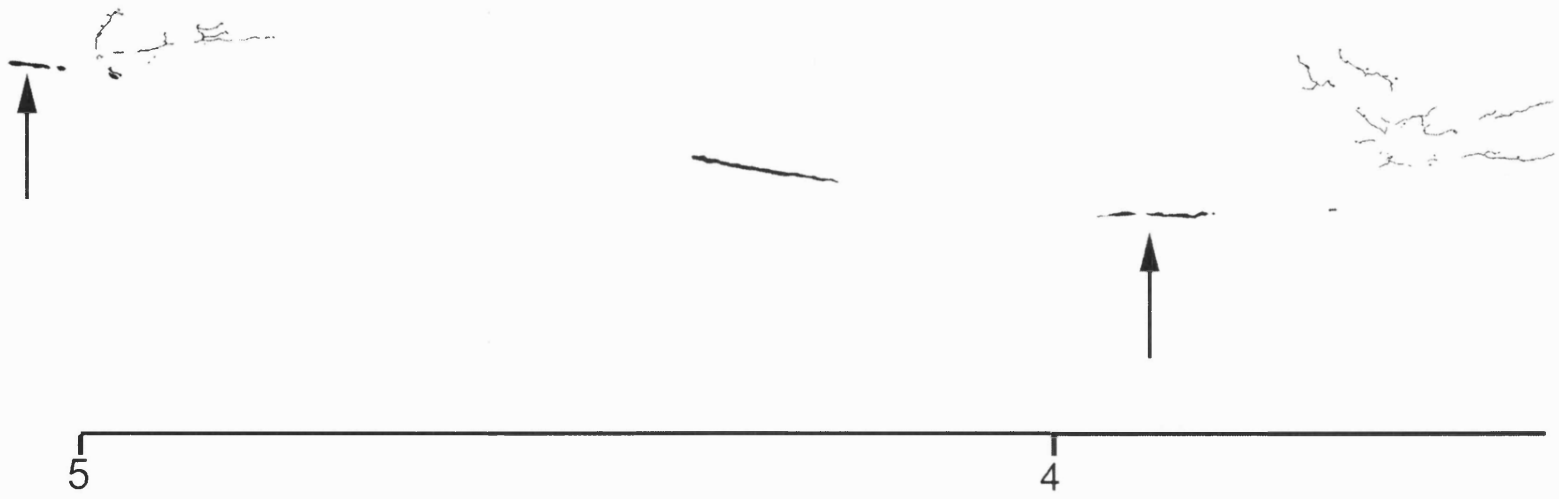

Figure 5.2.5. Continued, showing most distal projections.

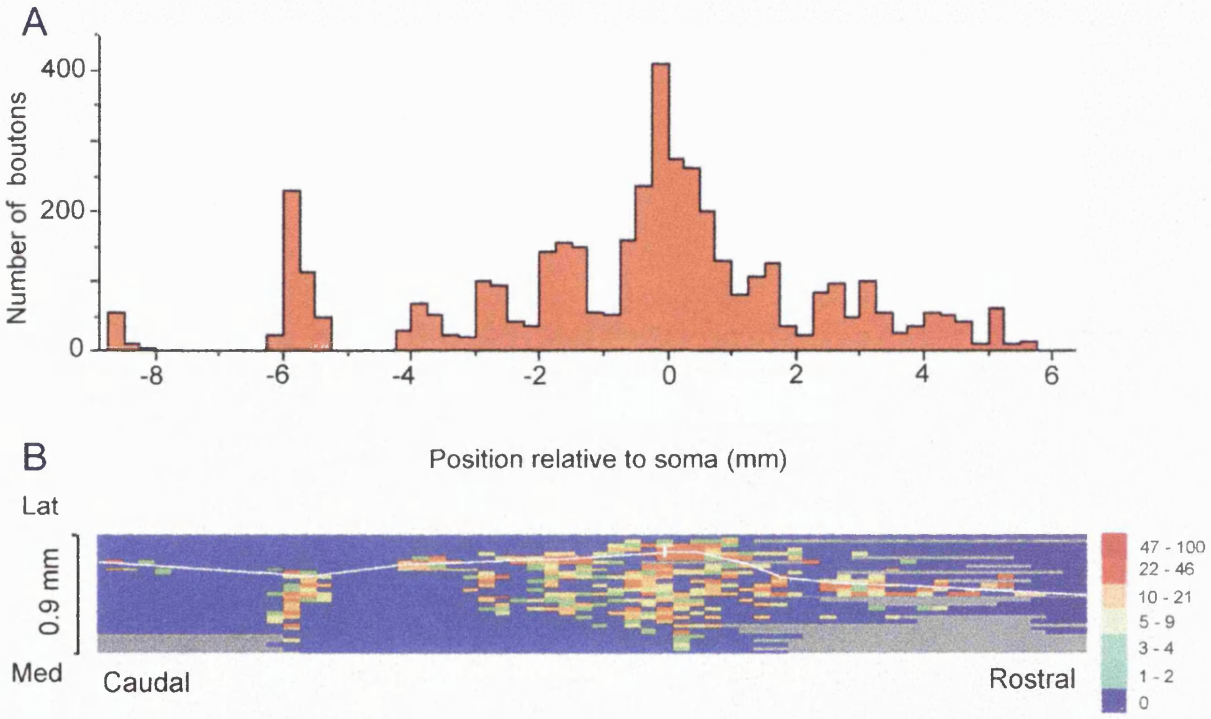

Figure 5.2.6. Distribution of Renshaw cell boutons. A. Rostrocaudal distribution of boutons in bin widths of 250 micrometers. B. Distribution of boutons in the horizontal plane; bin dimensions 250 * 30 micrometers. The trajectory of the axon is illustrated by the white line with the tick indicating the axon branch point. Grey areas are missing or unusable regions of the sections.

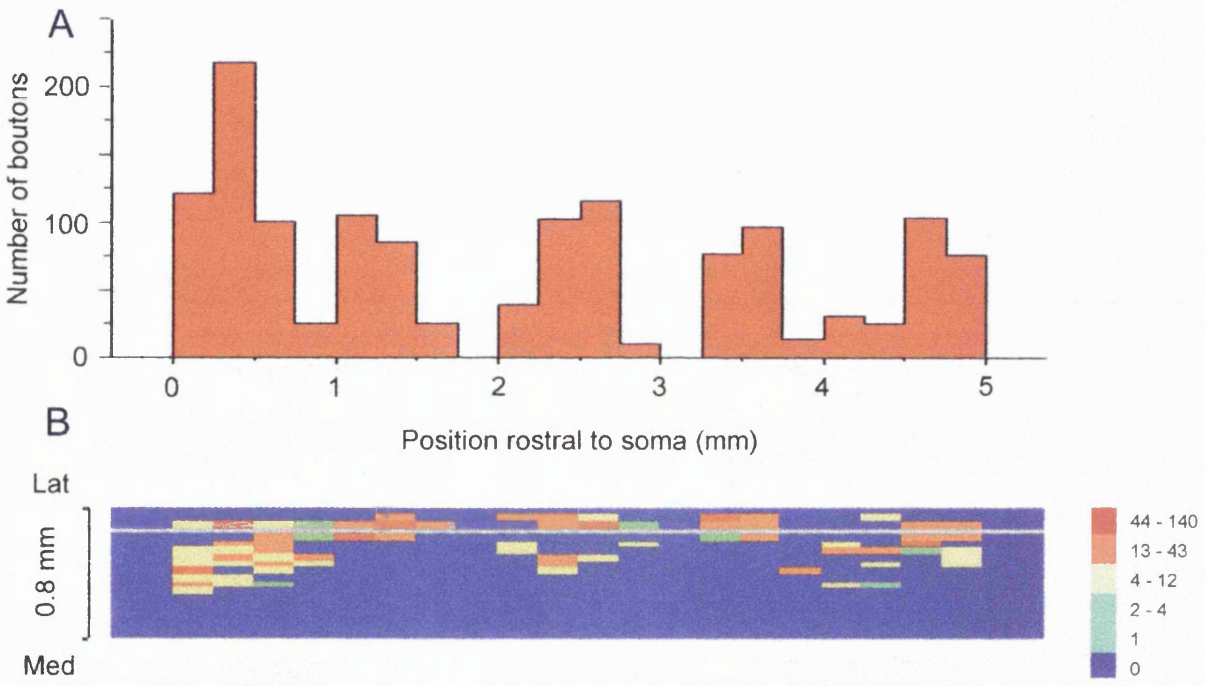

Figure 5.2.7. Distribution of Renshaw cell boutons. A. Rostrocaudal distribution of boutons in bin widths of 250 micrometers. B. Distribution of boutons in the horizontal plane;bin dimentions 250 * 30 micrometers.

seen to approach the soma of a presumed motoneurone. A further presumed contact with a motoneurone is shown in Figure 5.2.3 and Figure 5.2.4 where boutons can be seen to make contact with the middle portion of an intracellular labelled motoneurone dendrites.

The projections of individual collaterals in the rostrocaudal direction tended not to overlap each other, an example of this is shown in Figure 5.2.5, where a
drawing of all the collaterals in one parasagital section are shown. The collaterals of this Renshaw cell can be seen to occur at intervals and not overlap. To illustrate this further, for two Renshaw cells the distribution of the boutons has been counted and represented graphically in Figure 5.2.6. and Figure 5.3.7. It can be seen that the projections of the more distal collaterals do not appreciably overlap. The collateral branches also projected medially and occasionally dorsally approaching the level of the central canal.

5.3.1. Discussion.

5.3.1. Methodological Considerations.

Intracellular labelling with Neurobiotin successfully labelled three of the four Renshaw cells with one cell having irregular staining. For the 3 Renshaw cells the staining was intense and axons and collaterals were well stained at large distances from the soma. The collaterals and boutons of the Renshaw cell were well stained and there was no evidence of limited transport of the

label within the collateral branches. The only instance where there was a limitation in the transport of the label, was when a Renshaw cell was filled axonally, rostral to the point where the axon branched into rostral and caudal running axons. This branch point is illustrated in Figure 5.2.4.C., very little labelling was seen in the caudal branch of this axon. For the irregularly stained Renshaw cell the stain was present in granular aggregations and not evenly distributed throughout the cell as is usual. It is not clear why this occurred, it may be due to Neurobiotin toxicity, however, as it occurred in the cell that was penetrated in its soma it could be due to an injury response to penetration or current passage.

The degree of transport of Neurobiotin seen here, with intensely stained and profuse collaterals even several millimetres from the injection site, supports the observation that the collaterals of the other interneurones were indeed of small diameters with few boutons and these features are not due to limited transport of Neurobiotin. These collaterals were revealed with identical techniques and in the same animals as the other interneurones were identified.

5.3.3. Physiology of Renshaw Cells.

The Renshaw cells identified in this study were not discharging spontaneously, the discharges seen were in response to peripheral nerve stimulation. The stimulated discharge in all cases were modulated by respiration, this is likely due to input from firing motoneurones. Alternatively the Renshaw cells may receive an input from the respiratory bulbospinal neurones

similar to the Renshaw cells seen in the cervical cord (Hilaire, Khatib & Monteau 1986; Kirkwood *et al.* 1988). The fact that there is clear respiratory modulation suggests that they may be involved in inhibition of the internal and external intercostal muscles (Kirkwood, Sears & Westgaard 1981), the inhibition being facilitated during one phase of the respiratory cycle.

5.3.4. Morphology of the Renshaw Cells.

Intracellular labelling of identified Renshaw cells confirms their presence in the thoracic cord (Kirkwood, Sears & Westgaard 1981). The sizes of the Renshaw cell somata are comparable to those seen in the lumbosacral cord (Van Keulen 1979; Lagerbäck & Kellerth 1985; Fyffe 1990) with the exception of the study of Jankowska & Lindström 1973. The morphology of the somata are consistent with those previously reported (Largerbäck & Kellerth 1985; Largerbäck & Ronnevi 1982a), with no evidence of morphologically defined subtypes of Renshaw cell as suggested by Fyffe (1990). However, the sample size is appreciably lower here. The morphology and extent of the dendritic projections are also consistent with those previously reported (Van Keulen 1979; Largerbäck & Ronnevi 1982a; Lagerbäck & Kellerth 1985; Fyffe 1990) with the dendrites being tapered, sparsely branched, projecting rostrocaudally for up to 0.7 mm in laminae VIII and IX. It should be noted that according to Rexed (1954) the ventral portion of the thoracic ventral horn contains only lamina VIII and IX whereas in the cervical and lumbar cord lamina VII is described at the tip of the ventral horn. One new morphological observation is the presence of a microdendrite, and as for the interneurones discussed in

Chapter 4 the functional significance of these dendrites is obscure. The location of the Renshaw cells within the ventral horn is also consistent with that reported by other authors i.e. at the tip of the ventral horn (Jankowska & Lindström 1973; Van Keulen 1979; Largerbäck & Ronnevi 1982a; Lagerbäck & Kellerth 1985; Fyffe 1990). It is concluded that the Renshaw cell is found ubiquitously throughout the spinal cord and have a homogenous morphology, having oval/spindle shaped soma and sparsely branched dendrites that project in a rostrocaudal direction.

5.3.5. Axonal Projections and Bouton Distribution.

The caudal projection of Renshaw cell axons within the thoracic cord is extensive. An axonal projection has been identified here of up to 36 mm, much more extensive than that described in the lumbosacral cord (Jankowska & Smith 1973). In addition to this, intracellular labelling has here identified a rostral and caudal projection of the axon of up to 9 and 9.5 mm respectively, which is considerably more extensive than previously demonstrated anatomically (Lagerbäck & Kellerth 1985a; Fyffe 1990;1991). The diameters of the Renshaw cell axons seen here appear to show far less variation in diameter than the interneurones described in Chapter 4 or the study of Lagerbäck & Kellerth (1985a). As the Renshaw cells were processed identically to the other interneurones the lack of wide variation in the diameter of individual axons suggests that it is a genuine feature of the interneurones and not due to toxicity or other pathological processes. The Renshaw cells have axon collaterals occurring periodically along the length of the cord with dense clusters of

boutons. A similar pattern to this is seen in the lumbosacral cord (Lagerbäck & Kellerth 1985a; Fyffe 1991). However, we have identified clusters of boutons at much greater distances from the soma than previously reported. In previous studies collateral branches have been identified up to 2 mm from the soma (Lagerbäck & Kellerth 1985a; Fyffe 1991), whereas here collaterals have been identified as far as 9 mm from the soma. A common feature of the Renshaw cells described by Lagerbäck & Kellerth (1985a), Fyffe (1991) and those described here is the high density of boutons found close to the soma, as shown in Figure 5.3.6 and Figure 5.3.7.. It may be that in the study by Lagerbäck & Kellerth (1985a) and Fyffe (1991) the collateral branches described are similar to those described here within 2 mm of the soma. For these proximal collateral branches there is a decrease in the number of boutons with increasing distance from the soma, which was not seen by Lagerbäck & Kellerth (1985a), but was described by Fyffe (1991). The high density of boutons close to the soma appears to be a feature of all Renshaw cells, with the possible exception of Renshaw cells in the sacral cord that have crossing axons (Jankowska, Padel & Zarzecki 1978). This is consistent with the observation that recurrent inhibition is strongest in motoneurones close to those that induce it (Eccles 1961a), if the number of the boutons associated with a collateral branch, is considered an indication of the strength of the input to that region. In this study, due to a more widespread transport of label we have identified a new population of distal collateral branches. As the Renshaw cells labelled here are located in the rostral third of the segment the distal collaterals will be spreading recurrent inhibition to the adjacent segment. Overall there is a tendency for the strength of the projection (if proportional to the number of

boutons) to diminish with distance from the soma. This is illustrated in the bouton distribution in Figure 5.3.5. and Figure 5.3.7 but is less clear in Figure 5.3.6.. If this trend were to continue over the whole length of the axonal projection it could account for the decreasing strength of recurrent inhibition seen in the study of Kirkwood, Sears & Westgaard (1981).

The size of the boutons described here is consistent with those previously reported (Lagerbäck & Kellerth 1985a; Fyffe 1991). Many Renshaw cell boutons were seen close to the soma of counterstained neurones. The identity of these neurones is unknown but they were presumed to be motoneurones. These appositions cannot reliably be assumed to represent synapses. However, the close apposition of Renshaw cell boutons with a intracellularly labelled motoneurone is far more compelling evidence of connectivity, and is similar to that reported by Fyffe (1991). The synapsing of a Renshaw cell bouton and a motoneurone dendrite can however, only be fully confirmed by electron microscopy to identify synaptic specialisation, hence, the appositions described here must remain presumed connections.

The function of Renshaw cells remains obscure with many hypotheses being advanced to explain their function or more likely functions. It is known that thoracic motoneurones have dendrites that project rostrocaudally for up to 1 mm (Lipski & Martin-Body 1987) in either direction. Renshaw cell collaterals have been identified here to occur at regular intervals of around 1 mm, projecting for between 0.5 to 1 mm in a rostrocaudal and mediolateral direction. It is possible that this arrangement of collateral branching allows the Renshaw

cell to spread recurrent inhibition to all the motoneurones within the pool efficiently, as it would allow synapses to be made with the soma of motoneurones within the territory of the collateral and the mid to proximal dendrites of motoneurones outside the territory of the collateral. If this arrangement was repeated at intervals of 1 mm very few Renshaw cells would be required to achieve widespread inhibition of a large motoneurone pool such as those in the thoracic cord (Kirkwood, Sears & Westgaard 1981).

5.3.6. Summary.

Intracellular recordings have been made from respiratory modulated Renshaw cells. These Renshaw cells have then been intracellularly labelled confirming their location within the thoracic cord. The Renshaw cells are present in the same region of the ventral horn as Renshaw cells located in the lumbar cord and are morphologically similar. The thoracic Renshaw cells also possess axons that project rostrocaudally in the ventral funiculus. These axons give off collaterals that project into the ventral horn and possess both *en passent* and terminal boutons. These boutons are more abundant at regions close to the soma than more distant regions.

6.1.1. Concluding Remarks and Significance of Findings.

In this study intracellular recordings in interneurones and motoneurones of the thoracic cord have identified neurones with a both inspiratory and expiratory modulation. The motoneurones had similar CRDPs to those reported by Sears (1964). However, inspiratory and expiratory phasing of a new group of thoracic motoneurones, the dorsal ramus motoneurones has been demonstrated in this study. The dorsal ramus motoneurones innervate paravertebral muscles, whose primary function is likely to be maintenance of posture not effecting the movement of the radial pump. Respiratory modulation of the motoneurones innervating these muscles indicates that respiratory movements are coupled to other motor activities.

The dorsal ramus motoneurones also displayed a previously unreported expiratory decrementing CRDP. It is possible that these motoneurones cause the paravertebral muscles to contract thus increasing the rigidity of the spine during movements such as forced expiration when other expiratory muscles require a rigid structure to contract against. During forced expiration the rigidity of the spine would initially need to be maximal and there after could decline during the movement.

The interneurones also had similar firing patterns to those previously reported by Kirkwood *et al.* (1988) and Schmid *et al.* (1993). However, intracellular recording has allowed identification of new populations of interneurones according to their CRDPs. Interneurones with inspiratory and

expiratory CRDPs have been identified and the CRDPs were similar to those previously reported for thoracic motoneurones. The origin of the excitatory drive to these interneurones may be supraspinal as for the motoneurones although we are unable provide evidence for this. Interneurones with no apparent respiratory modulation were also identified, and it is possible that these interneurones have a respiratory modulation in the awake animal and are part of the same functional population as the respiratory phased interneurones. These intracellular recordings identify further thoracic interneurones that have a respiratory phasing of their membrane potential, and are likely to be involved in the transmission of the central respiratory drive to the musculature.

Spike-triggered averaging in motoneurones has revealed connections from expiratory bulbospinal neurones to motoneurones with axons in all of the thoracic nerves with inspiratory and expiratory activity. The input to the expiratory internal nerve motoneurones has been found to be larger than that previously reported by Lipski & Merrill (1987), being of the order of that reported by Kirkwood (1995) using a different technique. These data directly demonstrate that the monosynaptic drive from the EBSNs to expiratory thoracic motoneurones is more significant than previously shown from STA and consequently less of the central drive needs to be transmitted polysynaptically via interneurones than was thought previously.

Spike-triggered averaging in interneurones has failed to reveal any connections from the EBSNs. However, the sample size is comparatively small and the averages were technically difficult to perform. Consequently, few

conclusions regarding the input to interneurones can be drawn at present.

Intracellular labelling of the interneurones revealed neurones located in laminae VII to X, with varied somal morphologies. Their dendrites project widely throughout the ventral horn with a characteristic rostrocaudal orientation. The predominant axonal projection is to the contralateral cord, similar to that deduced electrophysiologically (Kirkwood *et al.* 1988). The axons run in the medial or ventral funiculus and are predominantly descending. The collaterals tend to be fine with small boutons, the first collateral generally originating close to the level of the soma. A predominant feature similar to that deduced electrophysiologically is that the interneurones with strong respiratory phasing tend to project more ventrally than those with a less powerful drive. Immunohistochemical staining has revealed interneurones that are inhibitory and excitatory with the inhibitory interneurone being respiratory modulated, whereas, the excitatory interneurones showing little respiratory modulation. These data are consistent with the hypothesis that tonically firing interneurones project to the distal dendrites of the motoneurones where they provide an excitatory drive increasing the overall excitability of the motoneurone, whereas, the phasically discharging interneurones project to the motoneurone somata and modulate the discharge pattern of the motoneurone by either an inhibitory or excitatory input.

Intracellular labelling of Renshaw cells has identified neurones with similar morphology and projections to those identified in the lumbar cord. Extensive, well-labelled terminal fields have been identified considerable

distances from the site of injection, thus supporting the observation that the collaterals of the other interneurones are in fact fine and their restricted size is not a result of limitations in the transport of label.

Renshaw cells thus appear to be ubiquitous within the spinal cord, characteristically found at homologous locations within the ventral horn. There are also very many similarities in the morphology of Renshaw cells and hence these neurones are likely to be a single population of neurones within the cord with any functional difference of these neurones related to differences in their projections.

References.

Alvarez.F.J., Dewey.D.E., Harrington.D.A. & Fyffe.R.E.W. (1997) Cell-type specific organisation of the glycine receptor clusters in the mammalian spinal cord. *J.Comp.Neurol.* **379**. 150-170.

Aminoff.M.J. & Sears.T.A. (1971) Spinal integration of segmental, cortical and breathing inputs to thoracic respiratory interneurones. *J.Physiol.* **215**. 557-575.

Aoki.M, Watanabe.H, Ebata.N & Mori.S. (1978) Spontaneous respiratory activity in spinal cats. *Brain Res.* **157**. 376-380.

Aoki.M, Mori.S, Kawahara.K, Watanabe.H & Ebata.N. (1980) Generation of spontaneous respiratory rhythm in high spinal cats. *Brain Res.* **202**. 51-63.

Arita.H., Kogo.N. & Koshiya.N. (1987) Morphological and physiological properties of caudal medullary expiratory neurons of the cat. *Brain Res.* **401**. 259-266.

Bellingham.M.C. & Lipski.J. (1990) Respiratory interneurones in the C5 segment of the spinal cord of the cat. *Brain Res.* **533**. 141-146.

Berger.A.J. (1977) Dorsal respiratory group neurons in the medulla of cat: spinal projections, responses to lung inflation and superior laryngeal nerve stimulation. *Brain Res.* **135**. 231-254.

Berger.A. (1979) Phrenic motoneurones in the cat: Subpopulations and nature of respiratory potentials. *J.Neurophysiology.* **42**. 76-90.

Berger.A.J., Averill.D.B. & Cameron.W.E. (1984) Morphology of inspiratory neurons located in ventrolateral nucleus of the tractus solitarius of the cat. *J.Comp.Neurol.* **244**. 60-70.

Berger.A.J., Cameron.W.E., Averill.D.B., Kramis.R.C. & Binder.M.C. (1984) Spatial distribution of phrenic and medial gastrocenemius motoneurones in the cat spinal cord. *Exp. Neurol.* **86**. 559-575.

Bianchi.A.L. (1971) Localisation et étude des neurones respiratoires bulbaires. Mais en jeu antidromique par stimulation spinale au vagale. *J.Physiol., Paris.* **63**. 5-40.

Bianchi.A.L. (1974) Modalités de décharge et propriété anatomo-fonctionnelles des neurones respiratoires bulbaires. *J.Physiol., Paris.* **68**. 555-587.

Bianchi.A.L & Barillot.J.C. (1982) Respiratory neurons in the retrofacial nucleus: Pontile, medullary, spinal and vagal projections. *Neurosci Letts.* **31**. 277-282.

Bianchi.A.L., Grélot.L., Iscoe.S. & Remmers.J.E. (1988) Electrophysiological properties of rostral medullary respiratory neurones in the cat: An intracellular study. *J.Physiol.* **407**. 293-310.

Bras.H. Cavallari.P & Jankowska.E. (1988a) Demonstration of initial axon collaterals of cells of origin of the ventral spinocerebellar tract in the cat. *J. Comp. Neurol.* **273**. 584-592.

Bras.H., Cavallari.P., Jankowska.E & Kubin.L. (1988b) Morphology of midlumbar interneurones relaying information from group II muscle afferents in the cat spinal cord. *J. Comp. Neurol.* **290**. 1-15.

Brink.E. & Suzuki.I. (1987) Recurrent inhibitory connexions among neck motoneurones in the cat. *J.Physiol.* **383**. 301-326.

Cameron.W.E., Averill.D.B. & Berger.A.J. (1983) Morphology of cat phrenic motoneurones as revealed by intracellular injection of horseradish peroxidase. *J.Comp.Neurol.* **219**. 70-80.

Cameron.W.E., Averill.D.B. & Berger.A.J. (1985) Quantitative analysis of the dendrites of cat phrenic motoneurones stained intracellularly with horseradish peroxidase. *J.Comp.Neurol.* **230**. 91-101.

Cohen.M.I., Piercey.M.F., Gootman.P.M. & Wolosky.P. (1974) Synaptic connections between inspiratory neurons and phrenic motoneurones as revealed by cross-correlation. *Brain Res.* **81**. 319-324.

Cohen.M.I. (1979) Neurogenesis of respiratory rhythm in the mammal. *Phys.*

Rev. **59**. 1105-1173.

Cohen.M.I. & Feldman.J.L. (1984) Discharge properties of dorsal medullary inspiratory neurons: Relation to pulmonary afferent and phrenic efferent discharge. *J. Neurophysiol.* **51**. 753-776.

Cohen.M.I., Feldman.J.L. & Sommer.D. (1985) Caudal medullary expiratory neurone and internal intercostal nerve discharges in the cat: effects of lung inflation. *J.Physiol.* **368**. 147-178.

Davies.J.G McF., Kirkwood.P.A, Sears.T.A. (1985a) The detection of monosynaptic connexions from inspiratory bulbospinal neurons to inspiratory motoneurones in the cat. *J.Physiol.* **368**. 33-62.

Davies.J.G McF., Kirkwood.P.A, Sears.T.A (1985b) The distribution of monosynaptic connexions from inspiratory bulbospinal neurons to inspiratory motoneurones in the cat. *J.Physiol.* **368**. 63-87.

De Troyer.A. & Ninane.V. (1986) Respiratory function of intercostal muscles in surpine dog: an electromyographic study. *J. Appl. Physiol.* **60**. 1692-1699.

De Troyer.A., Legrand.A. & Wilson.T.A. (1996) Rostrocaudal gradient of mechanical advantage in the parasternal intercostal muscles of the dog. *J.Physiol.* **495**. 239-246.

De Troyer.A., Legrand.A. & Wilson.T.A. (1999) Respiratory mechanical advantage of the canine external and internal intercostal muscles. *J.Physiol.* **518**. 283-289.

Dobbins.E.G. & Feldman.J.L. (1994) Brainstem network controlling descending drive to phrenic motoneurones in rat. *J.Comp.Neurol.* **347**. 64-86.

Douse.M.A & Duffin.J. (1993) Axonal projections and synaptic connections of the C5 segmental expiratory interneurones in the cat. *J.Physiol.* **407**. 431-444.

Duffin & Hoskin (1987) intracellular recordings from upper cervical inspiratory neurons in the cat. *Brain. Res.* **435**. 351-354.

Duron.B. (1981) Intercostal and Diaphragmatic muscle endings and afferents. In. *Regulation of Breathing*. Ed. T.F. Horbein. Dekker Inc. New York.

Eccles.J.C., Fatt.P. & Koketsu.K. (1954) Cholinergic and inhibitory synapses in a pathway from motor-axon collaterals to motoneurones. *J.Physiol.* **126**. 524-526.

Eccles.J.C., R.M..Eccles., Iggo.A. & Lundburg.A. (1961a) Electrophysiological investigations on Renshaw cells. *J.Physiol.* **159**. 461-478.

Eccles.J.C., Eccles.R.M., Iggo.A. & Ito.M. (1961b) Distributions of recurrent inhibition among motoneurones. *J.Physiol.* **159**. 478-499.

Eccles.R.M., Sears.T.A. & Shealy.C.N. (1962) Intra-cellular recording from respiratory motoneurones of the thoracic spinal cord of the cat. *Nature*. **193**. 844-846.

Ellaway.P.A. (1971) Recurrent inhibition of fusimotor neurones exhibiting background discharges in the decerebrate and the spinal cat. *J.Physiol.* **216**. 419-439.

Ellenberger.H.H & Feldman.J.L. (1988) Monosynaptic transmission of respiratory drive to phrenic motoneurones from brainstem bulbospinal neurons in the rat. *J.Comp.Neurol.* **269**. 47-57.

Fedorko.L. (1982) Localization of the respiratory motoneurone pools in the cat's thoracic spinal cord. *J.Physiol.* **332**. P28.

Feldman.J.L. (1981) Interactions between brainstem respiratory neurons. *Fed. Proc.* **40**. 2384-2388.

Feldman.J.L & Cohen.M.I. (1978) Relation between expiratory duration and rostral medullary expiratory neuronal discharge. *Brain Res.* **141**. 172-178.

Feldman.J.L., Loewy.A.D & Speck.D.F. (1985) projections from the ventral respiratory group to phrenic and intercostal motoneurones in the cat: An autoradiographic study. *J. Neurosci.* **5**. 1993-2000.

Ford.T.W., McWilliam.P.N, & Shepheard.S.L. (1986) A multibarrelled platinum-coated micro-electrode. *J.Physiol.* **386**. 9P.

Ford.T.W., Matsuyama.K., Mori.S. & Nakajima.K. (1997) Projections from the nucleus retroambigualis (nRA) to the thoracic spinal cord of the cat studied with the anterograde tracer *Phaseolus vulgaris*-leucoagglutinin (PHA-L). *J. Physiol.* **505.P**. 85P

Fyffe.R.E.W. (1990) Evidence for separate morphological classes of Renshaw cells in the cat's spinal cord. *Brain Res.* **536**. 301-304.

Fyffe.R.E.W. (1991) Spatial distribution of recurrent inhibitory synapses on spinal motoneurones in the cat. *J.Neurophysiol.* **65**. 1134-1148.

Goldman.M.D., Loh.L. & Sears.T.A. (1985) The respiratory activity of human levator costae muscles and its modification by posture. *J.Physiol.* **362**. 189-204.

Gordon.D.C. & Richmond.F.J.R. (1990) Topography in the phrenic motoneuron nucleus demonstrated by retrograde multiple labelling techniques. *J.Comp.Neurol.* **292**. 424-434.

Hamm.T.M., Sasaki.S., Stuart.D.G., Windhorst.U & Yuan.C-S. (1987) The measurement of single motor-axon recurrent inhibitory post-synaptic potentials in the cat. *J.Physiol.* **388**. 631-651.

Hamberger.G.E. (1749) De respirationis mechanismo et usu gnuino. Iena.

Hilaire.G., Nicholls.J.G. & Sears.T.A. (1983) Central and proprioceptive influences on the activity of levator costae motoneurones in the cat. *J.Physiol.* **342**. 527-548.

Hilaire.G., Khatib.M. & Monteau.R. (1986) Central drive on Renshaw cells coupled with phrenic motoneurones. *Brain Res.* **376**. 133-139.

Hongo.T., Kitazawa.S., Ohki.Y., Sasaki..M & Xi.M-C. (1989) A physiological and morphological study of premotor interneurones in the cutaneous reflex pathways of the cat. *Brain Res.* **505**. 163-166.

Hoskin.R.W. & Duffin.J. (1987) Excitation of upper cervical inspiratory neurons by inspiratory neurons of the nucleus retroambigualis in the cat. *Exp. Neurol.* **98**. 404-417.

Hultborn.H., Jankowska.E., & Lindström.S. (1971b) Recurrent inhibition of interneurones monosynaptically activated from group Ia afferents. *J.Physiol.* **215**. 613-636.

Hultborn.H. (1986) Recurrent inhibition - in search of a function. *Prog. Brain Res.* **80**. 269-281.

Iscoe.S. & Duffin.J.(1996) Effects of stimulation of phrenic afferents on cervical respiratory interneurons and phrenic motoneurones in cats. *J.Physiol.* **497.3**. 803-812.

Iscoe.S. (1998) Control of abdominal muscles. *Prog. Brain. Res.* **56**. 433-5606.

Jankowska.E. (1975) Identification of interneurones interposed in different spinal reflex pathways. Proceedings of the Golgi centennial symposium. Raven press. NY.

Jankowska.E. & Lindström (1971) Morphological identification of Renshaw cells. *Acta. Physiol. Scand.* **81**. 428-430.

Jankowska.E. & Smith.D.O. Antidromic activation of Renshaw cells and their axonal projections. (1973) *Acta. Physiol. Scand.* **88**. 198-214.

Jankowska.E., Padel.Y & Zarzecki.P. (1978) Crossed disynaptic inhibition of sacral motoneurones. *J.Physiol.* **285**. 425-444.

Jankowska.E & Odutola.A. (1980) crossed and uncrossed synaptic actions on motoneurones of back muscles in the cat. *Brain Res.* **194**. 65-78.

Jankowska.E. (1992) Interneuronal relay in spinal pathways from proprioceptors. *Prog. Neurobiol.* **38**. 335-378.

Jodkowasi.J.S., Viana.F., Dick.T.E. & Berger.A.J. (1987) Electrical properties of phrenic motoneurones in the cat: Correlation with inspiratory drive. *J. Neurophysiol.* **58**. 105-124.

Jodkowasi.J.S., Viana.F., Dick.T.E. & Berger.A.J. (1988) Repetitive firing properties of phrenic motoneurones in the cat. *J. Neurophysiol.* **60**. 687-702.

Kalia.M., Feldman.J.L. & Cohen.M.I. (1979) Afferent projections to the inspiratory neuronal region of the ventrolateral nucleus of the tractus solitarius in the cat. *Brain Res.* **171**. 135-141.

Kirkwood.P.A. & Sears.T.A. (1973) Monosynaptic excitation of thoracic expiratory motoneurones from lateral respiratory neurones in the medulla of the cat. *J.Physiol.* **232**. 87p-89p.

Kirkwood.P.A. (1979) On the use and interpretation of cross-correlation measurements in the mammalian central nervous system. *J. Neurosci. Methods.* **1**. 107-132.

Kirkwood.P.A., Sears.T.A. & Westgaard.R.H. (1981) Recurrent inhibition of intercostal motoneurones in the cat. *J.Physiol.* **319**. 111-130.

Kirkwood.P.A, Munson.J.B, Sears.T.A, Westgaard.R.H. (1988) Respiratory interneurones in the thoracic spinal cord of the cat. *J.Physiol.* **395**. 161-192.

Kirkwood.P.A, Schmid.K, Sears.T.A. (1993) Functional identities of thoracic respiratory interneurones in the cat. *J.Physiol.* **461**. 667-687.

Kirkwood.P.A. (1995) Synaptic excitation in the thoracic spinal cord from expiratory bulbospinal neurones in the cat. *J.Physiol.* **484.1**. 201-225.

Kirkwood.P.A., Donga.R., Ford.T.W., Saywell.S.A. & Holstege.G. (1999) Prog. Brain. Res. *In press (see appendix)*.

Lagerbäck.P-A. & Ronnevi.L-O. (1982) An ultrastructural study of serially sectioned Renshaw cells. I. Architecture of the cell body, axon hillock, initial axon segment and proximal dendrites. *Brain Res.* **235**. 1-15.

Lagerbäck.P-A. & Kellerth.J-O. (1985a) Light microscopic observations on cat Renshaw cells after intracellular staining with horseradish peroxidase. 1. The axonal systems. *J.Comp. Neurol.* **240**. 359-367.

Lagerbäck.P-A. & Kellerth.J-O. (1985b) Light microscopic observations on cat Renshaw cells after intracellular staining with horseradish peroxidase. 2. The cell bodies and dendrites. *J.Comp. Neurol.* **240**. 359-367.

Laricol.N., Rose.D., Marlot.D. & Duron.B. (1982) Spinal localization of the intercostal motoneurones innervating the upper thoracic spaces. *Neurosci. Letts.* **31**. 13-18.

Le Bars.P. & Duron.B. (1984) Are the external and internal intercostal muscles synergist or antagonist in the cat. *Neurosci Letts.* **51**. 383-386.

Legrand.A., Brancatisano.A., Decramer,M. & De Troyer.A. (1996) Rostrocaudal gradient of electrical activation in the parasternal intercostal muscles of the dog. *J.Physiol.* **495**. 247-254.

Legrand.A., & De Troyer.A. (1999) Spatial distribution of external and internal intercostal activity in dogs. *J.Physiol.* **518**. 291-300.

Lipski.J & Merrill.E.G. (1980) Electrophysiological demonstration of the projection from expiratory neurones in rostral medulla to contralateral dorsal respiratory group. *Brain Res.* **197**. 521-524

Lipski.J., Fyffe.R.E.W & Jodowski.J. (1985) Recurrent inhibition of cat phrenic motoneurones. *J. Neurosci.* **5**. 1545-1555.

Lipski.J & Duffin.J. (1986) An electrophysiological investigation of propriospinal inspiratory neurons in the upper cervical cord of the cat. *Exp. Brain Res.* **61**. 625-637

Lipski.J. & Martin-Body.R.L. (1987) Morphological properties of respiratory intercostal motoneurones in cats as revealed by intracellular injection of horseradish peroxidase. *J. Comp. Neurol.* **260**. 423-434.

Lipski.J. & Merrill.E.G. (1987) Inputs to intercostal motoneurones from ventrolateral medullary respiratory neurons in the cat. *J. Neurophysiol.* **57**. 1837-1853.

Mackel.R. (1979) Segmental and descending control of the external urethral and anal sphincters in the cat. *J.Physiol.* **294**. 105-122.

McCrea.D.A. (1992) Can sense be made of spinal interneuron circuits? *Behavioural and Brain Sciences*. **15**. 633-643.

Merrill.E.G. (1970) The lateral respiratory neurones of the medulla: Their associations with nucleus ambiguus, nucleus retroambigualis. The spinal accessory nucleus and the spinal cord. *Brain Res.* **24**. 11-28.

Merrill.E.G. (1982) One source of the expiratory inhibition of phrenic motoneurones in the cat. *J.Physiol.* **322**. 79p.

Merrill.E.G, Lipski.J, Kubin.L & Fedorko.L. (1983) Origin of the expiratory inhibition of nucleus tractus solitarius inspiratory neurones. *Brain Res.* **263**. 43-50.

Merrill.E.G. & Fedorko.L. (1984) Monosynaptic inhibition of phrenic motoneurones: A long descending projection from Bötzinger neurons. *J.Neurosci.* **4**. 2350-2353.

Merrill.E.G. & Lipski.J. (1987) Inputs to intercostal motoneurones from ventrolateral medullary respiratory neurons in the cat. *J. Neurophysiol.* **57**. 1837-1853.

Miller.A.D., Tan.L.K. & Suzuki.I. (1987) Control of abdominal and expiratory intercostal muscle activity during vomiting: Role of ventral respiratory group expiratory neurons. *J. Neurophysiol.* **57**. 1854-1866.

Monteau.R. & Hilaire.G. (1991) Spinal respiratory motoneurones. *Prog. In Neurobiol.* **37**. 83-144.

Munson.J.B. & Sypert.G.W. (1979) Properties of single central Ia afferent fibres projecting to motoneurones. *J.Physiol.* **296**. 315-327.

Nolan.C.N. & Waldrop.T.G. (1997) Integrative role of medullary neurons of the cat during exercise. *J. Physiol.*

Otake.K., Sasaki.H., Mannen.H. & Ezure.K. (1987) Morphology of expiratory neurones of the Bötzinger complex: An HRP study in the cat. *J.Comp.Neurol.* **258**. 565-579.

Ramón y Cajal.S. (1911) Histologie du systèms nerveux de l'homme et des vertébrés. Maloine, Paris.

Reklin.J.C & Feldman.J.L. (1998) PreBötzinger complex and pacemaker neurons: Hypothesized site and kernel for respiratory rhythm generation. *Annu. Rev. Physiol.* **60**. 385-405.

Renshaw.B. (1941) Influence of discharge of motoneurones upon excitation of neighbouring motoneurones. *J.Neurophysiol.* **4**. 167-183.

Renshaw.B. (1946) Central effects of centripetal impulses in axons of spinal ventral roots. *J. Neurophysiol.* **9**. 191-204.

Rexed.B. (1954) A cytoarchitectonic atlas of the spinal cord in the cat. *J.Comp Neurol.* **100**. 297-351.

Richter.D.W. & Ballantyne.D. (1983) A three phase theory about the basic respiratory pattern generator. In Central neurone environment, ed. Schläfke.M.E., Koepchen.H.P. & See.W.R. pp 164-174. Berlin. Springer-Verlag.

Rickard-Bell.G.C., Bystrzycka.E.K. & Nail.B.S. (1985) The identification of brainstem neurones projecting to thoracic respiratory motoneurones in the cat as demonstrated by retrograde transport of HRP. *Brain. Res. Bull.* **14**. 25-37.

Ryall.R.W., Piercey.M.F. & Polosa.C. (1971) Intersegmental and intrasegmental distribution mutual inhibition of Renshaw cells. *J. Neurophys.* **34**. 700-707.

Sasaki.H., Otake.K., Ezure.K. & Manabe.M. (1989) Morphology of augmenting inspiratory neurons of the ventral respiratory group in the cat. *J.Comp.Neurol.* **282**. 157-168.

Sears.T.A. (1964a) Efferent discharges in alpha and fusimotor fibers of intercostal nerves of the cat. *J.Physiol.* **174**. 295-315.

Sears.T.A. (1964b) Some properties and reflex connexions of respiratory motoneurones of the cat's thoracic spinal cord. *J.Physiol.* **175**. 386-403.

Sears.T.A. (1964c) The slow potentials of thoracic respiratory motoneurones and their relation to breathing. *J.Physiol.* **175**. 404-424.

Sears.T.A. (1977) The respiratory motoneuron and apneusis. *Fed. Proc.* **10**. 2412-2420.

Schmid.K, Kirkwood.P.A, Munson.J.B, Shen.E, Sears.T.A. (1993) Contralateral projections of the thoracic respiratory interneurones in the cat. *J.Physiol.* **461**. 647-665.

Smith.J.C., Morrison.D.E., Ellenberger.H.H., Otto.M.R. & Feldman.J.L. (1989) Brainstem projections to the major respiratory neuron populations in the medulla of the cat. *J.Comp.Neurol.* **281**. 69-96.

Stone.T.W. (1985) Micriontophoresis and pressure injection. IBRO handbook series. Methods in Neuroscience. Volume 8. Wiley.

Swadlow (1982) Antidromic activation: measuring the refractory period at the site of axonal stimulation. *Exp. Neurol.* **75**. 514-516.

Taylor.A. (1960) The contribution of the intercostal muscles to the effort of respiration in man. *J. Physiol.* **151**. 390-402.

Taylor.A. Stephens.J.A. Appenteng.K & O'Donovan.M.J. (1978) Extracellular spike triggered averaging for plotting synaptic projections. *Brain Res.* **140**. 344-348.

Tanaka.Y. & Hirai.N. (1994) Physiological studies of thoracic spinocerebellar tract neurons in relation to respiratory movement. *Neurosci. Res.* **19**. 317-326.

Tani.M., Kida.M.Y. & Akita.K. (1994) Relationship between the arrangement of motoneuron pools in the ventral horn and ramification pattern of the spinal nerve innervating trunk muscles in the cat (*Felis domestica*) *Exp. Neurol.* **128**. 290-300.

Thomas.R.C & Wilson.V.J. (1965) Precise localization of Renshaw cells with a new marking technique. *Nature.* **4980**. 211-213.

VanderHorst.V.G.J & Holstege.G. (1995) Caudal medullary pathway to

lumboscaral motoneuronal cell groups in the cat: Evidence for direct projections possibly representing the final common pathway for lordosis. *J.Comp.Neurol.* **359**. 457-475.

Van Keulen.L.C.M. (1979) Axon trajectories of Renshaw cells in the lumbar spinal cord of the cat, as reconstructed after intracellular staining with horseradish peroxidase. *Brain Res.* **167**. 157-162.

Van Keulen.L. (1981) Autogenetic recurrent inhibition of individual spinal motoneurones in the cat. *Neurosci. Letts.* **21**. 297-300.

Von Euler.C., Hayward.J.N., Marttila.I. & Wyman.R.J. (1973) Respiratory neurones of the ventrolateral nucleus of the solitary tract of the cat: vagal input, spinal connections and morphological identification. *Brain Res.* **61**. 1-22.

Von Euler.C., Hayward.J.N., Marttila.I. & Wyman.R.J. (1973) The spinal connections of the inspiratory neurones of the ventrolateral nucleus of the cat's tractus solitarius. *Brain Res.* **61**. 23-33.

Watt.D.G.D., Stauffer.E.K., Taylor.A., Reinking.R.M. & Stuart.D.G. (1976) Analysis of muscle receptor connections by spike-triggered averaging. 1. Spindle primary and tendon organ afferents. *J. Neurophysiology.* **39**. 1375-1392.

Walmsey.B. & Tracey.D.J. (1981) An intracellular study of Renshaw cells. *Brain Res.* **223**. 170-175.

Webber.C.L. Wurster.R.D. & Chung.J.M. (1979) Cat phrenic nucleus architecture as revealed by horseradish peroxidase mapping. *Exp.Brain.Res.* **35**. 395-406.

Willis.W.D & Willis.J.C. (1964) location of Renshaw cells. *Nature.* **204**. 1214-1215.

Windhorst.U. (1989) Do Renshaw cells tell spinal neurones how to interpret muscle spindle signals? *Prog in Brain Res.* **86**. 283-294.

Yates.B.J., Smail.J.A., Stocker.S.D. & Card.J.P. (1998) transneuronal tracing of neural pathways controlling activity of diaphragm motoneurones in the ferret. *Neuroscience.* **90**. 1501-1513.